Precursors of epi-/shamixanthone formed in Hülle cells cause oxidative stress sensitivity and repress sexual development of the filamentous fungus *Aspergillus nidulans*

Dissertation

for the award of the degree

"Doctor rerum naturalium"

of the Georg-August-Universität Göttingen

within the doctoral program "Microbiology and Biochemistry" of the Georg-August University School of Science (GAUSS)

submitted by

Li Liu

from Chongqing, P. R. China

Göttingen 2019

Thesis Committee:

Referee:

Prof. Dr. Gerhard H. Braus
Department of Molecular Microbiology and Genetics, Georg-August-Universität Göttingen

2nd referee:

Prof. Dr. Stefanie Pöggeler
Department of Genetics of Eukaryotic Microorganisms, Georg-August-Universität Göttingen

3rd referee:

Prof. Dr. Petr Karlovsky
Department of Molecular Phytopathology and Mycotoxin Research, Georg-August-Universität Göttingen

Further members of the examination board:

Prof. Dr. Rolf Daniel
Department of Genomic and Applied Microbiology, Georg-August-Universität Göttingen

Apl. Prof. Dr. Kai Heimel
Department of Molecular Microbiology and Genetics, Georg-August-Universität Göttingen

PD Dr. Michael Hoppert
Department of General Microbiology, Georg-August-Universität Göttingen

Date of oral examination: 14. 10. 2019

Declaration of independence

Herewith I declare that the dissertation entitled "**Precursors of epi-/shamixanthone formed in Hülle cells cause oxidative stress sensitivity and repress sexual development of the filamentous fungus *Aspergillus nidulans***" was written on my own and independently without any other aids and sources than indicated.

Li Liu

Göttingen 2019

This work was conducted in the group of Prof. Dr. Gerhard H. Braus at the Department of Molecular Microbiology and Genetics, Institute of Microbiology and Genetics, Georg- August-Universität Göttingen.

Parts of this work will be published in:

Li Liu, Jennifer Gerke, Rebekka Harting, Daniela Nordzieke, Gertrud Stahlhut, Brian Bannehr, Frank Kempken, Stefanie Pöggeler & Gerhard H. Braus (2019). Precursors of epi-/shamixanthone formed in Hülle cells cause oxidative stress sensitivity and repress sexual development of the filamentous fungus *Aspergillus nidulans*, in preparation.

Table of Contents

Summary **1**

Zusammenfassung **2**

1 Introduction **4**

1.1 The model organism *Aspergillus nidulans* **4**

1.1.1 Asexual development of *A. nidulans* 5

1.1.2 Sexual development of *A. nidulans* 6

1.1.2.1 Hülle cells 7

1.1.2.2 Cleistothecium 8

1.1.2.3 The regulation of *A. nidulans* sexual development 9

1.2 Secondary metabolites **12**

1.2.1 Categories of secondary metabolites 12

1.2.2 Biological functions in different organisms 13

1.2.2.1 The roles of secondary metabolites in interspecies interaction 13

1.2.2.2 The roles of secondary metabolites in intracellular regulation 14

1.2.3 The potential of fungal secondary metabolites for human society 15

1.2.4 Secondary metabolites in *A. nidulans* 16

1.2.4.1 The polyketide synthase *mdp/xpt* gene clusters in *A. nidulans* 17

1.3 Correlation of fungal development and secondary metabolism **23**

1.4 The aim of this work **26**

2 Materials and Methods **28**

2.1 Materials **28**

2.1.1 Reagents and materials 28

2.1.2 Strains, media and growth conditions 29

2.1.2.1 Bacterial strain and culture conditions 29

2.1.2.2 Fungal strains and culture conditions 29

2.2 Nucleic acid methods **31**

2.2.1 Plasmids and DNA fragments purification 31

2.2.2 Polymerase chain reaction 31

2.2.3 RNA purification and cDNA synthesis 32

2.2.4 Quantitative real-time polymerase chain reaction 32

2.3 The genetic manipulation of microorganisms **33**

2.3.1 Transformation of bacteria 33

2.3.2 Transformation of fungi 34

2.3.3 Plasmid construction for the genetic manipulation of fungi 35

2.3.3.1 Construction of *mdpG* overexpression strain 37

2.3.3.2 Construction of *mdp/xpt* deletion strains 37

2.3.3.3 Construction of *mdpG* and *mdpC* complementation strains 39

2.3.3.4 Construction of *sakA:gfp* strains 39

2.4 Southern hybridization 42

2.5 Secondary metabolites methods 46

2.5.1 Extraction of secondary metabolites 46

2.5.2 Separation of secondary metabolites by TLC 46

2.5.3 Identification of secondary metabolites by LC-MS 46

2.5.3 Relative quantification of secondary metabolites 47

2.6 Morphological and developmental analysis of *A. nidulans* 47

2.6.1 The productivity of conidiospores in the light 47

2.6.2 Analysis of viability of conidiospores 47

2.6.3 Analysis of germination of conidiospores 48

2.6.4 Monitor of sexual development under sexual growth conditions 48

2.6.5 Analysis of germination of Hülle nursing cells for sexual fruiting body formation 48

2.7 Protein methods 49

2.7.1 Protein extraction 49

2.7.2 SDS-PAGE and western hybridization 49

2.8 Stress tests 51

2.9 Bioactivity test of secondary metabolites 51

2.9.1 Secondary metabolites bioactivity of *mdp/xpt* clusters on fungi 51

2.9.2 Bioactivity of emodin on the egg laying activity of *Drosophila melanogaster* 52

3 Results 53

3.1 *A. nidulans mdp/xpt* secondary metabolite clusters produce emodins and benzophenones as intermediates resulting in epi-/shamixanthone as final products in Hülle cells during sexual development. 53

3.1.1 The *mdp/xpt* clusters produce emodins and benzophenones as intermediates resulting in epi-/shamixanthone as final products. 53

3.1.2 The *mdp/xpt* clusters derived metabolites are localized in Hülle cells 61

3.2 Precursors of epi-/shamixanthone repress sexual but not asexual development initially independent of the MAPK pheromone pathway or the velvet complex. 65

3.2.1 Precursors of epi-/shamixanthone mediated specific repression of sexual development in *A. nidulans* without an impact on vegetative growth or asexual development. 65

3.2.2 Repression of fruiting body maturation by epi-/shamixanthone precursors is independent of velvet gene expression and MAP kinase protein expression 72

3.3 Precursors of epi-/shamixanthone cause oxidative and weak acidic stress sensitivity and disturb reproduction of other fungi and flies. 75

3.3.1 Increased amounts of epi-/shamixanthone precursors cause oxidative and weak acidic stress sensitivity 75
3.3.2 Precursors of epi-/shamixanthone have a broad bioactivity on development of different fungi and fly egg depositing behavior. 78

4 Discussion.....83

4.1 Products of *mdp/xpt* clusters are localized in Hülle cells. 87

4.2 Precursors of epi-/shamixanthone repress sexual development of *A. nidulans*. 88

4.2.1 Emodins are the main factors of sexual development repression. 88
4.2.2 The repression of sexual development is independent of MAPK pheromone pathways or the velvet complex.....90

4.3 Increased amounts of epi-/shamixanthone precursors cause oxidative and weak acidic stress sensitivity. 93

4.4 Precursors of epi-/shamixanthone have a broad bioactivity on other organisms. 94

4.4.1 Repression of *Verticillium* spp. resting structure formation. 94
4.4.2 Repression of *S. macrospora* reproduction.....96
4.4.4 Repression of fly egg laying activity 97

4.5 Conclusion and outlook 98

References 104

List of abbreviations 122

Table of figures.....124

List of tables.....126

Acknowledgements 127

Summary

Fungal secondary metabolites are small molecular products that are not directly involved in survival but play a role as a reaction to environmental changes including multiple chemical structures and bioactivities. Fungal secondary metabolism and developmental programs are interconnected. The aim of this thesis was to analyze the biological activity of the *mdp/xpt* clusters derived metabolites in the sexual development of the filamentous soil fungus *Aspergillus nidulans*. This work firstly elucidated the negative effect of secondary metabolites derived by the polyketide synthase (PKS) encoding *mdp/xpt* gene clusters on sexual fruiting body maturation in *Aspergillus nidulans*. The *mdp/xpt* gene clusters derived intermediates such as emodins and benzophenones as well as the final products epi-/shamixanthone are produced during sexual development. The PKS MdpG and the other four members MdpH, MdpL, XptB and XptC are localized in sexual mycelia and Hülle cells. To obtain more insights about the metabolites derived by this clusters and their functions, the intact epi-/shamixanthone biosynthetic pathway was disrupted by deleting the PKS encoding gene *mdpG* and the biosynthetically following seven genes *mdpF*, *mdpC*, *mdpL*, *mdpD*, *xptA*, *xptB* and *xptC* separately. Deletion of the genes *mdpG* and *mdpF*, encoding the first two enzymes in the biosynthetic pathway, lost the yellowish products present in wild type during sexual developement, resulting in pale Hülle cells. Deletion of the genes *mdpC*, *mdpL*, *mdpD*, *xptA* and *xptB* resulted in the accumulation of various precursors of epi-/shamixanthone in Hülle cells. This led to smaller Hülle cells with reduced activity and a delayed maturation of sexual fruiting bodies. All five deletion strains were more sensitive to abiotic oxidative and weak acidic stress. All of them showed no remarkable changes in vegetative growth and the production and viability of asexual spores. The accumulated intermediates mainly consist of emodin and its derivatives, benzophenone-derived compounds, and xanthone derivatives. Therein, the most abundant and active ingredients are emodin and its derivatives particularly accumulated in Δ*mdpC* and Δ*mdpL* strains resulting in the strongest effect on Hülle cells and sexual fruiting bodies. They exhibited a broad bioactivity on other organisms, suppressing the resting structure formation of *Verticillum* sp., the fruiting body formation of *Sordaria macrospora*, and the egg-laying activity of *Drosophila melanogaster*. In summary, increased amounts of precursors of epi-/shamixanthone derived by *mdp/xpt* gene clusters, in particular emodin and its derivatives, repressed the development of cleistothecia and Hülle cells of *Aspergillus nidulans* and the formation of resting and reproductive structures of other fungi and insects.

Zusammenfassung

Pilzliche Sekundärmetaboliten sind kleine molekulare Produkte, welche nicht direkt zum Lebenserhalt beitragen, jedoch eine entscheidende Rolle bei der Anpassung an verschiedenste Umweltveränderungen spielen und wegen ihrer Struktur und bioaktiven Diversität auf ein großes Interesse in der Forschung stoßen. In der Regel sind sekundärmetabolische Prozesse mit den Entwicklungsprogrammen des Pilzes verbunden. Im Rahmen dieser Arbeit wurden Sekundärmetabolite identifiziert, welche die Entwicklung von Cleistothecien als sexuelle Fruchtkörper und Überdauerungsstrukturen des filamentösen Pilzes *Aspergillus nidulans* regulieren. Es wurde der Einfluss der Sekundärmetaboliten, welche durch das Polyketidsynthase- (PKS-) kodierende *mdp/xpt* Gen-Cluster produziert werden, auf die Fruchtkörperentwicklung im Modelorganismus *Aspergillus nidulans* untersucht. Frühere Untersuchungen ergaben, dass das *mdp/xpt*-Gencluster Emodin- und Benzophenon-Derivate als Zwischenprodukte, sowie Xanthone als Endprodukte während der sexuellen Entwicklung bilden, und dass die PKS MdpG sowie vier weitere vom Cluster produzierte Proteine, MdpH, MdpL, XptB und XptC, sowohl im sexuell entwickelten Myzel, als auch in Hülle-Zellen lokalisiert sind. Um weitere Informationen über diese Metaboliten und ihre Funktionen zu gewinnen, wurde der Xanthon-Stoffwechselweg durch die Deletion des PKS-kodierenden Gens *mdpG* und der biosynthetisch darauffolgenden sieben Gene *mdpF*, *mdpC*, *mdpL*, *mdpD*, *xptA*, *xptB* und *xptC* unterbrochen. Die Deletionen der Gene *mdpG* und *mdpF*, die die ersten beiden Enzyme im Biosyntheseweg codieren, resultierten im Verlust der gelben Pigmentbildung der Hülle-Zellen. Die Deletion der Gene *mdpC*, *mdpL*, *mdpD*, *xptA* und *xptB* führte zur Akkumulation verschiedener Xanthon-Vorläufer in Hülle-Zellen, welche sich durch kleinere Hülle-Zellen mit reduzierter Aktivität und einer verzögerten Reifung der sexuellen Fruchtkörper äußerte. Diese fünf Deletionsstämme waren empfindlicher gegenüber abiotischem oxidativem und schwach-saurem Stress. Keiner der Deletionsstämme zeigte signifikante Veränderungen im vegetativen Wachstum und in der Produktion und Lebensfähigkeit von asexuellen Sporen. Die akkumulierten Zwischenprodukte bestanden hauptsächlich aus Emodin und Emodin-Derivaten, von Benzophenon abgeleiteten Verbindungen und Xanthonderivaten. Hierbei ist eine besonders hohe Ansammlung von Emodin und seinen Derivaten im Δ*mdpC*- und Δ*mdpL*-Stamm zu vermerken, was zu der stärksten Wirkung auf Hülle-Zellen und Fruchtkörper führte. Auch in anderen Organismen hatte die Akkumulierung von Emodin und seinen Derivaten einen Einfluss auf Entwicklungsprozesse und Wachstum, welcher sich in der verringerten Produktion persistierender Überlebensstrukturen in *Verticillium* sp., verringertem und Fruchtkörperbildung

in *Sordaria macrospora* und der verringerten Eiablagetätigkeit von *Drosophila melanogaster* äußerte.

Zusammenfassend hemmen erhöhte Mengen der Vorläufer von Epi-/Shamixanthone vom *mdp*/*xpt* Gencluster, insbesondere Emodin und dessen Derivate, die Entwicklung von Cleistothecien und Hülle Zellen von *Aspergillus nidulans*. Ebenso unterdrücken sie die Bildung von reproduktiven und zur Überdauerung dienenden Strukturen von anderen Pilzen und Insekten.

1 Introduction

1.1 The model organism *Aspergillus nidulans*

Aspergillus nidulans is one of many species of filamentous fungi in the phylum Ascomycota. It is a fast-growing, ubiquitous saprophytic soil fungus and not very selective with respect to abiotic growth conditions. For instance, it can grow over a wide range of temperature (6-51°C) and a wide range of pH (2-12) (Krijgsheld *et al.*, 2013). Since 1953 introduced by Guido Pontecorvo and co-workers (Pontecorvo *et al.*, 1953) and due to its haploid, homothallic growth, it has been considered as an important research model organism for studying eukaryotic cell biology. It has been widely used to understand genetic recombination, DNA repair, mutation, cell cycle control, multicellular development, tubulin, chromatin, nucleokinesis, pathogenesis, primary and secondary metabolism, compounds heterologous production and experimental evolution (Frandsen *et al.*, 2018, Nierman *et al.*, 2005, Park *et al.*, 2019, Schoustra *et al.*, 2005, Etxebeste *et al*., 2019). Its complete genome has been sequenced in 2003 and revealed that it is 31 million base pairs in size and predicted to contain around 10,687 protein-coding genes on eight chromosomes (Arnaud *et al.*, 2012, Galagan *et al.*, 2005). This well-annotated genome resource facilitates the research work to the molecular level and builds a well-developed genetic system.

A. nidulans possesses a well-characterized life cycle (Park *et al*., 2019). After spore germination, a network of vegetative hyphae develops and then it can undergo two different developmental programs. When the fungus is cultivated on surface and exposed to air with enough oxygen and light, asexual development is induced forming conidiophores with asexual spores (conidia). When the fungus is cultivated in dark with low oxygen levels and nutrient, sexual development is induced. Its sexual development can also be triggered by pheromones or cellular redox status. It forms sexual fruiting bodies as overwintering structures, called cleistothecia, with sexual spores (ascospores) (Fig. 1). These two different developmental programs are not separated but coexisting. During asexual development, it can form sexual fruiting bodies, while, during sexual development, it can also form asexual structures lately. The differentiation and regulation between these two developmental pathways are controlled by multiple regulators including the trimeric velvet complex consisting of velvet domain proteins velvet A (VeA), velvet-like B

(VelB) and the methyltransferase LaeA (lack of aflR expression A). LaeA is a global regulator of secondary metabolism and development (Bayram *et al.*, 2010). *A. nidulans* is able to self-fertilize and form fruiting bodies in the absence of a mating partner and form sexual spores through meiosis. This allows crossing of strains in the laboratory.

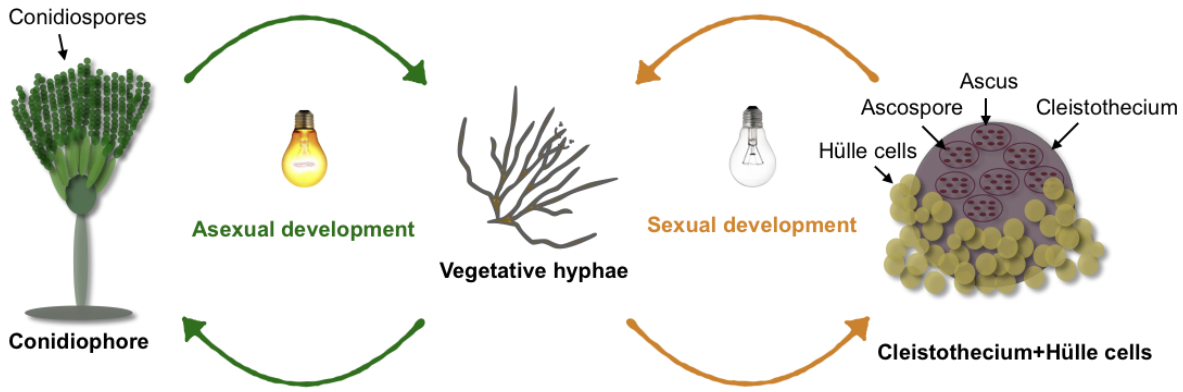

Figure 1. Life cycles of *A. nidulans*.
Asexual development (left hand side) in *A. nidulans* begins with superficial hyphae, which are exposed to the atmosphere and light. This initiates a sequence of developmental changes leading to the formation of conidiophores. Approximately 35 h after inoculation at 37°C, conidiophores are mature and carry green conidiospores (Etxebeste *et al.*, 2010a). Sexual development (right hand side) is triggered by environmental and endogenous factors like low nutrient, low oxygen, darkness, pheromones or cellular redox status. The sexual tissue Hülle cells differentiate from hyphae forming a nest-like structure around the developing cleistothecium. After 120 h, a cleistothecium is mature with a pigmented shell and reddish ascospores inside (Busch *et al.*, 2007).

1.1.1 Asexual development of *A. nidulans*

Colonies of *A. nidulans* are constituted by apically growing pluripotent hyphae that extend away from germination points. When these superficial hyphae are exposed to air and light, they initiate a sequence of morphological changes leading to the formation of the conidiophores, which bear green asexual spores. The process starts from vegetative hyphae to apical cell swelling and subapical branching, to metulae and phialide formation, which continuously generate conidia (Ugalde *et al.*, 2007). Every single stage is activated and regulated by certain regulators. Previous findings already identified over 20 regulators for the whole developmental pathway (Etxebeste *et al.*, 2010b).

For example, in the early response to the environmental changes, the scaffold protein VeA plays a key role in transduction of the light signal. VeA interacts with the red-light receptor, FphA.

This protein interacts with the blue-light-sensing protein apparatus, LreA and LreB (Purschwitz *et al.*, 2008). This large protein complex senses red and blue light from the environment and initiates asexual development. The functional FluG (fluffy G) protein is a derepressor of SfgA (suppressor of *fluG* A), what releases the repression of the downstream transcriptional activators FlbD, FlbC, FlbB (fluffy low *brlA* D, C and B), and BrlA (encoded by *bristle* gene *brlA*) necessary for normal conidiation (Seo *et al.*, 2005). As the central regulator of phialide formation and conidia production, BrlA controls the expression of a number of downstream conidiation-specific genes including *abaA* (*abacus A*) and *wetA* (*wet-white A*) (Ojeda-López *et al.*, 2018). AbaA regulates its own expression in metula and phialide (Andrianopoulos *et al.*, 1994), whereas WetA is required for the conidia pigmentation and integrity (Sewall *et al.*, 1990). An additional actor is VosA (viability of spores A), which is essential for spore maturation and trehalose production (Ni *et al.*, 2007). VosA is expressed during the spore formation and plays a dual role as a putative activator of *wetA* and as a repressor of *brlA*. Furthermore, VosA interacts with VeA-VelB dimer involved in initial stages of asexual developmental induction (Bayram *et al.*, 2008).

Available evidence indicates that environmental abiotic stimuli such as osmotic stress (Vargas-Pérez *et al.*, 2007), and carbon or nitrogen starvation (Skromne *et al.*, 1995, Wang *et al.*, 2019) can also be integrated into single or multiple signals that shut down vegetative growth and initiate conidiophore development. The interrelationships between molecular and morphological changes open new avenues for interpretation of these modes of action.

1.1.2 Sexual development of *A. nidulans*

About one-third of the described Aspergillus species have a known sexual stage (Geiser, 2009). Aspergillus with a sexual stage can be either self fertile (homothallic) or require a partner (heterothallic) (Ojeda-López *et al.*, 2018). *A. nidulans* is known to be homothallic and can form fruiting bodies with or without a partner (Paoletti *et al.*, 2007). The sexual development of *A. nidulans* is influenced by both environmental and intrinsic signals. It starts after 18-20 h of cultivation at 37°C with the first sign of sexual development- Hülle cells production. A dikaryon is formed by hyphal fusion and surrounded by a nest of Hülle cells. The cleistothecial shell is

developed and nuclear fusion takes place inside, which means the young asci formation. The following processes are meiosis and post-meiotic mitosis resulting in eight nuclei. These nuclei are then separated from each other by membrane, giving rise to eight red spores in each of the 10,000 asci within one fruiting body (Pöggeler *et al.*, 2006).

1.1.2.1 Hülle cells

Hülle cells are large (ca. 5-40 µm diameter), thick-walled, multinucleate (a volume 20x that of normal nuclei) (Fig. 2) and have long been described to "nurse" the cleistothecium during development (Nahlik *et al.*, 2010). In recent years, further evidence contributed to elucidate their biologic functions, such as the production of α-1,3 glucanase in Hülle cells that mobilizes carbon sources for fruiting body development (Wei *et al.*, 2001). Hülle cells also exhibit the activity of laccase II and chitin synthase (Bayram *et al.*, 2012b, Lee *et al.*, 2005), which are required for cleistothecial shell pigments and cell wall formation (Hermann *et al.*, 1983). The accumulation of laccase II enzyme in Hülle cells leads to strong phenoloxidase activity and the formation of multiple reactive oxygen species (ROS) (Siegmund *et al.*, 2015). ROS represent an essential endogenous signals that are required for further development of cleistothecia (Lara-Ortíz *et al.*, 2003, Gulko *et al.*, 2018). The *noxA* gene encoding NADPH oxidase of *A. nidulans* produces ROS induced at the start of sexual development. Suppression of Nox enzymes results in a ROS decrease in the accumulation of Hülle cells and cleistothecial precursors (primordia). ROS, however, are toxic to cells. Hülle cells produce increased catalase, peroxidases or superoxide dismutase activities to cope with the increased ROS formation. Additionally, the normal formation and development of cleistothecia are depending on Hülle cells. The methyltransferase LaeA deficient mutant strain can just produce 2-5 Hülle cells surrounding the cleistothecium, which resulted in significantly smaller cleistothecia (ca. 40 µm diameter) in comparison to wild type (ca. 200 µm diameter) (Bayram *et al.*, 2010). Indeed, the initial developmental program related to Hülle cell production can proceed independently of the subsequent cleistothecia and ascospores production. For instance, a CsnE (COP9 signalosome) null mutant strain is capable of initiating Hülle cell production and develops the precursor cleistothecia- primordia, but maturation to sexual fruiting bodies is blocked (Busch

et al., 2003). This fact emphasizes that Hülle cells are essential for cleistothecia and ascospores formation, but they are regulated by independent pathways. Hülle cells are not just cleistothecia nursing cells but can also germinate to initiate growth of new hyphae (Ellis *et al.*, 1973). Adult Hülle cells harbor several nuclei, mitochondria, lipid bodies and storage products. When detached from subtending hyphae, Hülle cells can germinate new hyphae and form conidiophores with asexual spores (Dr. Danielle M. Troppens, personal communication).

Figure 2. Detached Hülle cells of *A. nidulans*.
Photomicrograph of *A. nidulans* Hülle cells after three days of sexual development. Hülle cells are globose shaped with a thick cell wall. The cell wall is open on one side, where it is connected to hyphae. Scale bar = 10 µm.

1.1.2.2 Cleistothecium

In *A. nidulans*, the cleistothecium is the container of ascospores and is a globose, darkly pigmented structure of 100-200 µm in diameter (Scazzocchio, 2009). Cleistothecium formation of *A. nidulans* is initiated with two separate hyphal branches coiled together to form a simple and loose structure, also named cleistothecial initials, at the very early stage (Sohn *et al.*, 2002). With the increased number of turns of the wrapping coils, the core cell of initials also enlarged with multinucleate, thus form a tighter and more complete investment. At this stage, Hülle cells appear in the vicinity of cleistothecial initials. Along with the hyphal wrapping (peridium) becoming pseudoparenchymatous, the number of peridial layers is increased in the median section of cleistothecial initials. With the increasing size of the peridium, peridial layer is further increased, and peridium is surrounded with numerous aerial hyphae and Hülle cells. When the young cleistothecium grow up to approximately 100 µm in diameter, the centrum portion start

to form ascogenous cells. Spontaneously, the inner peridial layers are reduced. At this stage, the cleistothecium is wrapped by numerous Hülle cells (Fig. 3) and the shell become more and more dark. At the late stage of the cleistothecium development, the peridium just is composed of two layers of flattened cells with dark pigmented smooth surface, and abundant matured ascospores inside.

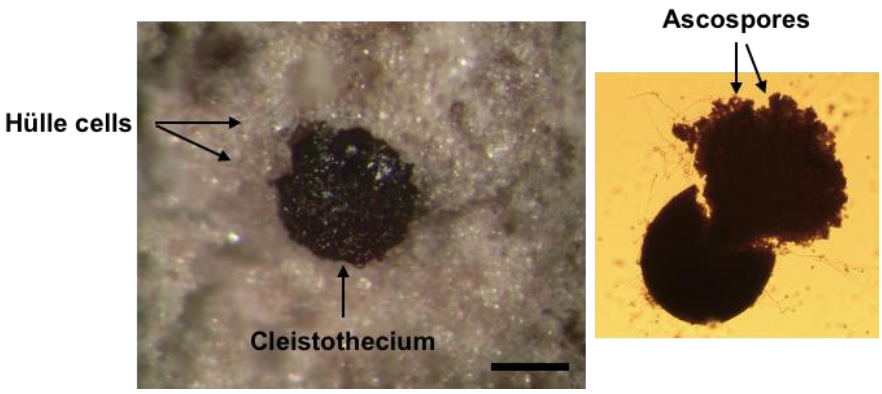

Figure 3. Sexual structure of *A. nidulans*.

Photomicrograph of sexual structure of *A. nidulans* after five days of sexual development. Transparent bubble-shaped cells are Hülle cells and the centre dark pigmented structure is a cleistothecium (left hand side). Part of Hülle cells were stripped to make the cleistothecium more visible. Scale bar = 100 µm. The cleistothecium is the closed type of sexual fruiting body containing about ten thousand of ascospores inside (Pöggeler *et al*., 2006). The image on the right shows the naked manually opened cleistothecium and released ascospores.

1.1.2.3 The regulation of *A. nidulans* sexual development

Fungal sexual development provides a complex, diverse, and intriguing system to study tissue differentiation in eukaryotes. As mentioned above, these complex processes are regulated by both environmental and intrinsic signals and rely on very strictly regulated gene, protein, and metabolite pathways (Wilson *et al*., 2019). The environmental factors include the absence of light, nutrients and pH of the growth medium, the presence of atmospheric gases and temperature (Dyer *et al.*, 2012). In general, the balance of the carbon/nitrogen ratio is critical for the organism's growth. A slight increase in carbon and a decrease in nitrogen can favor cleistothecia development (Swart *et al.*, 2001). Meanwhile, phosphorus and manganese ions also influence cleistothecia development (Bussink *et al.*, 1998). Development of cleistothecia normally only occurs on an air interface. This is commonly achieved in the laboratory by cultivating the fungus on agar medium plates, which are sealed by parafilm to enrich carbon

dioxide and reduce oxygen levels to further induce the sexual development. As carbon dioxide is needed for both the synthesis and breakdown of α-1,3 glucan, a lack of carbon dioxide reduces cleistothecia production (Zonneveld, 1988). Plate sealing also reduces the oxygen concentration, partly blocks the electron transport system and entry into the sexual cycle (Han *et al.*, 2003a). Nitric oxide also has been shown to promote cleistothecia production (Baidya *et al.*, 2011). For initiation of sexual development, from environmental stimuli to intrinsic regulation, serious signal transduction pathways are required.

For intrinsic regulation, multiple transcriptional regulators and proteins balance the asexual/sexual development (Fig. 4). The well-known and characterized regulators are velvet complex members (VeA-VelB heterodimer with the methyltransferase LaeA), the interaction and localization patterns of which can control developmental pathway (Bayram *et al.*, 2012b). NsdD (never in sexual development D) is a sexual development regulator, crucial for cleistothecia production and a repressor of the asexual regulator encoding gene *brlA* (Han *et al.*, 2003b, Han *et al.*, 2001, Lee *et al.*, 2014). The stunted protein StuA is a morphological modifier required for the early stage of asexual reproduction until completion of conidiophore development but not for differentiation of conidia (Miller *et al.*, 1991, Park *et al.*, 2014). Mario Schere and co-workers also found that StuA can regulate the transcriptional activation of the catalase-peroxidase gene (*cpeA*) gene, which is especially expressed in Hülle cells during early sexual development (Scherer *et al.*, 2002). A putative helix-loop-helix (HLH)-type regulator, UrdA, is a negative regulator of sexual development and sterigmatocystin production (Pandit *et al.*, 2018). Deletion of the gene *urdA* induced the expression of sexual regulator genes, *steA*, *nsdD* and *veA*, which induced the sexual fruiting body formation finally. SakA, a member of the Hog1/Spc1/p38 MAPK family, regulates fungal sexual development by repressing the transcription of genes needed for cleistothecia in *A. nidulans* (Furukawa *et al.*, 2005, Kawasaki *et al.*, 2002, Lara-Ortíz *et al.*, 2003). SakA null mutant displays premature *steA*-dependent sexual development. High mobility group box (HMGB), chromatin-associate architecture proteins, are also involved in sexual development of *A. nidulans* (Bokor *et al.*, 2019). Deletion of HMGB encoding genes, namely *hmbA*, *hmbB* and *hmbC*, extremely down-regulated the expression of mating-type coding genes (*matA* and *matB*), which resulted in deficient ascospore

production and viability. HmbA and HmbB play a role in response to environmental signals, while HmbC functionally interacts with VeA, a key regulator of the coordination of asexual and sexual development, as well as of secondary metabolism.

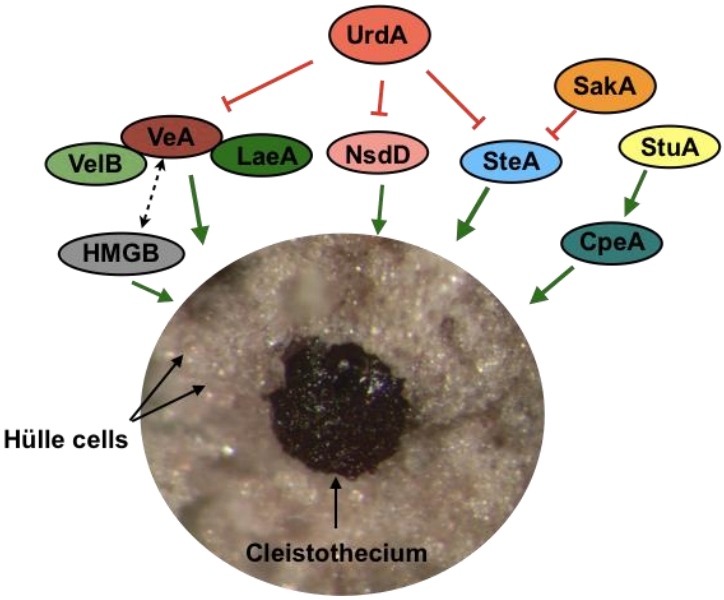

Figure 4. The sexual development regulatory network in *A. nidulans*.
Under sexual growth conditions, the velvet complex VelB-VeA-LaeA triggers the gene expression required for sexual development. VeA functionally interacts with one of the HMGB members HmbC to regulate sexual development in *A. nidulans*. The protein UrdA is a negative regulator of sexual development through repressing the gene expression of *veA*, *nsdD* and *steA*. The MAP kinase SakA is activated in response to osmotic stress and reduces the activity of the transcription factor SteA, which is a positive regulator of sexual development in *A. nidulans*. StuA is required for expressing the catalase CpeA encoding gene *cpeA*, which is especially expressed in Hülle cells at the early stage of sexual development. The positive regulatory influences are shown in green, negative regulatory influences in red and functional interaction is shown in black dashed. Summarized from Bayram *et al.*, 2012b, Bokor *et al*., 2019, Han *et al*., 2003b, Han *et al*., 2001, Lee *et al*., 2014, Miller *et al*., 1991, Scherer *et al*., 2002, Pandit *et al*., 2018, Furukawa *et al*., 2005, Kawasaki *et al*., 2002 and Lara-Ortíz *et al*., 2003.

In summary, sexual development of *A. nidulans* is transited from vegetative hyphae to multicellular fruiting bodies, which is activated by development triggers, and then sensed by G-protein coupled receptors and transduced by G-proteins, kinases and transcription factors. In post-transcription stage, protein modification and degradation also play important roles in sexual development. On other layers, metabolism, cytoskeleton and cell wall construction are essential for fruiting body formation (Busch *et al.*, 2007).

1.2 Secondary metabolites

Secondary metabolites (SMs) are low molecular weight organic compounds produced by certain fungi, plants, bacteria, and a small number of invertebrate and vertebrate animals (Bainbridge, 1989, Bills *et al.*, 2016, Croteau *et al.*, 2000, Giovannini *et al.*, 1987, Myers *et al.*, 1983, Zasloff, 1987). Due to their occurrence, they are also called natural products. Unlike primary metabolites, they are not directly involved in the survival of the producing organisms. Absence of secondary metabolites does not result in immediate death, but rather in long-term impairment of the organism's survivability, fertility, or aesthetics. The reasons for the production of secondary metabolites have been discussed and investigated over decades. The various hypotheses range from genetic mutations and evolution in progress to waste or detoxification products from metabolism and a measure of the fitness of the organism to survive (Firn *et al.*, 2000, Haslam, 1986, Wink, 2003, Holighaus *et al*., 2019).

1.2.1 Categories of secondary metabolites

All reactions of secondary metabolism use ubiquitous intermediates of primary metabolism to produce a large body of natural products. These products are structurally and functionally diverse. One hypothesis is the structure-function hypothesis: the function of a natural product is a direct consequence of its structure (Williams *et al.*, 1989, Teh *et al*., 2016). For instance, the absorbance of UV radiation is due to the presence of conjugated double bonds. Antioxidant and antiradical properties are governed by the availability of -OH, -NH_2, and -SH groups, aromatic nucleus and unsaturated aliphatic chains. The presence of -COOH, -OH, -NH_2, mono-, O-diphenol-, and O-quinoid groups allows polymerization, condensation and complexation, which provide the structure-stabilizing, antimicrobial and hypersensitive response activities. Based on this fundamental theory and biosynthesis and occurrence, secondary metabolites can be roughly categorized into alkaloids, terpenoids, flavonoids, natural phenols, polyketides, nonribosomal peptides, *etc*. For large and complex molecules, it is difficult to ascribe them to one class, because they can be synthesized by a combination of various biosynthetic pathways with various functional groups.

1.2.2 Biological functions in different organisms

The high structural diversity of secondary metabolites has puzzled researchers for some time. More than 100 years ago, most botanists speculated that secondary metabolites were waste products of primary metabolism or detoxification products and their structural diversity only reflected a play of nature. Today, more adaptive explanations facilitate us to understand the existence and the diversity of secondary metabolites (Haslam, 1986, Williams *et al.*, 1989, Wink, 2003, Wink *et al.*, 2018). There are two typical hypothetical functions now widely accepted that the main role of many secondary metabolites as chemical defense and signal compounds benefit the host organism in interspecies interaction and intracellular regulation (Vining, 1990, Wink, 2003, Wink *et al.*, 2018).

1.2.2.1 The roles of secondary metabolites in interspecies interaction

Plants and fungi are sessile organisms and cannot run away when they are attacked by insects, vertebrate herbivore, fungivore, or even surrounding competitors, nor have an immune system to rely on. In order to survive, these organisms have developed defense strategies. Therefore, interspecies antagonism is commonly happening in every natural niche. A large body of experimental, toxicological data and circumstantial evidence support the view that many secondary metabolites (SMs) are toxic or deterrent to animals, and display antibiotic or even allelopathic activities (Wink *et al.*, 2018). The structurally diverse SMs have a wide spectrum of targets. SMs can interact with proteins by changing conformation to inactivate their bioactivity, intercalate DNA to cause mutations, interfere with biomembranes to induce cell death, and modulate signal transduction by interfering with ion channels, monoamine oxidase and other enzymes related to signal transduction pathways.

In filamentous fungi, interspecies antagonism can occur over a distance or at hyphae contact level (Hiscox *et al.*, 2018). Over a distance, many fungi can produce volatile or diffusible organic compounds (VOCs and DOCs), some of which possess antibiotic or antifungal activity to inhibit growth of competitors (Holighaus *et al.*, 2019, Hynes *et al.*, 2007). For example, *Escovopsis weberi* strongly inhibits the growth of the garden fungus *Leucoagaricus gongylophorous* without direct contact by producing cycloarthropsone and emodin, and its

emodin is also active against *Streptomyces* microbial symbionts of ants (Dhodary *et al*., 2018). At hyphae contact level, VOCs and DOCs may alter qualitatively and quantitatively, and toxic SMs may be produced (El Ariebi *et al.*, 2016).

However, organisms also need to cooperate with neighboring organisms to improve their survival and/or fitness. In these cases, SMs can act as signal compounds to attract or communicate with insects, microbes, host, *etc*. For example, the plant SMs fragrant monoterpenes, coloured anthocyanins or carotenoids can serve to attract animals for pollination or seed dispersal (Wink, 2003).

1.2.2.2 The roles of secondary metabolites in intracellular regulation

Above mentioned are extrinsic functions of secondary metabolites. Many secondary metabolites also possess various intrinsic functions by incorporating the SMs into developmental structures or function as signals to initiate developmental programs (Keller, 2018). Secondary metabolites can act as substrate storages for cell cycle or as structural components (Barber *et al.*, 1988, Bu'lock, 1967). Some of the excreted SMs have a role in the uptake of available trace elements by chelating iron from surroundings (Weinberg, 1969, Winkelmann, 1986, Burnside *et al*., 2019). For instance, the siderophore rhizoferrin is capable of binding iron and promoting the growth of *Legionella pneumophila* in iron-limited media (Cianciotto *et al*., 2015). SMs can also serve as differentiation signals to modulate cellular metabolism and development. For instance, fungal SMs as hormones induce fruiting body formation or sporulation (Manoil *et al.*, 1980, Rodríguez-Urra *et al.*, 2012) or protect spores and/or inhibit germination (Allen, 1976, Calvo *et al.*, 2002, Demain *et al.*, 2000, Khalid *et al.*, 2017, Murrell, 1981). Several SMs required for the formation of fungal resting or sexual structures have been verified. Fusarubins are required for pigmentation of the perithecia in *Fusarium* species (Studt *et al.*, 2012). The anthraquinone asparasone A is the precursor of the sclerotial pigment (Calvo *et al.*, 2015). One PKS gene *pks4* is essential for *Sordaria macrospora* perithecial maturation (Schindler *et al.*, 2014).

Besides, many secondary metabolites possess protective functions in the adaptation of organisms to the changing environment and in coping with stress constrains. For instance,

DOPA-melanin produced by *A. nidulans* has photoprotective functions to protect the fungus from UV light-induced and oxidant-mediated damages (Gonçalves *et al.*, 2012). Flavonoids are endowed with high capability of ROS scavenging (Pietta, 2000, Sarker *et al*., 2018).

1.2.3 The potential of fungal secondary metabolites for human society

Nature produces an amazing variety and number of SM products. Countless of secondary metabolites have been characterized and are mainly produced by microbes and plants. Since last decades, SMs display a broad range of useful properties in pharmaceutical, food, cosmetic, and agricultural industry, *etc*. The traditional Chinese medicine has more than 2,500 years history by obtaining active metabolites from natural herbs to treat diseases (McNamara *et al.*, 1996, Wang *et al.*, 2008). Furthermore, by connecting with modern technologies and tools, traditional Chinese medicine provides useful databases for identifying novel drug candidates effectively. Microbial SMs display a broad range of useful activities for pharmaceutical purposes, such as antibiotics, antifungal, antivirals and antitumor activities. Exemplified best by the antibiotic penicillin, their introduction into clinical use saved countless lives (Miller, 2002). Other most famous fungal metabolites in successful clinical use include the antihypercholestemic drug lovastatin and its derivatives, the immunosuppressant cyclosporin and ergotamine (Misiek *et al.*, 2007). The chemical complexity of SMs, however, not only enriches the sources of drug candidates and medicinal design but also represents some obstacles in the production of pharmaceutical industry. Chemical synthesis is often difficult and expensive, and isolation from natural resources is typically in low yields. In recent years, more and more researchers focused on improving SMs mining and practical use. By heterologous expressing the putative SMs genes increase the interest in drug research and development. For instance, *Saccharomyces cerevisiae*, one of the most intensely studied eukaryotic model organisms, which hardly produces secondary metabolites on its own, produced as a heterologous host a large-scale commercial SMs as pharmaceuticals (Huang *et al.*, 2008). The growing rich density of knowledge about fungal or plant genetics, biochemistry, physiology, *etc.* makes them an overwhelming metabolic wealth for using SMs in the pharmaceutical industry.

SMs of plants and fungi are the major source of biologically active substances of the human diet. Vegetables, fruit and mushroom can provide rich nutritional SMs, which also enriched the food color, smell, and taste (Hounsome *et al.*, 2008). Due to the advantages of natural SMs, they are also be widely used in food or drink manufactures as flavoring compounds or colorants (Caputi *et al.*, 2011, Mapari *et al.*, 2010, Patakova, 2013). In cosmetic industry, new trends are extracting SMs from plant, algae or other microorganisms, or even from fish, meat and dairy products, as cosmetics active ingredients (Ariede *et al.*, 2017, Barbulova *et al.*, 2015, Kusumawati *et al.*, 2013).

Bioactive SMs also play important roles in agricultural management. The worldwide spread of crop pests and pathogens is a significant problem that results in large crop yield reduction and food and feeds contamination, which has adverse effects on humans and animals in health and economy. In the last decades, the agricultural management is facing the economic and ecological challenge. The widespread use of farm chemicals, although, can solve part of the problems, which also result in severe eco-environmental damage and the second contamination of the residues. As mentioned above, SMs can be treated as chemical weapons against competitors or predators for host organisms. These advantages inspired ecologically friendly insecticide, fungicide development. The natural SMs are used for effective and specific insecticide and fungicide design, while ensuring the economic and ecological sustainability (Bebber *et al.*, 2014, Hussein *et al.*, 2001, Rattan, 2010).

Unexpected functions of known or unknown secondary metabolites are continuously being unraveled, fulfilling some of the needs of the present day, and showing great promise for the future.

1.2.4 Secondary metabolites in *A. nidulans*

A. nidulans is also used as a model organism to investigate bioactive natural products. The antibiotic penicillin is produced by filamentous fungi from the species *Penicillium* and *Aspergillus* (Foster *et al.*, 1945). It has been produced industrially by *Penicillium chrysogenum* and widely used in the pharmaceutical industry over decades. However, its biosynthesis genetic regulations were identified in *A. nidulans*, because of its well characterized genetics, which

permits precise manipulation of the genome and genetic control of the biosynthesis of penicillin. In the genome of *A. nidulans* 248 genes are GO annotated for secondary metabolism (Inglis *et al.*, 2013). Secondary metabolite biosynthetic genes often occur in clusters and are expressed under certain conditions (Bouhired *et al.*, 2007, Palmer *et al.*, 2010). Typically, a secondary metabolite biosynthetic gene cluster harbors one or several "backbone" enzymes for the secondary metabolite biosynthetic process: polyketide synthase (PKS), non-ribosomal peptide synthetase (NRPS), polyketide synthase/non-ribosomal peptide synthetase hybrid (PKS-NRPS), prenyltransferase known as dimethylallyl tryptophan synthase (DMATS) and/or a diterpene synthase (DTS), and several "tailoring" genes. Predicted by SMURF and antiSMASH, *A. nidulans* has 71 non-redundant clusters, which contain 24 PKS/PKS-like/PKS hybrid clusters, 24 NRPS/NRPS-like clusters, 10 DMATS and DTS clusters as well as 4 putative gene clusters without PKS/NRPS backbone genes (Andersen *et al.*, 2013, Inglis *et al.*, 2013). Whereas, 24 out of 71 non-redundant clusters just have been determined in experiments. Their products include asperfuranone (Chiang *et al.*, 2009), asperthecin (Szewczyk *et al.*, 2008), aspyridone (Bergmann *et al.*, 2007), austinol/dehydroaustinol (Lo *et al.*, 2012), 2,4-dihydroxy-3-methyl-6-(2-oxopropyl) benzaldehyde (DHMBA) and F9775 (Gerke *et al.*, 2012b, Sanchez *et al.*, 2010), emericellamide (Chiang *et al.*, 2008), microperfuranone (Andersen *et al.*, 2013), monodictyphenone (Andersen *et al.*, 2013, Chiang *et al.*, 2010), penicillin (Martin, 1992), nidulanin A (Inglis *et al.*, 2013), sterigmatocystin (Brown *et al.*, 1996) and terriquinone (Bok *et al.*, 2006). More than half of the non-redundant clusters are still to be elucidated, which indicates that *A. nidulans* has a huge biosynthetic potential to identify novel secondary metabolites.

1.2.4.1 The polyketide synthase *mdp/xpt* gene clusters in *A. nidulans*

As mentioned above, *A. nidulans* has 71 non-redundant SMs clusters and almost 60% of its products and regulation mechanisms still remain veiled (Inglis *et al.*, 2013). This is due to the fact that most of the secondary metabolite genes are silent under normal growth conditions and/or the production level is below the detection limit of our current methods. Genome sequencing also showed that many of these clusters are located near the telomeres of

chromosomes (Keller, 2018, Macheleidt *et al.*, 2016), where transcription is normally controlled by epigenetic regulation, such as DNA methylation and histone deacetylation (Shwab *et al.*, 2007). Loss of the critical member CclA of COMPASS (complex associated with Set1) complex, which methylates the histone H3 (Mueller *et al.*, 2006), activated the expression of at least two secondary metabolites clusters (Bok *et al.*, 2009). One of the clusters is the *mdp* cluster, which is responsible for monodictyphenone, emodin and emodin derivatives production (Chiang *et al.*, 2010). The *mdp* cluster can also be activated by nitrogen and phosphorous limitation in growth conditions (Sarkar *et al.*, 2012). Recently, Grau and co-workers identified a conserved negative master regulator of secondary metabolites production, McrA, and a positive master regulator of secondary metabolism, LlmG (Grau *et al.*, 2019). Both, artificially downregulated McrA and upregulated LlmG result in increased production of emodins, chrysophanol, monodictyphenone and prenyl xanthone derived by the *mdp* cluster. Deletion of the gene *bagA* (Bcl-2 associated athanogene) up-regulated the production of metabolites, such as variecoxanthone A, monodictyphenone and 2, ω-hydroxyemodin, during sexual development in *Aspergillus nidulans* (Jain *et al*., 2018).

Table 1. Gene designation of *mdp/xpt* clusters of *Aspergillus nidulans* (Arnaud *et al*., 2012).

Systematic name	Gene designation	Putative function of encoding protein
AN10021	*mdpA*	regulatory gene
AN10049	*mdpB*	dehydratase
AN0146	*mdpC*	ketoreductase
AN0147	*mdpD*	monooxygenase
AN0148	*mdpE*	regulatory gene
AN0149	*mdpF*	Zn-dependent hydrolase
AN0150	*mdpG*	polyketide synthase
AN10022	*mdpH*	hypothetical protein
AN10035	*mdpI*	acyl-CoA synthase
AN10038	*mdpJ*	glutathione S transferase
AN10044	*mdpK*	oxidoreductase
AN10023	*mdpL*	Baeyer-Villiger oxidase
AN6784	*xptA*	prenyltransferase
AN12402	*xptB*	prenyltransferase
AN7998	*xptC*	GMC oxidoreductase

The *mdp* gene cluster consists of one nonreduced polyketide synthase (PKS) encoding gene *mdpG* as the backbone and 11 *mdp* tailoring genes (Table 1). MdpE, a putative AflR homolog, can activate the *mdp* gene cluster in the requirement of the coactivator MdpA. The PKS MdpG is localized at the first place in the biosynthetic pathway and catalyzes the starter units to form the octaketide. The hydrolase MdpF playing a role in the second step catalyzes polyketide, released from MdpG lacking a TE domain. Further spontaneous decarboxylation, dehydration and oxidation lead to the formation of the crucial intermediate emodin and its derivatives, 2, ω-hydroxyemodin and ω-hydroxyemodin. MdpK, MdpC, MdpB, and MdpL are involved in the biotransformation from emodin to monodictyphenone (Chiang *et al.*, 2010).

The following finding is that the *mdp* cluster is not ended and monodictyphenone and emodin are not the final products but the shunt ones. Another three genes *xptA*, *xptB* and *xptC* work together with the *mdp* cluster to synthesize other secondary metabolites. The whole *mdp/xpt* gene clusters consist of three subunits scattered in three different chromosomes (Fig. 5).

The monooxygenase MdpD hydroxylates the compound 1-hydroxy-6-methyl-8-hydroxy-methylxanthone derived from monodictyphenone for Xpt enzymes. Prenyltransferases XptB as the bridge connecting the Mdp and Xpt pathways forms the variecoxanthone A. This compound is further converted by another prenyltransferases XptA and oxidoreductase XptC to form emericellin and the final products shamixanthone and epishamixanthone (Fig. 6) (Sanchez *et al.*, 2011).

In addition to emodin, monodictyphenone and final products epi-/shamixanthone, there are a lot of shunt pathways occurring spontaneously. Atrochrysone carboxylic acid is unstable and converted into endocrocin. Emodin can be modified into ω-hydroxyemodin, chrysophanol and aloe-emodin. Pockrandt and co-workers also found two novel branches from chrysophanol to xanthones (Pockrandt *et al.*, 2012). MdpL and MdpJ converted chrysophanol into thiolester intermediate, and the oxidoreductase MdpK took it to undergo either a benzophenone alcohol pathway or the aldehyde arugosin F pathway. The benzophenone alcohol pathway is fused into the main pathway as mentioned above. Another is arugosin F pathway. Arugosin F is firstly formed. XptA converts it into Arugosin I, which is hydroxylated by MdpD to form arugosin H.

XptB furtherly converts arugosin H into arugosin A and B, and finally form the final shamixanthone and epishamixanthone (Fig. 6).

The intact *mdp*/*xpt* clusters has been identified harboring 15 genes (Table 1) and can produce over 33 compounds theoretically. Most of them are ubiquitous in plants and microbes and have a wide spectrum of bioactivities.

Monodictyphenone, 2-(2,6-dihydroxybenzoyl)-3-hydroxy-5-me-thylbenzoic acid, has been previously isolated from a marine fungus *Monodictys putredinis* (Krick *et al.*, 2007). Its benzophenone structure is related to sulochrin and balanol. The former, derived from the anthraquinone emodin (Couch *et al.*, 2004), is an inhibitor of the degranulation, activation and chemotaxis of eosinophils (Ohashi *et al.*, 1997). The latter is a potent inhibitor of the serine/threonine kinases protein kinase A and protein kinase C (Koide *et al.*, 1995). However, the bio-functions of monodictyphenone still need to be elucidated.

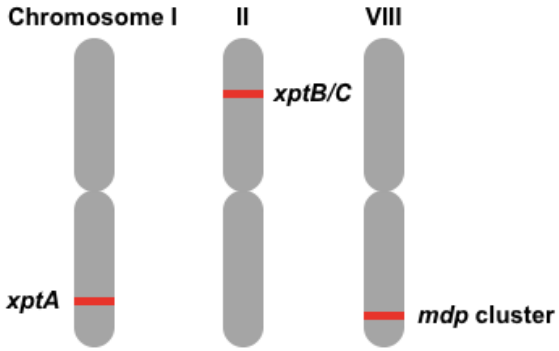

Figure 5. The chromosome locations of *mdp/xpt* clusters in *A. nidulans*.
Three subunits of the *mdp/xpt* clusters are scattered in three different chromosones. The gene *xptA* is localized in the chromosome I, the genes *xptB* and *xptC* are localized in the chromosome II and 12 *mdp* genes are localized in the chromosome VIII. Modified from Macheleidt *et al.*, 2016.

Emodin is commonly present in the roots and barks of numerous plants and an active ingredient of Chinese herbs including *Rheum officinale* and *polygonam cuspidatum* (Dorland, 2011, Xiao *et al.*, 1984, Won Jang *et al.*, 2018) but also produced as a secondary metabolite by molds and lichens (Wells *et al.*, 1975, Goga *et al.*, 2018). Researchers are deciphering the biological properties of emodin, such as genotoxic activity (Moreira *et al.*, 2018, Mueller *et al.*, 1999, Müller *et al.*, 1996), anti-inflammatory (Chang *et al.*, 1996, Park *et al.*, 2009), chemopreventive activity (Duvoix *et al.*, 2004, Koyama *et al.*, 2002), cell cycle inhibitory activity (Shieh *et al.*, 2004), protein kinases inhibitors (Jayasuriya *et al.*, 1992, Wang *et al.*, 2006, Xue *et al.*, 2015),

antitumor (Wang *et al.*, 2012, Wei *et al.*, 2013), inducer of apoptosis in tumor cells (Shieh *et al.*, 2004, Wang *et al.*, 2007), and inhibitor of key regulators in angiogenesis pathways and metastasis (Kwak *et al.*, 2006). It also efficiently acts as an agent controlling various cellular processes on molecular level, like interacting with protein, DNA and glutathione (GSH) (Panigrahi *et al.*, 2015a, Panigrahi *et al.*, 2015b, Panigrahi *et al.*, 2018, Srinivas *et al.*, 2007). Besides, current researches state that emodin, the main ingredient in fungal colorants, as the natural dye is used for the dyeing and printing of natural and synthetic fibers (Räisänen, 2019, Räisänen *et al.*, 2001). Emodin derivatives, ω-hydroxyemodin, chrysophanol, and aloe-emodin have also various bioactivities in microbes and mammalian cells. For instance, ω-hydroxyemodin possesses antibacterial activity by direct binding to the response regulator of quorum sensing (QS) resulting in reducing the virulence of *Staphylococcus aureus* (Daly *et al*., 2015); chrysophanol extracted from the root of *Colubrina greggii S.* Watson shows antimicrobial activity against *Bacillus subtilis* and *Staphylococcus aureus*, and it induces cancer cells death through increasing reactive oxygen species and decreasing the level of mitochondrial membrane potential (Chen *et al.*, 2004, Daly *et al.*, 2015, García-Sosa *et al.*, 2006, Lin *et al.*, 2006); aloe-emodin inhibits cell proliferation and induced G2/M arrest and apoptosis in mammalian cells (Chen *et al*., 2004, Quan *et al*., 2019).

Xanthones are dibenzo-γ-pyrone derivatives produced by higher plants, lichens and fungi (Masters *et al*., 2012, de Almeida *et al*., 2019, Chen *et al.*, 2018). Natural xanthones contain different substituents at various positions on the two benzene rings, thus resulting in large structure diversity, which means the potential to bind to a variety of targets. Hundreds of xanthones exhibit diverse biological and pharmacological activities, including antimicrobial, antioxidant, cytotoxic, and neuropharmacological activities (El-Seedi *et al.*, 2010). In many cases, activity is associated with prenylation of the xanthone skeleton (Pinto *et al.*, 2005). Ascomycetes, especially of the genera *Aspergillus* and *Penicillium*, are known producers of prenylated xanthones (Masters *et al.*, 2012). *A. nidulans* can produce at least 4 prenylated xanthones, variecoxanthon A, emericellin, shamixanthone and epishamixanthone, and also produce structurally related prenylated benzophenones, arugosins A, B, H and I (Sanchez *et al.*, 2011, Simpson, 2012).

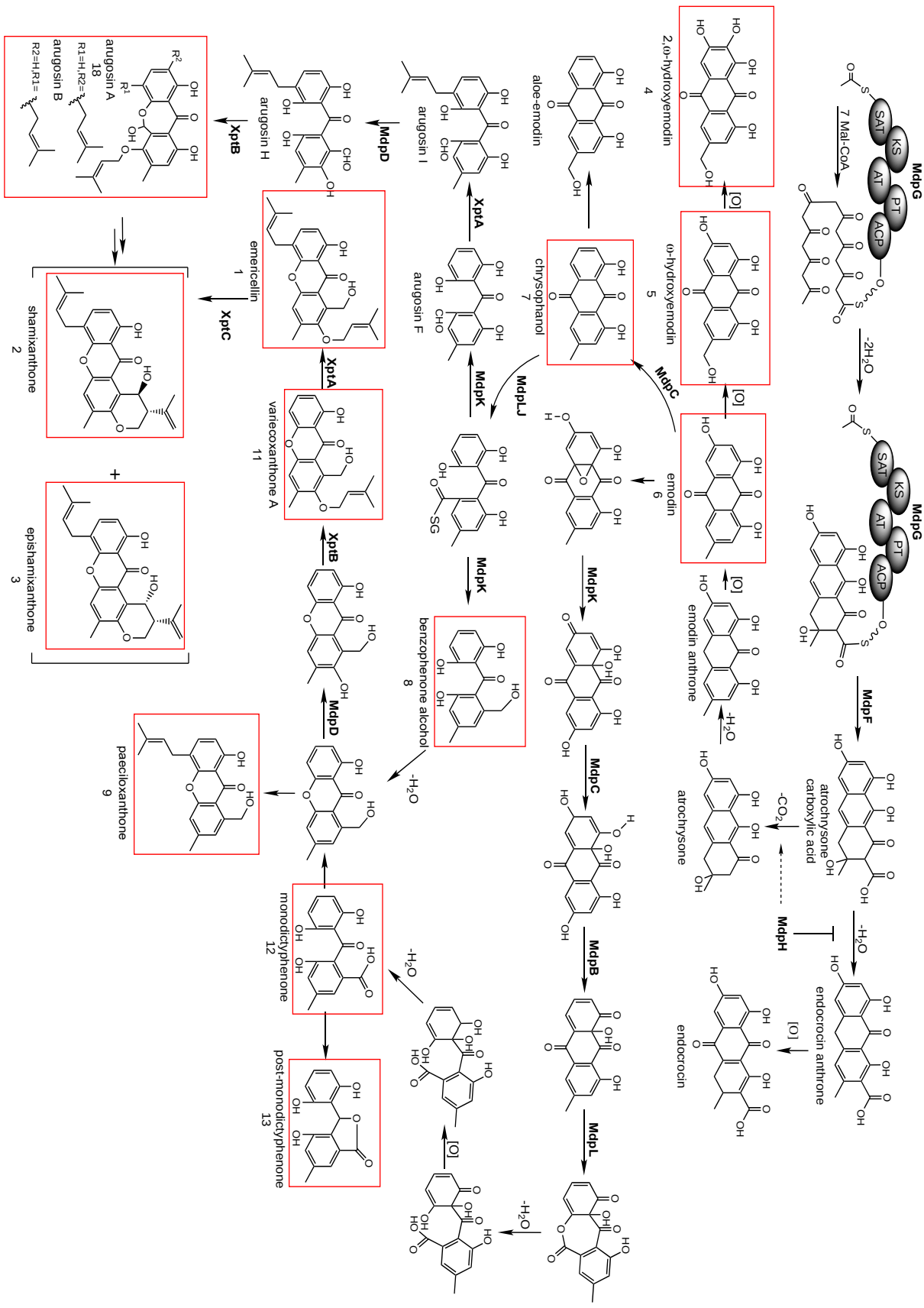

Figure 6. Proposed biosynthetic pathway of prenyl xanthones.

Modified from Chiang *et al.*, 2010, Pockrandt *et al.*, 2012 and Sanchez *et al.*, 2011. Compounds highlighted in red frames were detected in this study.

Furthermore, *mdpG* is known to influence the production of orsellinic acid, sterigmatocystin, and agnestins in *A. nidulans* and other fungi (Sarkar *et al.*, 2012, Simpson, 2012, Szwalbe *et al.*, 2019). According to bioinformatic analyses, monodictyphenone and epi-/shamixanthone biosynthetic processes are reasonably conserved in *A. fumigatus*, *A. niger* and *A. oryzae* (Inglis *et al.*, 2013).

1.3 Correlation of fungal development and secondary metabolism

Unlike primary metabolites, secondary metabolites are not directly required to ensure the growth of the organisms that produce them. SMs production is usually associated with cell differentiation or development, and in fact, most secondary metabolites are produced by organisms that exhibit special growth and have a relatively complex morphology (Calvo *et al.*, 2002). Their biosynthetic gene clusters are controlled by a complex regulatory network involving interconnected networks consisting of multiple proteins and complexes that respond to various abiotic and/or biotic stimuli (Brakhage, 2013, Collemare *et al*., 2019).

SMs can regulate fungal growth and development. For instance, linoleic-acid derived psi factors can induce sporulation and affect the asexual/sexual spore ratio in *A. nidulans* (Calvo *et al.*, 2001, EbrahimáEl-Zayat, 1991). Abscisic acid of plant regulates the growth and metabolism of *A. nidulans* (Xu *et al*., 2018). Zearalenone produced by *Fusarium graminearum* induces sporulation and perithecial formation in *Fusarium roseum* (Wolf *et al.*, 1973). Butyrolactone I, an inhibitor of eukaryotic cyclin-dependent kinases produced by *Aspergillus terreus*, increases hyphal branching, sporulation, and production of another secondary metabolite, lovastatin (Schimmel *et al.*, 1998). The diorcinol-dehydroaustinol adduct rescued a non-sporulation mutant in *A. nidulans* (Rodríguez-Urra *et al.*, 2012). The production of fungal development affecting secondary metabolites is characterized as well. Normally, fungal SMs production happens at the late stage of cultivation. Numerous genes' mutant phenotypes affect the production of secondary metabolites such as asperthecin, austinol, dehydroaustinol, emericellin, fumiquinazolines, orsellinic acid, pseurotin A, shamixanthones and violaceol among others (Inglis *et al.*, 2013, Jain *et al.*, 2018).

Secondary metabolism and fungal development are coordinated processes (Calvo *et al*., 2002, Braus *et al*., 2010, Bayram *et al*., 2016). There are global regulatory complexes, including the light-operated heterotrimeric VeA-VelB-LaeA velvet complex, mitogen activated protein (MAP) kinase cascades and striatin-interacting phosphatase and kinase (STRIPAK) complex, which are playing crucial roles in regulating the secondary metabolism and fungal development processes.

The velvet family proteins, VeA and VelB, interact with each other and with the methyltransferase LaeA to form the central VeA-VelB-LaeA complex in the nucleus where it controls gene expression required for SMs production and sexual development (Bayram *et al.*, 2012b, Bayram *et al.*, 2008). The velvet family regulatory proteins are widely conserved in the fungal kingdom, and further controlled by the MAPK signaling pathway. MAPK signaling cascades are composed of MAPK kinase kinases (MAP3Ks), MAPK kinases (MAP2Ks), and MAPKs (Marshall, 1994). MAP3K phosphorylates MAP2K, which in turn phosphorylates the MAPK. This final kinase MpkB (yeast Fus3 ortholog) enters into the nucleus and phosphorylates VeA and is involved in regulation of cell fusions, sexual development and SMs production. The upstream members of MpkB, like SteC, MkkB and adaptor SteD, and downstream adaptor SteA can also participate in sexual development and SMs production (Bayram *et al.*, 2012a, Frawley *et al.*, 2018). MAPKs that specifically transmit environmental stress signals are also known as stress-activated protein kinases. Members of this MAPK subfamily include SakA and MpkC in *A. nidulans*. Activated SakA is involved in the repression of sexual development by reducing the activity of SteA presented in the downstream of MpkB pathway (Kawasaki *et al.*, 2002). Although SakA and MpkC show physical interaction, they play major, distinct and sometimes opposing roles in conidiation and in response to stress (Aguirre *et al.*, 2018). However, the roles of MpkC in sexual development are still not known. MpkA is the core signaling protein in the cell wall integrity pathway activating expression of genes which encode cell wall biosynthetic enzymes and other repair functions (Li *et al*., 2011). MpkA also plays roles outside of cell wall stress during steady state growth (Chelius *et al*., 2019). For instance, MpkA enhances the expression of ROS generating NoxR/IDC/HAM,

regulates the syntheisis of aspernidine A and siderophore, and is also required for the phosphorylation of SteC (Chelius *et al*., 2019).

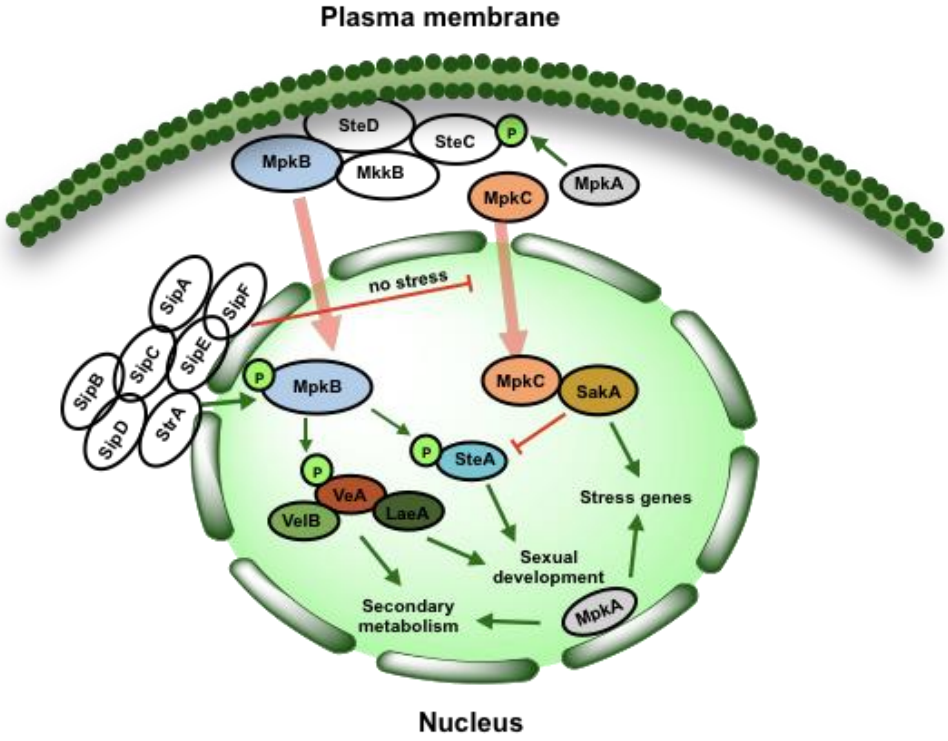

Figure 7. The regulation models of secondary metabolism and fungal development in *A. nidulans*. *An*STRIPAK complex sits on the nuclear envelope and controls two major MAPK signaling pathways. One is promoting MpkB phosphorylation, which in turn promotes VeA and SteA phosphorylation to control fungal sexual development and secondary metabolism. Another is limiting MpkC nuclear localization under resting conditions. Under stress conditions, MpkC enters into nucleus to form a heterodimer with SakA. This complex activates stress response genes and generates cross-talking with MpkB pathway negatively regulating sexual development by reducing the activity of SteA. MpkA is required for SteC phosphorylation showing cross-talk with MpkB pathway and regulates secondary metabolism and the expression of stress genes for cell wall integraty and reparation. The positive regulatory influences are shown in green, negative regulatory influences in red and entering into the nucleus is shown in pink arrow. Summarized from Bayram *et al.*, 2012a, Bayram *et al.*, 2012b, Elramli *et al.*, 2019, Frawley *et al.*, 2018, Jaimes-Arroyo *et al.*, 2015, Kawasaki *et al.*, 2002 and Chelius *et al.*, 2019.

The STRIPAK complex has been studied from yeast to human and plays a range of roles in development, cellular transport and signal transduction. In fungi, STRIPAK complex is required for coordination of multicellular fungal development with secondary metabolism (Bloemendal *et al.*, 2012, Dettmann *et al.*, 2013, Elramli *et al.*, 2019). The *An*STRIPAK complex consists of striatin (StrA) and six members, the Mob3-type kinase coactivator SipA,

the SIKE-like protein SipB, the STRIP1/2 homolog SipC, the SLMAP-related protein SipD and the catalytic and regulatory phosphatase 2A subunits SipE (PpgA), and SipF, which sits on the nuclear envelope and is required for proper expression of the heterotrimeric VeA-VelB-LaeA complex and controls activities of two major MAPK signaling pathways through either promoting MpkB phosphorylation or limiting MpkC nuclear localization under resting conditions (Elramli *et al.*, 2019). These global regulator complexes show independent actions and cross-talk regulations to control fungal development and secondary metabolism (Fig. 7).

1.4 The aim of this work

Emodin, monodictyphenone and epi-/shamixanthone are widely present secondary metabolites in fungi. The biosynthetic gene clusters, by which they are produced, normally harbor a backbone PKS encoding gene and several of "tailoring" enzyme encoding genes. These PKS gene clusters can produce various anthraquinone and derivatives thereof and are also involved in other secondary metabolite biosynthetic pathways. According to the structure-function theory, these metabolites must have a high diversity in bioactivity. *A. nidulans* is a model organism for studing eukaryotic cell biology, with an available genome sequence and well-characterized growth and development. It can undergo asexual and sexual development to form conidiophores and cleistothecia, which are surrounded by hundreds of yellowish Hülle cells. These special cells vary in size and number of nuclei and their functions are still to be elucidated. It was previously found that the genes of *mdp/xpt* clusters were especially up-regulated during fungal sexual development, and that the PKS MdpG and other four enzymes in the biosynthetic pathway, namely MdpH, MdpL, XptB and XptC, were mainly located in sexual mycelia and Hülle cells. This suggests that the expression of *mdp/xpt* clusters and the sexual development of *A. nidulans* must have correlations and this is a good model to investigate the biological functions of secondary metabolites in fungal sexual development.

The aims of this work are the: 1) localization of the products of the *mdp/xpt* clusters during fungal sexual development; 2) analysis of the effects of the *mdp/xpt* clusters products on fungal growth, reproductive development and morphology in *A. nidulans*; 3) elucidation of the bioactivities on other fungi and insects, e.g., the plant pathogenetic fungi *Verticillium dahliae,*

Verticillium longisporum and *Colletotrichum graminicola*, the model organism *Sordaria macorospora*, and the model insect *Drosophila melanogaster*. This study gives insight into the direct relationships between secondary metabolism and fungal development and the biological functions of secondary metabolites in interspecies antagonism.

2 Materials and Methods

2.1 Materials

2.1.1 Reagents and materials

Deoxynucleotide mix, restriction enzymes, DNA 1kb Ladder, PageRuler™ Prestained Protein Ladder, Phusion High fidelity DNA polymerase and RNaseA were purchased from the companies: Thermo Fisher Scientific (Waltham, Massachusetts, USA), Roche Diagnostics GmbH (Mannheim, Germany), New England Biolabs (Massachusetts, USA) and SERVA Electrophoresis GmbH (Heidelberg, Germany).

The selection antibiotics of microorganism, such as ampicillin, clonNAT nourseothricin dihydrogen sulfate and phleomycin were purchased from Roth, Werner-BioAgents (Jena, Germany), Invivogen (CA, USA) and Cayla-InvivoGen (Toulouse, France).

The lab-expendables such as plastic tubes, Filtropur filters (a pore size of 0.45 µm), plastic petri dishes, pipette tips, inoculation loops, *etc*., were obtained from the companies Sarstedt AG & Co. (Nümbrecht, Germany), StarLab GmbH (Hamburg, Germany) and Nerbe Plus GmbH (Hamburg, Germany). The Miracloth was obtained from Merck KGaA (Darmstadt, Germany).

DNA purification from *E. coli*, gel extraction and cleaning, RNA isolation and cDNA-synthesis kits were purchased from Macherey-Nagel GmbH & Co. KG (Düren, Germany) and Qiagen (Hilden, Germany).

DNA, RNA and protein concentrations were measured using the NanoDrop ND-1000 photospectrometer from Peqlab Biotechnologie GmbH (Erlangen, Germany).

The agarose gel electrophoresis was performed with Mini-Sub® Cell GT chambers and the PowerPac™ 300 power supply. SDS-polyacrylamide gel electrophoresis and subsequent blotting with the Mini-Protean® Tetra Cell, Mini Trans-Blot® Electrophoretic Cell and powered with the PowerPac™ 3000 from Bio-Rad Laboratories (Hercules, CA, USA).

For Southern hybridization, DNA was transferred to the Amersham™ Hybond-N™ ECL nylon membranes. For western hybridization, proteins were transferred to Amersham™ Protran™ 0.45 µm NC nitrocellulose blotting membranes from GE Healthcare Life Sciences (Buckinghamshire, United Kingdom) and Amersham™ Hyperfilm™-ECL for chemiluminescence detection.

Primers were ordered from Eurofins Genomics GmbH (Ebersberg, Germany) and Sigma-Aldrich Chemie GmbH (Schnelldorf, Germany).

Further materials and suppliers are indicated in the following sections.

2.1.2 Strains, media and growth conditions

2.1.2.1 Bacterial strain and culture conditions

The *Escherichia coli* strain DH5α [F-, Δ(*arg*F-*lac*ZYA) U169, φ80d*lac*ZΔM15-1, Δ*pho*A8, λ-, *gyr*A96 (NalR), *rec*A1, *end*A1, *sup*E44, *thi*E1, *hsd*R17 (rK-, mK+), *rel*A1] (Woodcock *et al.*, 1989) was used for general cloning procedures and expression of recombinant plasmids in this study. *E. coli* was grown in Lysogeny Broth medium (LB) (Bertani, 1951), containing 1% bactotryptone, 0.5% yeast extract and 1% NaCl, pH 7.5, at 37°C on a shaker, for cultivation in liquid LB medium. Solid LB medium was prepared by addition of 2% agar. The antibiotic ampicillin was used as selective agent at a concentration of 100 µg/ml.

2.1.2.2 Fungal strains and culture conditions

In this study, *A. nidulans* strains were cultivated in minimal medium (MM) [1% Glucose, 1x AspA (3.5 M $NaNO_3$, 350 mM KCl, 560 mM KH_2PO_4, pH 5.5 with KOH), 2 mM $MgSO_4$, 1x trace elements (5 g/L $FeSO_4$ x $7H_2O$, 50 g/L EDTA, 22 g/L $ZnSO_4$ x $7H_2O$, 11g/L H_3BO_3, 5 g/L $MnCl_2$ x $4H_2O$, 1.6 g/L $CoCl_2$ x $6H_2O$, 1.6 g/L $CuSO_4$ x $5H_2O$, 1.1 g/L $(NH_4)_6Mo_7O_{24}$ x 4 H_2O; pH 6.5 with KOH)] (Käfer, 1977)). For solid MM medium plates, 2% agar was added. Standard growth of *Aspergillus* strains was performed at 37°C under the white light or dark conditions. Different antibiotics and supplements were added to the medium according to the experimental requirements. For selection of *A. nidulans* transformants, phleomycin (final concentration 80 µg/ml) was added. In this study, the *A. nidulans veA*+ strain AGB552 (Bayram *et al.*, 2012a) was used as the wild type (wt) host for *A. nidulans* strains construction. Cultivation of strains with AGB552 background required the addition of 4-aminobenzoic acid (PABA, final concentration 0.0001%).

Table 2. Fungal strains used in this study

$_R$ = resistance gene, $_P$ = promoter, *six* = *β-rec* recognition sequences

Strain name	Genotype/Information	Reference
AGB552	*pabaA1; ΔnkuA::argB; veA+*	Gerke *et al*., 2012a
AGB596	*$_P$gpdA:sgfp:phleo$_R$; pabaA1; yA2; veA+*	Bayram *et al*., 2012a
AGB611	*ΔmpkB::ptrA; pabaA1; ΔnkuA::argB; veA+*	Bayram *et al*., 2012a
AGB1235	*$_P$gpdA:mdpG:six; pabaA1; ΔnkuA::argB; veA+*	This study
AGB1236	*ΔmdpG::six; pabaA1; ΔnkuA::argB; veA+*	Fekete-Szücs, 2016
AGB1237	*ΔmdpF::six; pabaA1; ΔnkuA::argB; veA+*	This study
AGB1238	*ΔmdpC::six; pabaA1; ΔnkuA::argB; veA+*	This study
AGB1239	*ΔmdpL::six; pabaA1; ΔnkuA::argB; veA+*	This study
AGB1240	*ΔmdpD::six; pabaA1; ΔnkuA::argB; veA+*	This study
AGB1241	*ΔxptA::six; pabaA1; ΔnkuA::argB; veA+*	This study
AGB1242	*ΔxptB::six; pabaA1; ΔnkuA::argB; veA+*	This study
AGB1243	*ΔxptC::six; pabaA1; ΔnkuA::argB; veA+*	This study
AGB1244	*sakA:sgfp:nat$_R$; pabaA1; ΔnkuA::argB; veA+*	This study
AGB1245	*sakA:sgfp:nat$_R$; ΔmdpG::six; pabaA1; ΔnkuA::argB; veA+*	This study
AGB1246	*sakA:sgfp:nat$_R$; ΔmdpC::six; pabaA1; ΔnkuA::argB; veA+*	This study
AGB1247	*sakA:sgfp:nat$_R$; ΔmdpL::six; pabaA1; ΔnkuA::argB; veA+*	This study
AGB1248	*ΔmdpG::six, mdpG:six::six; pabaA1; ΔnkuA::argB; veA+*	This study
AGB1249	*ΔmdpC::six, mdpC:six::six; pabaA1; ΔnkuA::argB; veA+*	This study
***Sordaria macrospora* Taxid5147**	wild type isolate	Nowrousian *et al.* 2010
***Colletotrichum graminicola* CgM2**	wild type isolate	O'Connell *et al.* 2012
***Verticillium longisporum* VL43**	wild type isolate	Zeise *et al.* 2002
***Verticillium dahliae* JR2**	wild type isolate	Fradin *et al.* 2009

For fungal vegetative growth, *Aspergillus nidulans* strains were cultivated in liquid MM at 37°C in baffled flasks under shaking conditions for 16-24 h. For inducing the asexual development, spores were incubated on solid MM plates and under illumination at 37°C for three days. Sexual

development was induced by cultivation on solid MM plates at 37°C in darkness and sealing the plates with Parafilm® M (Merck, Darmstadt, Germany) to restrict aeration. For conidiospores were collected in 0.96% NaCl with 0.02% Tween-80 (Sigma-Aldrich, Schnelldorf, Germany) and stored at 4°C. The concentration of these spore solutions was determined using a spore counter Beckman Coulter Z2 (Beckman Coulter GmbH, Krefeld, Germany). Otherwise, these culture conditions can be modified for special experimental requirements and they will be properly detailed when it corresponds.

Sordaria macrospora, *Colletotrichum graminicola*, *Verticillium longisporum* and *Verticillium dahliae* were kindly provided by Prof. Dr. Stefanie Pöggeler, Dr. Daniela Nordzieke and Dr. Rebekka Harting separately. *S. macrospora* was cultivated on cornmeal malt fructification medium (BMM) plates at 27°C (Dirschnabel *et al.*, 2014, Nowrousian *et al.*, 1999). *C. graminicola* was cultivated on complete medium (CM) (Leach *et al.*, 1982) at room temperature under continuous fluorescent light (Climas Control CIR, UniEquip, Martiensried, Germany). *Verticillium* sp. were cultivated on the simulated xylem medium (SXM) agar plate at 25°C (Singh *et al.*, 2010).

Fungal strains used in this study are listed in table 2.

2.2 Nucleic acid methods

2.2.1 Plasmids and DNA fragments purification

Plasmids were extracted from o/n cultures of *E. coli* by utilization of the NucleoSpin® Plasmid Kit (Macherey-Nagel) according to manufacturer's specifications. Plasmids were eluted from spin columns with 50 µl dH_2O and stored at -20°C. The DNA fragment purification is the same as the manufacturer's specifications in the NucleoSpin® Gel and PCR Clean-up Kit (Macherey-Nagel).

2.2.2 Polymerase chain reaction

Polymerase chain reaction (PCR) is a efficient way to amplify DNA fragments from different sources, such as plasmid-DNA and gDNA (Saiki *et al.*, 1988). In this study, PCRs were performed in T Professional Standard 96, T Professional Trio 48 and T Professional Standard 96 Gradient thermocyclers from Biometra GmbH (Göttingen, Germany) or in Primus 96

Thermal Cyclers from MWG Biotech AG (Ebersberg, Germany). Phusion® High-Fidelity DNA Polymerase (Thermo Fisher Scientific, Schwerte, Germany) was used for DNA amplification. PCR programs were designed according to the manufacturer's instructions and calculated melting temperatures (Tm) of utilized primers. The online 'Tm calculator' tool from New England Biolabs was used to determine the Tm of the designed primers and to estimate the annealing temperature of the reaction grograms.

2.2.3 RNA purification and cDNA synthesis

Mycelia were harvested from liquid vegetative growth, agar surface asexual/sexual growth for RNA extraction. Mycelia were washed by 0.96% NaCl solution and filtered through sterile Miracloth filters and immediately frozen in liquid nitrogen. Frozen mycelia were ground with a table mill fastly and approximately 200 µl of the resulting powder was processed for RNA isolation using the RNeasy® Plant Miniprep Kit from Qiagen (Hilden, Germany) according to manufacturer's instructions without β-mercaptoethanol. Concentrations of total RNA were measured with the Nanodrop ND-1000 (PeqLab). Approximate 0.8 µg of the total RNA was used for cDNA synthesis with the QuantiTect® Reverse Transcription Kit (Qiagen) according to manufacturer's conditions.

2.2.4 Quantitative real-time polymerase chain reaction

Gene expression was measured with the quantitative real-time polymerase chain (qRT-PCR) reaction by the use of MESA GREEN qPCR MasterMix Plus for SYBR® Assay purchased from Eurogentec (Lüttich, Belgium) in a CFX Connect™ Real-Time System (BioRad, Germany). The used primers of qRT-PCR were designed through the online tool 'Primer3 software' (Untergasser *et al.*, 2012) and they are listed in the table 3. Gene expression was measured from 1:5 dilutions of respective cDNA. Obtained qRT-PCR data were analyzed with the CFX Manager™ 3.1 software package (BioRad) using the 2-ΔΔCT method for relative quantification of gene expression (Schmittgen *et al.*, 2008). Expression of the genes *h2A* (AN3468) and *S15* (AN5997) was used as the reference for relative quantification. qRT-PCR measurements were conducted in at least two independent biological replicates for each treatment as indicated. Each

biological replicate was performed in three technical replicates.

Table 3. Primers for qRT-PCR used in this study

Primer	5'-sequence-3'	Size/bp
JG795(*laeA*)	TGA AGA GAA CGG ACG CAC CTA C	22
JG796(*laeA*)	CAA ATC CAC ACC AGC GAC AAA C	22
JG814(*veA*)	CAA CGA GCA TCA GCA CAA ACA T	22
JG815(*veA*)	AGC AGG AAT CGG CGT AGA AGA T	22
JG816(*velB*)	CCC CTC CGT GTA TCC GTC TAA T	22
JG817(*velB*)	AGC CGA GTG CTT CAC AAG ATT T	22
kt491(*nsdD*)	TCA TCT CAC CAG CCA CAA TTA C	22
kt492(*nsdD*)	CAG AGG TCA TAA CAG TGC TTG C	22
kt395(*stuA*)	GAT CGA ATC TGA TGT CAA GAC G	22
kt396(*stuA*)	CGA CCA GTG TTG TAT CCA CTG T	21
LL232(*mutA*)	TCC AGT CAA GAG GGC AGT AGA T	22
LL233(*mutA*)	ACG AAA ACG CTC CAT CAA TC	20
LL237(*sakA*)	CAG TTT TCC ATC ATC ACA GAG C	21
LL238(*sakA*)	ACG AAC CGC AGA GTG TTT TC	20
LL265(*mpkB*)	GTT GTT TGC TCT GCT ATC CAC A	21
LL266(*mpkB*)	CTT CAT CTC TCG TAG GGT TCG	20
LL35(*mdpG*)	CAG GTT GAG GTT GTG TCT GAA A	22
LL36(mdpG)	CTG TTT GTG AGG AGT GAA ATG C	22
LL267(*mpkC*)	CCT TTG AGA CCA CCA GCA GAT A	22
LL268(*mpkC*)	CAA GTC GTA AGC GGA ACA TAC A	22
JG882(*h2A*)	GCC GCT GTT TTG GAG TAT CT	20
JG882(*h2A*)	TAC GAG TCT TCT TGT TGT CAC G	22
JG884(*S15*)	GCC GAG ATC AAG AAG AGA AGA C	22
JG885(*S15*)	GAA GCT GTT CAG AGG AGA GGT C	22

2.3 The genetic manipulation of microorganisms

2.3.1 Transformation of bacteria

The transformation of *E. coli* was performed using the heat-shock method (Hanahan *et al.*, 1991, Inoue *et al.*, 1990). The procedure was as follows, competent *E. coli* cells were incubated with plasmid for 25 min on ice and subsequently heat shocked at 42°C for 60 s to allow plasmid uptake, and immediately cells were cooled down on ice for one to 2 min. 800 µl of liquid LB was added and cultures were incubated for 30 to 60 min at 37°C on a rotary shaker. 200 µl of *E. coli* cells were inoculated on solid LB plates. The antibiotic ampicillin was added (final concentration 100 µg/ml) to prevent plasmid loss and allow for selection of the clones, which

successfully incorporated the plasmid. Plates were grown o/n (no more than 14 h) at 37°C. *E. coli* colonies were picked and checked by colony PCR (Woodman, 2008) for positive clones.

2.3.2 Transformation of fungi

A. nidulans strains were transformed by polyethylene glycol-mediated protoplast fusion (Punt *et al.*, 1992). For all genetic modifications in *A. nidulan*s, AGB552 was used as the original host for the subsequent transformations. All the strains used in this study harbor the Δ*nkuA* and *pabaA1* mutations (see genotypes in the strains table 2). Loss of *nkuA* orthologous genes remarkably increases homologous recombination during transformation and results in on-locus integration of linearized genetic constructs (Krappmann *et al.*, 2006).

Fresh spores of the host *A. nidulans* strains were inoculated into liquid MM medium and grown for o/n on a rotary shaker at 37°C. Next day, mycelia were harvested through sterile Miracloth filters (Merck, Germany) and washed with sterile citrate buffer (150 mM KCl, 580 mM NaCl, 50 mM Na-citrate pH 5.5) three times. These mycelia were transferred into new autoclaved flasks and mixed with protoplastation solution (20 mg/ml Vinoflow® Max or Vinotaste® Pro from Novozymes (Bagsværd, Denmark) and 20 mg/ml of lysozyme (Serva)), which were dissolved in citrate buffer and sterile filtered through 0.45 µm Filtropur filters (Sarstedt AG & Co). The protoplastation was performed by incubating the mycelia in protoplastation solution for 80 min at 30°C under constant gentle agitation (75 rpm/min). The formed protoplasts were monitored by microscopy. Protoplasts were filtered through sterile Miracloth filters and collected in 50 ml pre-cooled sterile centrifuge tubes. Then, protoplasts solution was filled up to 50 ml with ice cold STC 1700 buffer (1.2 M sorbitol, 10 mM Tris pH 5.5, 50 mM $CaCl_2$, 35 mM NaCl) and incubated in ice for 10 min. Subsequently, protoplasts were centrifuged at 2500 rpm at 4°C for 12 min and washed with ice cold STC1700 gently. This step was repeated twice and discarded the supernatant after the second centrifuge. Protoplasts were resuspended and 200 µl of protoplast supernatant was incubated in 15 ml tubes with approximately ~ 5 µg of respective DNA linear constructs (after excision from respective plasmids) for 25 min in ice. 250 µl of sterile PEG solution (10 mM Tris pH 7.5, 50 mM $CaCl_2$, 60% (v/v) PEG4000) was added sequentially and mixed with protoplast supernatant gently. This step was repeated twice

and 850 µl PEG solution was added finally. This PEG solution induces the DNA uptake of protoplasts. The mixture was incubated for another 35 min on ice to avoid crystal formation. After that, the tubes were filled up to 15 ml with ice cold STC 1700 buffer again and centrifuged at 2700 rpm for 15 min. Supernatants were discarded and resuspended protoplasts distributed in 5 ml of 0.7% top agar (MM) and placed on freshly prepared solid MM plates, supplemented with 1.2 M sorbitol and respective selecting agents (phleomycin 1:1000). After five days, individual positive clones were picked and they were singularized twice on selective MM plates. Successful transformation of constructs into *A. nidulans* hosts was verified by Southern hybridization. Recyclable marker cassettes were eliminated from the genome of respective mutants by growing the fungus in the presence of xylose (1% xylose MM plate) and isolating single colonies twice (Hartmann *et al.*, 2010). Successful marker recycling was monitored by growing transformants on phleomycin containing agar plates and by Southern hybridization.

2.3.3 Plasmid construction for the genetic manipulation of fungi

In this study, fungal strains carrying NHEJ-deficient (Non-Homologous End Joining repair) mutations (Δ*nkuA*) were used as transformation hosts (Nayak *et al.*, 2006). They have an increased frequency of Homologous Recombination (HR) that allows transformation on-locus with higher efficiency and yields as described above. For the mutant strains generation, ~ 1.5 kilobases fragments of the flanking regions (FR) of the gene of interest were amplified and inserted into a cloning vector. As shown in figure 8, a recyclable marker is placed between these two FRs that consists of a resistance cassette against an antibiotic as selective agent, a prokaryotic small β-serine recombinase (*β-rec*) under the control of a xylose-inducible promotor followed by a fungal terminator region ($trpC_t$), and its six recognition sequences (*six*) flanking this whole recyclable marker (Canosa *et al.*, 1996, Hartmann *et al.*, 2010, Rojo *et al.*, 1993).

This system allows the removal of the marker cassette from the fungal genome once the transformation succeeded by growing the fungus in the presence of xylose. Therefore, a marker-free deletion mutant has the possibility to use the same antibiotic as a selective agent for a next round of transformation over the same host. This system also prevents the accumulation of large

resistance cassettes integrated in the genome of the fungus, which can lead to undesired side effects.

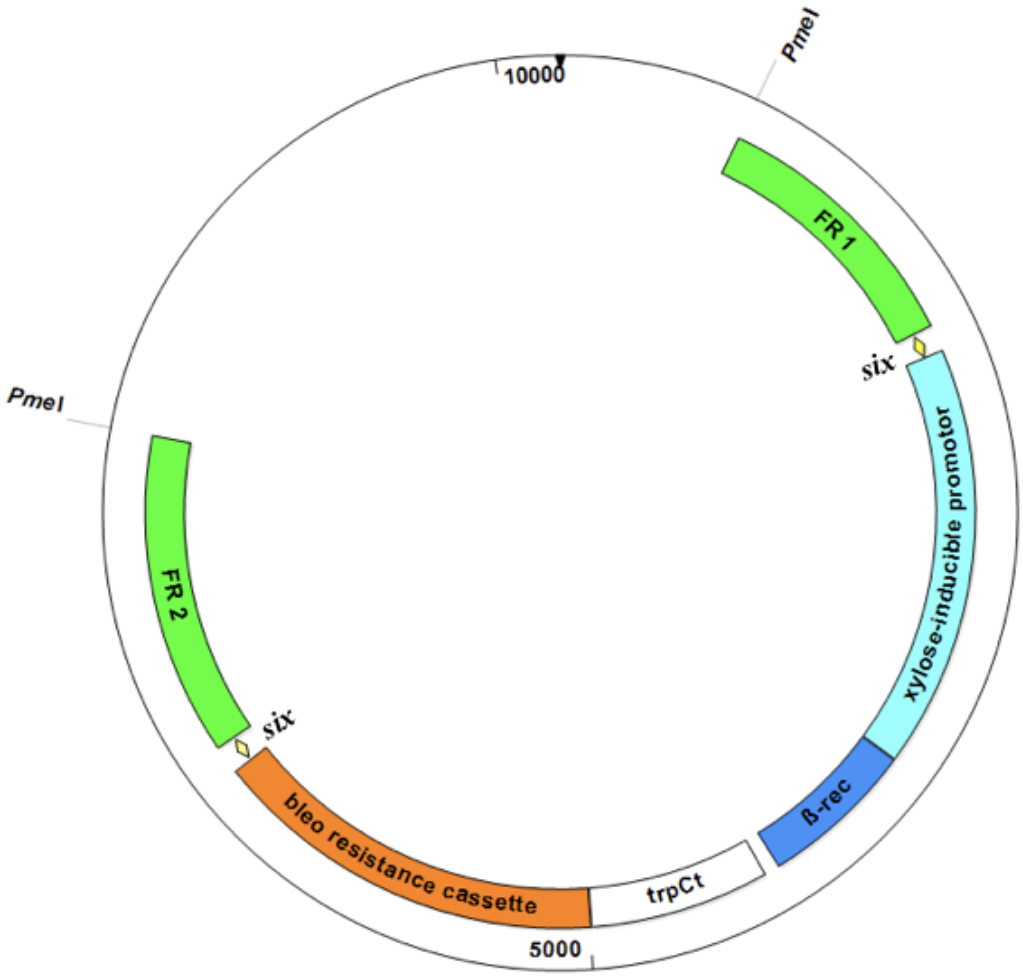

Figure 8. Schematic diagram of a resistance recyclable marker in a fragment construct.
FR1 and FR2 are flanking regions of the target gene and amplified with overhang regions (15 bp) complementary to the cloning vector and to the recyclable marker. Also, two unique *Pme*I restriction sites are generated at both sides of the fragment construct to allow scission from the plasmid (procedure of plasmid design and construction is detailed in the text). *β-rec* = prokaryotic small β-serine recombinase, *trpC*$_t$ = fungal terminator region of gene *trpC*, *six* = *β-rec* recognition sequences.

The recyclable marker cassette containing plasmid pME4319 was kindly provided by Dr. Jennifer Gerke, which harbors the *bleo* gene from *Streptoalloteichus hindustanus* conferring resistance to phleomycin (Drocourt *et al.*, 1990).

Primer design and cloning strategy for the generation of the different individual constructs were detailed in the corresponding sections. For ‘on-locus’ transformation of fungi, a linear fragment will consist in two regions (FR1 and FR2 in figure 8) where the recombination will occur

flanking the recyclable marker. This fragment will be integrated in the fungal genome due to the two FRs that will take place in the flanking homologous regions. The restriction sites are recognized and cut by the specific nuclease *Pme*I (also called *Mss*I), whose target sequence is GTTT/AAAC.

In this study, we focused on the backbone PKS encoding gene *mdpG* and other seven *mdp/xpt* genes *mdpF*, *mdpC*, *mdpD*, *xptA*, *xptB* and *xptC* playing key roles in intermediates and final products in the *mdp/xpt* clsuters (Sanchez *et al.*, 2011). The overexpression and deletion plasmid constructions were based on pME4319.

2.3.3.1 Construction of *mdpG* overexpression strain

1.5 kb of 5'UTR of *mdpG* was amplified with primers LL63/64 as FR1. The constitutive promoter of *gpdA* was amplified with primers LL101/102. The first 1.5 kb of *mdpG* was amplified with primers LL65/66. These two fragments were fused by fusion PCR (Szewczyk *et al.*, 2006) with primers LL101/66 as FR2. Plasmid of overexpression *mdpG* was generated by two steps: pME4319 was linearized by *Swa*I and spliced the FR1 in a seamless cloning reaction according to manufacturer's instructions; linearized again by *Pme*I and spliced the FR2 in a seamless cloning reaction, giving rise to pME4841. The OE*mdpG* cassette was excised from the plasmid and integrated into AGB552, resulting in AGB1235.

2.3.3.2 Construction of *mdp/xpt* deletion strains

Deletion strains were generated by inserting the FR1 (5'UTR of *mdp/xpt* genes) and the FR2 (3'UTR of *mdp/xpt* genes) before and behind the recyclable marker cassette in pME4319.

1.5 kb of FR1 (5'UTR of *mdpG*) was amplified with primers LL139/140 and 1.6 kb of FR2 (3'UTR of *mdpG*) was amplified with primers LL141/142. Both fragments, respectively, were cloned into pME4319 in a seamless reaction, giving rise to pME4842. The Δ*mdpG* cassette was excised from the plasmid and integrated into AGB552, resulting in AGB1236 (Fekete-Szücs, 2016).

1.0 kb of FR1 (5'UTR of *mdpF*) was amplified with primers LL197/198 and 1.0 kb of FR2 (3'UTR of *mdpF*) was amplified with primers LL199/200. Both fragments, respectively, were

cloned into pME4319 a seamless reaction, giving rise to pME4843. The Δ*mdpF* cassette was excised from the plasmid and integrated into AGB552, resulting in AGB1237.

1.0 kb of FR1 (5'UTR of *mdpC*) was amplified with primers LL223/224 and 1.1 kb of FR2 (3'UTR of *mdpC*) was amplified with primers LL225/226. Both fragments, respectively, were cloned into pME4319 a seamless reaction, giving rise to pME4844. The Δ*mdpC* cassette was excised from the plasmid and integrated into AGB552, resulting in AGB1238.

1.2 kb of FR1 (5'UTR of *mdpL*) was amplified with primers LL193/194 and 1.2 kb of FR2 (3'UTR of *mdpL*) was amplified with primers LL195/196. Both fragments, respectively, were cloned into pME4319 a seamless reaction, giving rise to pME4845. The Δ*mdpL* cassette was excised from the plasmid and integrated into AGB552, resulting in AGB1239.

1.1 kb of FR1 (5'UTR of *mdpD*) was amplified with primers LL162/163 and 1.3 kb of FR2 (3'UTR of *mdpD*) was amplified with primers LL164/165. Both fragments, respectively, were cloned into pME4319 a seamless reaction, giving rise to pME4846. The Δ*mdpD* cassette was excised from the plasmid and integrated into AGB552, resulting in AGB1240.

1.3 kb of FR1 (5'UTR of *xptA*) was amplified with primers LL211/212 and 1.3 kb of FR2 (3'UTR of *xptA*) was amplified with primers LL213/214. Both fragments, respectively, were cloned into pME4319 a seamless reaction, giving rise to pME4847. The Δ*xptA* cassette was excised from the plasmid and integrated into AGB552, resulting in AGB1241.

1.5 kb of FR1 (5'UTR of *xptB*) was amplified with primers LL215/216 and 1.3 kb of FR2 (3'UTR of *xptB*) was amplified with primers LL217/218. Both fragments, respectively, were cloned into pME4319 a seamless reaction, giving rise to pME4848. The Δ*xptB* cassette was excised from the plasmid and integrated into AGB552, resulting in AGB1242.

1.0 kb of FR1 (5'UTR of *xptC*) was amplified with primers LL219/220 and 1.1 kb of FR2 (3'UTR of *xptC*) was amplified with primers LL221/222. Both fragments, respectively, were cloned into pME4319 a seamless reaction, giving rise to pME4849. The Δ*xptC* cassette was excised from the plasmid and integrated into AGB552, resulting in AGB1243.

2.3.3.3 Construction of *mdpG* and *mdpC* complementation strains

In this study, we complemented the PKS encoding gene *mdpG* and the most interesting gene *mdpC* in the deletion strains. The plasmid of *mdpG* and *mdpC* complementation was generated by the same protocol as mentioned above.

5'UTR of *mdpG* was amplified with primers LL59/60 and the complete *mdpG* was amplified with primers LL61/62. Both fragments were cloned into pME4319 (linearized by *Swa*I). The plasmid was linearized again by *Pmi*I and spliced the FR2 fragment (1.6 kb of 3'UTR of *mdpG* was amplified with primers JG1076/EFS46) in the back of the recyclable marker cassette, giving rise to pME4850. The *mdpG* complementation cassette was excised from the plasmid and integrated into AGB1236, resulting in AGB1248.

1.9 kb of FR1 (5'UTR+ *mdpC* was amplified with primers LL223/236) was cloned into pME4319 (linearized by *Swa*I). The plasmid was linearized again by *Pmi*I and spliced the FR2 fragment (1.1 kb of 3'UTR of *mdpC* was amplified with primers LL225/226) in the back of the recyclable marker cassette, giving rise to pME4851. The *mdpC* complementation cassette was excised from the plasmid and integrated into AGB1238, resulting in AGB1249.

2.3.3.4 Construction of *sakA:gfp* strains

The plasmid pME4852 of *sakA:gfp* was constructed by assembly of the pBluescript SK+ vector (*EcoR*V linearized) with *sakA:gfp:nat*$_R$*:*3'UTR fusion fragment. The last 1.3 kb of *sakA* (no termination codon) was amplified with primers LL261/262. 2.1 kb of the *gfp:nat*$_R$ fusion fragment was amplified from plasmid pJG121 with primers LL55/56. 1.3 kb of 3'UTR of *sakA* was amplified with primers LL263/264. These three fragments were fused by fusion PCR with primers LL261/56 and LL261/264 successively. 4.7 kb of the fusion fragment cloned into pBluescript SK+ vector in a seamless reaction, giving rise to pME4852. The *sakA:gfp* cassette was excised from the plasmid and integrated into AGB552 resulting in AGB1244, into AGB1236 resulting in AGB1245, into AGB1238 resulting in AGB1246 and into AGB1239 resulting in AGB1247.

The plasmids constructed and used in this study are listed in the table 4. The primers used for amplifying DNA fragments to construct all the different plasmids of this study are listed in the

table 5. The software used for designing the maps of the constructs and the primers was Lasergene from DNA Star Inc (Madison, WI, USA). Genetic sequences and information were obtained from AspGD (Arnaud *et al.*, 2012, Cerqueira *et al.*, 2013).

Table 4. Plasmids used and constructed in this study

$_P$ = promoter, $_t$ = terminator, $_R$ = resistance gene. *phleo*$_{RM}$ = recyclable *phleo* resistance cassette from pME4319. All plasmids constructed in this study use pBluescript SK+ as vector.

Plasmid	Description	Reference
pBluescript SK+	Cloning vector, *amp*$_R$	Fermentas GmbH
pME4319	*six:*$_P$*xylP:β-rec:trpC*$_t$*:phleo*$_{RM}$*:six*	J. Gerke
pJG121	Plasmid containing *sgfp*	J. Gerke
pME4841	$_P$*gpdA:mdpG:phleo*$_{RM}$	This study
pME4842	Δ*mdpG::phleo*$_{RM}$	This study
pME4843	Δ*mdpF::phleo*$_{RM}$	This study
pME4844	Δ*mdpC::phleo*$_{RM}$	This study
pME4845	Δ*mdpL::phleo*$_{RM}$	This study
pME4846	Δ*mdpD::phleo*$_{RM}$	This study
pME4847	Δ*xptA::phleo*$_{RM}$	This study
pME4848	Δ*xptB::phleo*$_{RM}$	This study
pME4849	Δ*xptC::phleo*$_{RM}$	This study
pME4850	Δ*mdpG::phleo*$_{RM}$*:mdpG*	This study
pME4851	Δ*mdpC::phleo*$_{RM}$*:mdpC*	This study
pME4852	*sakA:gfp:nat*$_R$	This study

For the integration of all the fragments into the backbone vector, the GeneArt® Seamless Cloning and Assembly Kit (Invitrogen) or the GeneArt® Seamless Cloning and Assembly Enzyme Mix (Invitrogen) was used. Primers used for seamless cloning reactions were designed to introduce 15 base pairs (bp) complementary to adjacent sequences in the way that two adjacent sequences share a 15 bp homology region. As templates for DNA amplification in *A. nidulans*, gDNA from AGB552 strain was used.

Generated plasmids were sequenced, when necessary, by Seqlab Sequence Laboratories GmbH (Göttingen, Germany) and the obtained sequences were analyzed with the Basic Local Alignment Search Tool (BLAST) (NCBI, NIH, USA).

Table 5. Primers used in this study for DNA sequence amplification and plasmid construction

Primer	5'-sequence-3'	Size/bp
LL55	GGT GGT AGC GGT GGT ATG GTG	21
LL56	TCA GGG GCA GGG CAT GCT CAT	21
LL59	ACG GTA TCG ATA AGC TTG ATG TTT AAA CCA TCG TTT TAC ACC TCC TC	47
LL60	CAT CAC GAT TGA GCC TAT ACC G	22
LL61	GTA TAG GCT CAA TCG TGA TGA AGC GCC TTG AAG ATG CTG AG	41
LL62	TAT TGA CCT ATA GGC CTG AGC TAA TTA TAG TAC TCT AAT AGC CAG	45
JG1076	ATA ATA TGG CCA TCT GCA GTA TGT TAA CCG GTA GTG AA	38
EFS 46	TCC CCC GGG CTG CAG GAA TTC GAT GTT TAA ACC CGA CAA GAG CAG CTT TG	50
LL63	ACG GTA TCG ATA AGC TTG ATG TTT AAA CGG CTC CAA TGC CAT CTT G	46
LL64	TAT TGA CCT ATA GGC CTG AGT CTG AGG CGA TGG AAC CAC CA	41
LL65	TTC CTA TCC CAT ACT CTC ACA TGC CCG TAT ATA CTC CTC AAT CA	44
LL66	CCG GGC TGC AGG AAT TCG ATG TTT AAA CAA GCC AGG CTC ATC AAT AAA	48
LL101	ATA TGG CCA TCT CAC GAT CTT TGC CCG GTG TAT GAA A	37
LL102	CGG TGA TGT CTG CTC AAG CG	20
LL139	AGG AAT TCG ATA TTT GTT TAA ACC ATC GTT TTA CAC CTC CTC	42
LL140	ATA GGC CTG AGA TTT TCT GAG GCG ATG GAA CCA CC	35
LL141	ATA TGG CCA TCT CAC GCA GTA TGT TAA CCG GTA GTG A	37
LL142	GAT AAG CTT GAT CAC GTT TAA ACC CGA CAA GAG CAG CTT TG	37
LL162	AGG AAT TCG ATA TTT GTT TAA ACC CTT CAC TAT CAT GCG TG	41
LL163	ATA GGC CTG AGA TTT TGT GAC TCT CAG TGC TGG TGG	36
LL164	ATA TGG CCA TCT CAC TTA CCT TTT CTC CAA AGA TTT AGA AT	41
LL165	GAT AAG CTT GAT CAC GTT TAA ACA TGT CCG TCA CCG TTC C	40
LL193	AGG AAT TCG ATA TTT GTT TAA ACA CCC AAC CAC CAT CAA CC	41
LL194	ATA GGC CTG AGA TTT TTT TGA CGC CGT ATT CGT GCT T	37
LL195	TAT GGC CAT CTC ACT TAG ATA TAC GCA GTG CTG TAT AT	38
LL196	GAT AAG CTT GAT CAC GTT TAA ACT CTG AAT TTT TAG ATG CGA AT	44
LL197	AGG AAT TCG ATA TTT GTT TAA ACT CGC ACT ACC TCG GCA C	40
LL198	ATA GGC CTG AGA TTT TGT GTC TGG TTA GAA AAT GCA CAA	39
LL199	ATA TGG CCA TCT CAC TTA AGC GAG GCA TTG GAT GGA G	37
LL200	GAT AAG CTT GAT CAC GTT TAA ACT ATA AAT CAA GCA TTA ACC AAG	45
LL211	AGG AAT TCG ATA TTT GTT TAA ACA TGC AGA TCA AGC CTT ACT	42
LL212	ATA GGC CTG AGA TTT CTT GGA GGT ACT TTT CAG ATT CTA A	40
LL213	ATA TGG CCA TCT CAC TCT ACA CCT TGA CCA CAA CCG	36

LL214	GAT AAG CTT GAT CAC GTT TAA ACT CTA TAT CAT CCT GGT CAA C	43
LL215	AGG AAT TCG ATA TTT GTT TAA ACC CAT CCC CAT CCC TTT G	40
LL216	ATA GGC CTG AGA TTT GCT GGT CAG TTT GCA TGA TGG	36
LL217	ATA TGG CCA TCT CAC TTC CTC TCT AGA AAC TTC TCA AAT	39
LL218	GAT AAG CTT GAT CAC GTT TAA ACA AGC AGA GGG ATA CCG C	40
LL219	AGG AAT TCG ATA TTT GTT TAA ACA CAA GGA CCC ATT ATC GTA	42
LL220	ATA GGC CTG AGA TTT TTT CTC ACA AGC GAA GGA TAC C	38
LL221	ATA TGG CCA TCT CAC ATT AGA TCT ATT AGA CCG CAG GC	38
LL222	GAT AAG CTT GAT CAC GTT TAA ACA GCT CAA ATA CTC TCG AGC	42
LL223	AGG AAT TCG ATA TTT GTT TAA ACG GAG GCT CGC AGG CCT	38
LL224	ATA GGC CTG AGA TTT TGG TGC TTT CCT ACC TAC CTT A	36
LL225	ATA TGG CCA TCT CAC TTC TGC TAG ATT TAG TAG CTA AGT	38
LL226	GAT AAG CTT GAT CAC GTT TAA ACT ACC TTT CCT CAG TAC CAA	41
LL236	ATA GGC CTG AGA TTT CTA AGC AGC GCC TCC GTC GA	35
LL261	ATC GAT AAG CTT GAT GTT TAA ACG TCA GTC CTC GTT CGA AG	41
LL262	ACC ACC GCT ACC ACC TTG GAA ACC TTG CTG GTT GAG C	37
LL263	ATG CCC TGC CCC TGA AGC CCT AAT GAA TCG CGT GGA	36
LL264	CTG CAG GAA TTC GAT GTT TAA ACC ATG CCG AGG TGA CGA C	40

2.4 Southern hybridization

Southern hybridization (Southern, 1975) was performed to confirm successful mutagenesis of genetic loci. Genomic DNA of the generated mutant clones was digested with restriction enzymes (Thermo Fisher Scientific) o/n according to its temperature requirement. Samples were loaded onto 1% (w/v) agarose gel with the DNA loading dye and DNA fragments were separated according to different size. After separation, gels were washed for 10 min in the wash buffer 1 (0.25 M HCl) (depurination), followed by washing with the buffer 2 for denaturation (0.5 M NaOH, 1.5 M NaCl) for 25 min and finally, 30 min in the buffer 3 (0.5 M Tris, 1.5 M NaCl, pH 7.4) for neutralization. All these washing steps were performed under constant gentle agitation at room temperature (rt). Subsequently, DNA was transferred onto Amersham™ Hybond™-N nylon membranes (GE Healthcare) by dry blotting for at least 2 hours or o/n at rt. Membranes were subsequently dried at 75°C for 10 min, and DNA was cross-linked to the membrane by UV light exposure (λ = 254 nm) for 3 min per side. Membranes were pre-hybridized in hybridization solution from the Amersham™ Gene Images AlkPhos Direct Labelling and Detection System (GE Healthcare, prepared after manufacturer's instructions)

for at least 30-60 min at 55°C in a HERA hybrid R hybridization oven (Heraeus Instruments) prior to application of the DNA probe. DNA probes were prepared with the aforementioned kit according to manufacturer's instructions (GE Healthcare). Hybridization of the membranes with the respective DNA probes was performed o/n at 55°C in the same rotor. Membranes were washed twice in post-hybridization buffer I (1 mM $MgCl_2$, 3.5 mM SDS, 50 mM sodium phosphate buffer, 150 mM NaCl, 2 M urea, 0.2% blocking reagents) for 10 min at 55°C, and twice in post-hybridization buffer II (2 mM $MgCl_2$, 50 mM Tris, 100 mM NaCl, pH 10) for 10 min at rt under constant agitation. For detection of DNA bands, the detection solution CDP-Star (GE Healthcare) was applied and membranes were exposed to Amersham™ Hyperfilm™ ECL (GE Healthcare). The Southern hybridization verification of all the mutants in this study is shown in figure 9.

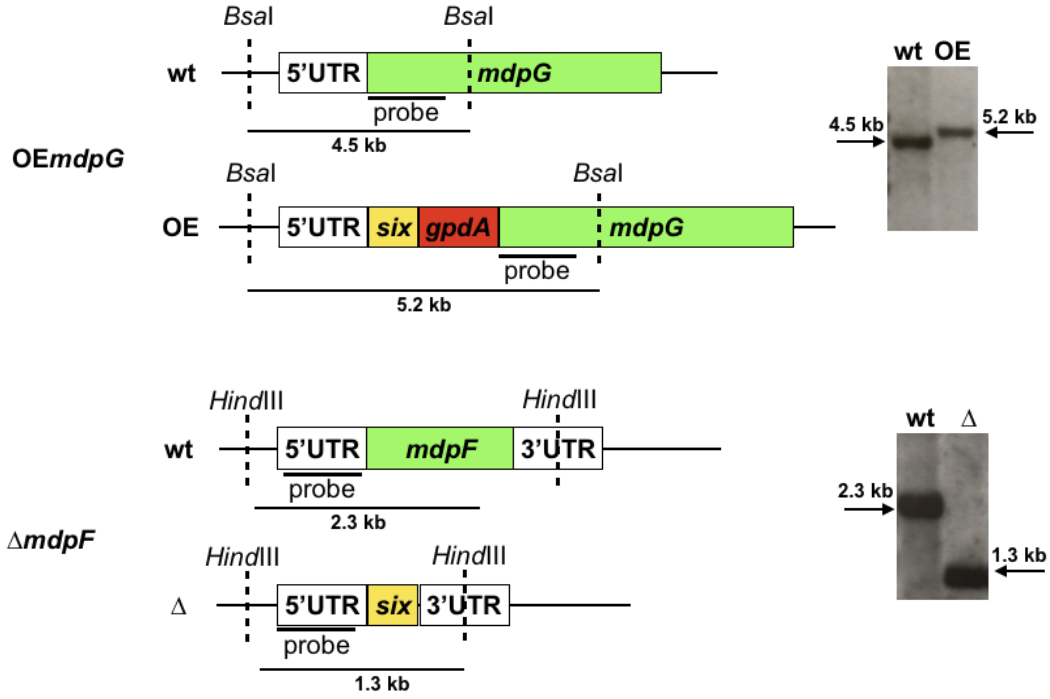

Figure 9. Restriction map and Southern hybridization after the marker was recycled.
For OE*mdpG*, *Bsa*I was used and the first 1.5 kb of *mdpG* was used as the probe. The probe targeted fragment of the wild type is 4.5 kb and the OE*mdpG* is 5.2 kb. For deletion of the *mdpF*, *Hind*III was used and the 5'UTR of *mdpF* was used as the probe. The probe targeted fragment of the wild type is 2.3 kb and the Δ*mdpF* is 1.3 kb.

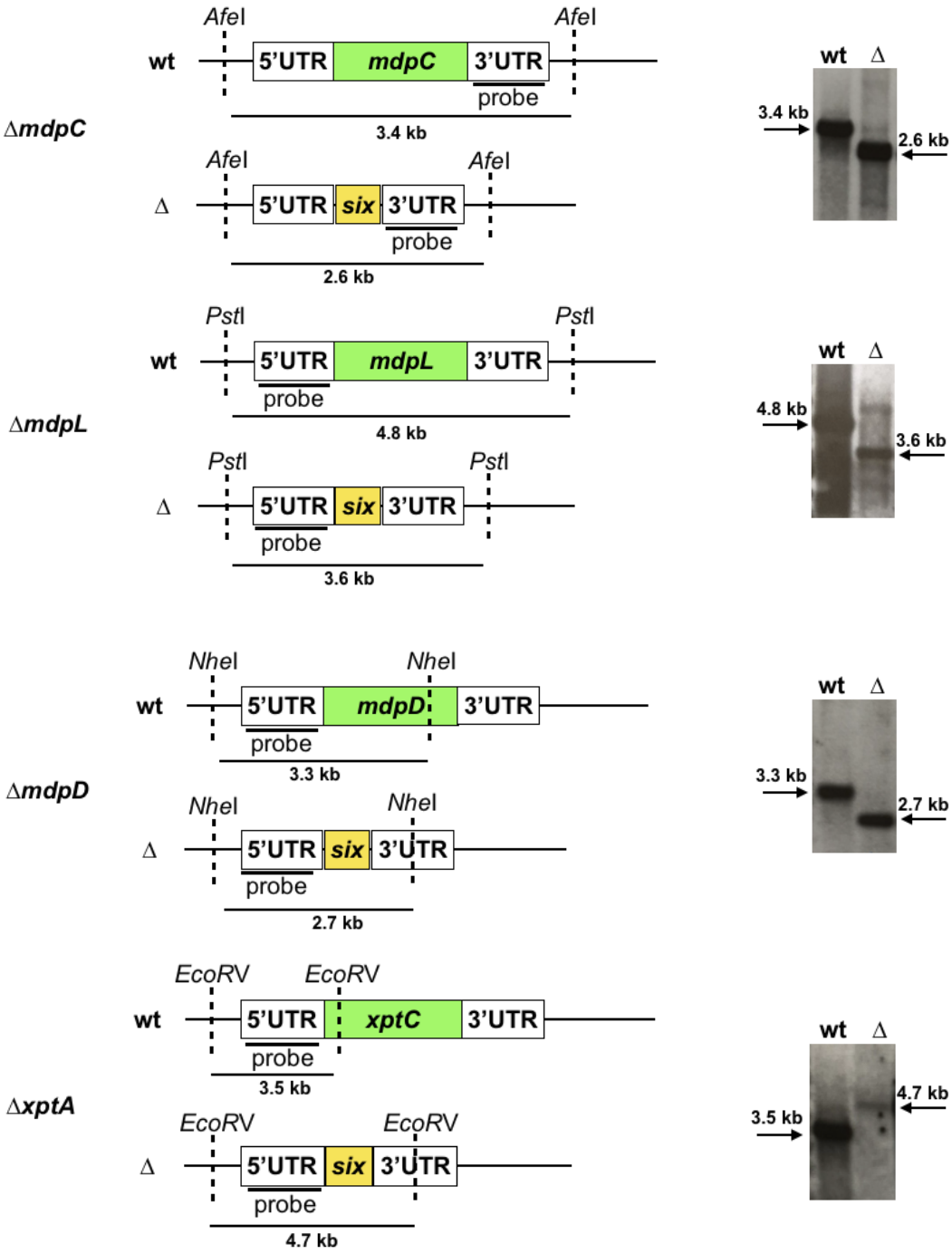

Figure 9. Continued, Restriction map and Southern hybridization after the marker was recycled. For deletion of the *mdpC*, *Afe*I was used and the 3'UTR of *mdpC* was used as the probe. The probe targeted fragment of the wild type is 3.4 kb and the Δ*mdpC* is 2.6 kb. For deletion of the *mdpL*, *Pst*I was used and the 5'UTR of *mdpL* was used as the probe. The probe targeted fragment of the wild type is 4.8 kb and the Δ*mdpL* is 3.6 kb. For deletion of the *mdpD*, *Nhe*I was used and the 5'UTR of *mdpD* was used as the probe. The probe targeted fragment of the wild type is 3.3 kb and the Δ*mdpD* is 2.7 kb. For deletion of the *xptA*, *EcoR*V was used and the 5'UTR of *xptA* was used as the probe. The probe targeted fragment of the wild type is 3.5 kb and the Δ*xptA* is 4.7 kb.

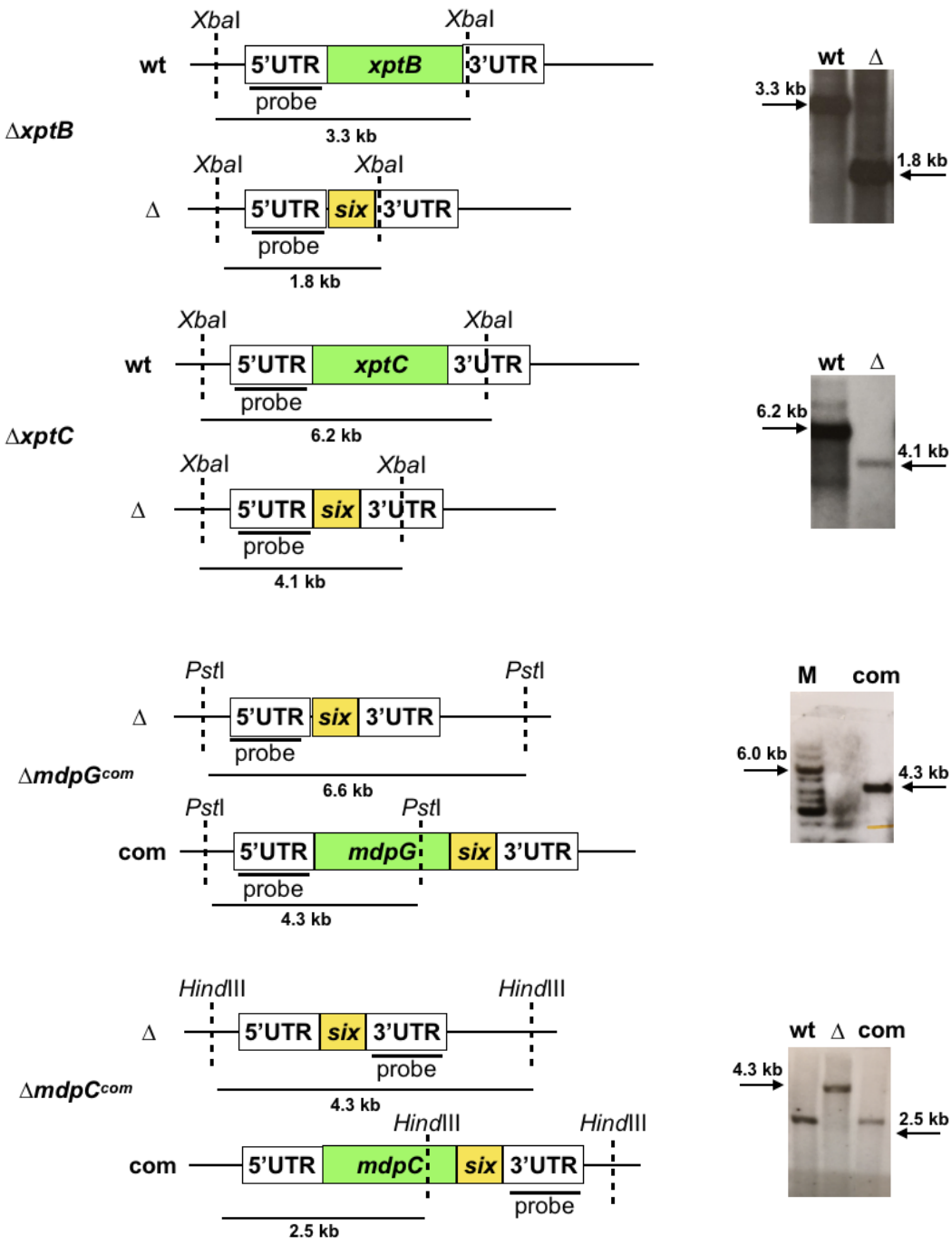

Figure 9. Continued, Restriction map and Southern hybridization after the marker was recycled. For deletion of the *xptB*, *Xba*I was used and the 5'UTR of *xptB* was used as the probe. The probe targeted fragment of the wild type is 3.3 kb and the Δ*xptB* is 1.8 kb. For deletion of the *xptC*, *Xba*I was used and the 5'UTR of *xptC* was used as the probe. The probe targeted fragment of the wild type is 6.2 kb and the Δ*xptC* is 4.1 kb. For *mdpG* complementation, *Pst*I was used and the 5'UTR of *mdpG* was used as the probe. The probe targeted fragment of the deletion strain is 6.6 kb and the complementation and the wild type is 4.3 kb (M: 1kb DNA ladder, com: complementation). For *mdpC* complementation, *Hind*III was used and the 3'UTR of *mdpC* was used as the probe. The probe targeted fragment of the deletion strain is 4.3 kb and the complementation and the wild type is 2.5 kb.

2.5 Secondary metabolites methods

2.5.1 Extraction of secondary metabolites

Extraction of secondary metabolites was performed from solid agar plates. 4 µl containing approximate 1000 fresh conidiospores were point-inoculated on MM agar plate and grown sexually in dark conditions for three and five days. Subsequently, the colonies were digged by 50 ml tube (Φ = 2.7 cm) with 5.7 cm^2 agar piece and cut into small pieces (0.5 cm^2, approximately), transferred into 50 ml tube and covered with 5 ml ethyl acetate. Samples were shaken at 200 rpm at rt for 30 min followed by 10 min ultra-sonication in a Bandelin Sonorex™ Digital 10P ultrasonic bath from Bandelin Electronic GmbH & Co. KG (Berlin, Germany) at highest level. 3 ml ethyl acetate was transferred to glass tube and evaporated in a Hei-VAP-Advantage rotary evaporator from Heidolph Instruments GmbH & Co. KG (Schwabach, Germany) with a MWG Lauda RM6 from Lauda-Brinkmann LP (Delran, NJ, USA) and a Laboxact KNF vacuum system (Sigma-Aldrich, Germany) at 37°C under constant gyration (200 rpm) and samples were stored at -20°C.

2.5.2 Separation of secondary metabolites by TLC

-20°C stored SM extracts were resolved in 700 µl methanol, 15 µl of SMs and 5 µl of 25mg/ml pure emodin and chrysophanol were separated on TLC in chloroform / methanol 9:1 (v/v) with trifluoroacetic acid (0.1% (v/v)) (Gerke *et al.,* 2012a). Metabolites were visualized under UV light λ = 366 nm, 254 nm and white light. The data were documented using CAMAG TLC Visualizer (CAMAG, Muttenz, Switzerland).

2.5.3 Identification of secondary metabolites by LC-MS

-20°C stored SM extracts were resolved in 700 µl methanol and centrifuged 10 min at 13,000 g at 4°C (table top centrifuge). 500 µl supernatant was transferred to LC-MS vial. Liquid chromatography-coupled mass spectrometry was done using a Q ExactiveTM Focus orbitrap mass spectrometer coupled to a Dionex Ultimate 3000 HPLC (Thermo Fisher Scientific). 5 µl of each sample was injected on a HPLC column (AcclaimTM 120, C_{18}, 5 µm, 120 Å, 4.6 x 100 mm). A linear gradient from 5-95% (v/v) acetonitrile/0.1 formic acid in 20 min, plus additional 10 min with 95% (v/v) acetonitrile/0.1 formic acid) with a flow rate of 0.8 ml/min at 30°C was

used. The measurements were performed in a mass range of 70-1050 m/z in positive and negative mode. Data analysis was performed with FreeStyle™ 1.4 (Thermo Fisher Scientific, Schwerte, Germany).

2.5.3 Relative quantification of secondary metabolites

SMs extracted from three and five days of sexual growth were measured with LC-MS as described above. PABA with final concentration of 0.002% (w/v) was added to each SMs sample for relative quantification. Relative quantification of each component was calculated from relative peak area (detected with a charged aerosol detector (CAD)) compared to the peak area of internal standard PABA (set to 100%).

2.6 Morphological and developmental analysis of *A. nidulans*

A. nidulans phenotypical analysis was performed for asexual and sexual development. Approximate 1000 fresh conidiospores per strain were point-inoculated on minimal medium agar plate and cultivated for three days in light to induce asexual development and in dark and sealed by parafilm to induce sexual development, respectively. Developmental analysis was performed from conidiospores, sexual fruiting bodies and Hülle cells.

2.6.1 The productivity of conidiospores in the light

Conidiospores productivity was detected as follows. Spores were collected from a single colony by using 200 µl pipette tips to dig 0.2 cm^2 agar pieces from colony center, middle and border, separately. The agar pieces were vortex-washed 15 min in 1ml tween-80 buffer. The spores containing buffer was collected for spore concentration measurement by spore counter (Backman Coulter Z2). The relative spore productivity was calculated relative to wild type. This detection was performed in two biological replicates with three technical replicates.

2.6.2 Analysis of viability of conidiospores

Viability of spores over time was analyzed as described (Thieme *et al.*, 2018). 100 µl of 200 fresh conidiospores per strain were stored at 4°C and completely separated on 20 ml MM agar plate after zero, two, five and 14 days with triplicates and germinated for two days at 37°C.

Spore viabilities were calculated as a ratio of the number of countable colonies relative to the initial spore formed colonies. This analysis was performed in three biological replicates.

2.6.3 Analysis of germination of conidiospores

The spore germination was analyzed as follows. Fresh spores with 20 (±1) per strain were picked by MSM System 300 micromanipulator (Singer Instruments) separately and placed on fresh agar plate in matrix. After two days at 37°C, the spore germination was calculated as a ratio of the visible colonies to the number of the placed spores. This analysis was performed in two biological replicates with two technical replicates.

2.6.4 Monitor of sexual development under sexual growth conditions

Monitoring of sexual fruiting body development was traced from two, three, four, five, seven and 10 days under sexual growth. The formation and maturation of the cleistothecia at the colony center were recorded over time with photomicrograph. Up to 10 days, mature cleistothecia were collected as above described of conidiospore collection. Cleistothecia were vortex-washed 4 times in water to take off the covering Hülle cells. The naked cleistothecia were counted and their sizes were measured by microscope with software cellSens Dimension. Detached Hülle cells from cleistothecia were collected at the third and fifth day, respectively, by rolling cleistothecia on agar surface. The size of Hülle cells with 150 (±10) per strain was measured by microscope with software cellSens Dimension. All measurements were performed in two biological replicates.

2.6.5 Analysis of germination of Hülle nursing cells for sexual fruiting body formation

Hülle cells of three and five days old, sexually grown wild type, Δ*mdpG*, Δ*mdpC* and Δ*mdpL* colonies were used to pick cleistothecia with attached Hülle cells, which were then transferred to a fresh MM agar plate. 40 (±1) Hülle cells were picked using an MSM System 300 micromanipulator (Singer Instruments) and placed on separate fresh MM plates to directly compare the germination of Hülle cells. It was taken particular care that no spores were “sticking” to Hülle cells while transferring them. Plates were incubated 48 hours at 37°C

under light conditions. The rate of germination of Hülle cells was quantified by countable colonies after 48 hours' cultivation. The test was performed in three biological replicates.

2.7 Protein methods

2.7.1 Protein extraction

Approximate 1000 fresh conidiospores were point-inoculated on MM agar plates and grown for three days and five days under sexual growth conditions at 37°C. For protein isolation from sexual tissues, samples were harvested from plate colonies directly and frozen in liquid nitrogen immediately. Frozen samples were ground in a MM400 table mill (Retsch) and approximately 200 mg of the resulting powder was mixed with 300 µl of B_+ buffer (300 mM NaCl, 100 mM Tris pH 7.5, 10% glycerol, 1 mM EDTA, 0.1% NP-40) supplemented with 1.5 mM DTT, 1 tablet/50 ml complete EDTA-free protease inhibitor cocktail (Roche), 1 mM PMSF and phosphatase inhibitor mix (1 mM NaF, 0.5 mM sodium-orthovanadate, 8 mM ß-glycerolphosphate disodium pentahydrate and 1.5 mM benzamidine). The powder mixture was centrifuged for 10 min at 13000 rpm at 4°C. Supernatant was stored in ice and transferred into a fresh tube and protein concentration was measured with the NanoDrop ND-1000 spectrophotometer (Peqlab). Protein samples were mixed with 3x SDS sample buffer (250 mM Tris-HCl pH 6.8, 15% β-mercaptoethanol, 30% glycerol, 7% SDS, 0.3% bromophenol blue) and denatured at 95°C for 5 min followed by 5 min incubation on ice. Samples were stored at -20°C for further experiments.

2.7.2 SDS-PAGE and western hybridization

SDS-polyacrylamide gel electrophoresis (SDS-PAGE) is used to separate proteins according to size for western hybridization (Laemmli, 1970, Schinke *et al.*, 2016). Equal amounts of protein were loaded on SDS gel and separated according to size. Stacking gel: 3.67 ml H_2O, 625 µl 1 M Tris pH 6.8, 30 µl 10% SDS, 650 µl 30% acrylamide, 5 µl TEMED and 25 µl 10% APS. Separation gel: 2.8 ml H_2O, 3.75 ml 1 M Tris pH 8.8, 100 µl 10% SDS, 3.3 ml 30% acrylamide, 10 µl TEMED and 50 µl 10% APS. First at 100 V during ca.10 min to let all of the samples reach to the same level and then at 200 V in running buffer (25 mM Tris, 0.25 M glycine, 0.1% SDS) for 45 min. Proteins from SDS gels were blotted for 60 min at 100 V on Amersham™

Protran™ 0.45 µm NC nitrocellulose membranes (GE Healthcare) in ice cooled transfer buffer (25 mM Tris, 192 mM glycine, 0.02% SDS) (Towbin *et al.*, 1979). After the transfer, membranes were stained with Ponceau staining as loading control before the blocking step (Romero-Calvo *et al.*, 2010). Membranes were blocked with 5% skim milk powder dissolved in TBS-T buffer (10 mM Tris-HCl pH 8.0, 150 mM NaCl, 0.05% Tween 20) for at least 1 hour at rt and subsequently probed with the first antibody in TBST-M (blocking solution) (TBS-T buffer, supplemented with 5% skim milk powder or BSA, according to antibody requirement) and incubated o/n at 4°C (incubation with the first antibody can be also performed 1 hour at rt). Antibody solution(s) was (were) collected and membranes were washed three times in TBS-T for 10 min each step under constant agitation at rt. After the last washing step, membranes were directly incubated for 1 hour at rt with the secondary antibody in TBST-M. Membranes were washed thrice for 10 min with TBS-T under constant agitation at rt. For target protein detection, membranes were covered with a 1:1 mixture of solution A (2.5 µM luminol, 400 µM paracoumarat, 100 mM Tris-HCl pH 8.5) and solution B (5.4 mM H_2O_2, 100 mM Tris-HCl pH 8.5) and incubated for 2-5 min under constant agitation at rt in the dark (Suck *et al.*, 1996). Chemiluminescent signals were detected by exposing the membranes to Amersham™ Hyperfilm™ ECL (GE Healthcare).

In this study, we examined one of the MAPK member SakA protein expression levels in *mdp* mutant strains. For total SakA-GFP protein, the first antibody was 1:1000 mouse α-GFP antibody (sc-9996, Santa Cruz Biotechnology, Dallas, TX, USA) in TBST-M (TBST buffer, supplemented with 5% (w/v) skim milk powder), and the second antibody was 1:1000 horseradish peroxidase coupled goat α-mouse antibody (115-035-003, Jackson Immuno Research, West Grove, CA, USA) in TBST-M (TBST buffer, supplemented with 5% (w/v) skim milk powder). For phosphorylated SakA protein, the first antibody was 1:2000 P-p38 ((Thr180/Tyr182) (D3F9) XP® Rabbit mAb #4511) in TBST-M (TBST buffer, supplemented with 5% (w/v) BSA), and the second antibody was 1:2000 horseradish peroxidase coupled goat anti-rabbit lgG (H+L) antibody (659520, Themo Fisher Scientific) in TBST-M (TBST buffer, supplemented with 5% (w/v) BSA).

2.8 Stress tests

Stress tests affecting fungal growth were performed as follows. 0.01 mM menadione sodium bisulfite, 1 mM diamide and 1 mM potassium sorbate were mixed in MM medium separately, and UV stress test was performed by cultivating MM medium plate under UV 366 nm (Sylviana UV light, 5 µW) for five days. 4 µl containing approximate 1000 fresh conidiospores per strain were point- inoculated on the same plate with different stressing agents. The impact of the different treatments over the mutants was always in comparison with the wild type present in each plate as well as with the control plate (only MM grown under the same conditions). Plates were cultivated for five and 10 days at 37°C in darkness. The colonies were recorded after five days and the analysis of development of the sexual fruiting bodies was performed after five and 10 days separately. Further information about the stress tests will be detailed in the corresponding Results section.

2.9 Bioactivity test of secondary metabolites

2.9.1 Secondary metabolites bioactivity of *mdp/xpt* clusters on fungi

Secondary metabolites of *mdp/xpt* mutant strains and *A. nidulans* wild type, extracted from single colonies as described in **2.5.1** with nine replicates, were dissolved in 450 µl methanol. 30 µl extract solution was loaded on filter paper disc (Φ = 9 mm) individually. 30 µl pure methanol was used as a blank control. Before placing on spore-inoculated ager plates, filter paper discs were dried completely in sterile bench with air flow. 0.075 mg pure emodin and chrysophanol were dissolved in methanol and also loaded on the paper disc for following tests. The next step was placing these SMs loaded paper discs on tested fungi. For *A. nidulans* wild type, $1x10^5$ fresh conidiospores were completely separated on 80 ml minimal medium (MM) agar plates. The SMs loaded and blank control paper discs were placed and the plates were sealed by parafilm and covered by aluminum foil for induction of sexual development and were incubated for five days at 37°C. The confocal microscope with software cellSens Dimension was used to measure the size and count the amount of sexual fruiting bodies on each paper disc. For *Sordaria macrospora*, $2x10^5$ spores were pre-inoculated on cornmeal malt fructification medium (BMM) agar plates and placed with the SMs loaded paper discs as described above,

grown for 7 days at 27°C. For *Verticillium* sp., $1x10^5$ spores were pre-inoculated on simulated xylem medium (SXM) agar plates and placed with the SMs loaded paper discs, grown for 10 days at 25°C. For *Colletotrichum graminicola*, $5x10^6$ spores were inoculated on complete medium (CM) agar plates and placed with the SMs loaded paper discs, grown for 7 days at room temperature under continuous fluorescent light (Climas Control CIR, UniEquip, Martiensried, Germany).

2.9.2 Bioactivity of emodin on the egg laying activity of *Drosophila melanogaster*

2 ml of a combination of DPM and GMM (6.25% cornmeal, 6.25% brewer's yeast, 2% glucose, 4% sucrose, 1.2% 1 M phosphate buffer, 2% 50x MM salts, 0.1% 1000x Hutner's trace elements, 1% agar) was boiled up for 15 min and autoclaved at 112°C. For phosphate buffer, 50x MM salts and Hutner's trace elements see (http://www.fgsc.net/Aspergillus-/asperghome.html) were filled in 24-well plates and mixed with 0.04 mg/ml (final concentration) of emodin, and pure ethanol as blank control. One fertilized female *Drosophila melanogaster* of the same generation was added in each well. After three days at 30°C in darkness, the flies were removed and the deposited eggs were enumerated under the binocular. Additionally, one fertilized female was set on emodin-free DPM/GMM as a control (Goldman *et al.*, 2018).

3 Results

3.1 *A. nidulans mdp/xpt* secondary metabolite clusters produce emodins and benzophenones as intermediates resulting in epi-/shamixanthone as final products in Hülle cells during sexual development.

3.1.1 The *mdp/xpt* clusters produce emodins and benzophenones as intermediates resulting in epi-/shamixanthone as final products.

The *mdp/xpt* gene clusters consist of three subunits scattered on three different chromosomes in *A. nidulans*. They harbor one polyketide synthase (PKS) gene and 14 "tailoring" genes. Previous researches showed that the whole gene clusters can produce approximately 33 compounds (summarized in figure 6). 10 out of 15 genes of the *mdp/xpt* clusters, namely *mdpC, mdpD, mdpE, mdpF, mdpH, mdpL, mdpI, mdpJ, mdpK* and *xptA*, were specifically up-regulated after 72 hours of fungal sexual development (Bayram *et al.*, 2016). Furthermore, proteomics data showed that the PKS MdpG and the other four "tailoring" enzymes, MdpH, MdpL, XptB and XptC were localized in sexual mycelia and Hülle cells (Dirnberger, 2018).

In an effort to get more insights into the products of the *mdp/xpt* clusters during fungal sexual development, the backbone PKS encoding gene *mdpG* was overexpressed and deleted and the following seven key genes in the biosynthetic pathway, *mdpF, mdpC, mdpL, mdpD, xptA, xptB* and *xptC*, were deleted separately.

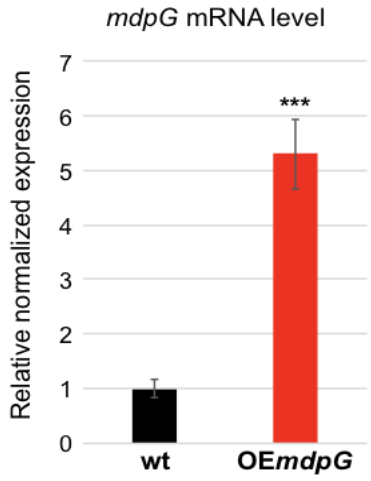

Figure 10. The gene *mdpG* was upregulated in OE*mdpG* mutant strain (AGB1235) in comparison to wild type (AGB552).

RNA samples were collected from vegetatively grown mycelium after 24 hours. Gene expression of *mdpG* was measured with qRT-PCR and *h2A* (AN3468) served as house-keeping gene. Data were collected from two biological and three technical replicates. Error bar means standard deviation, ***$P < 0.005$, wt = wild type, OE = overexpression.

As shown in figure 10, the gene *mdpG* was up-regulated more than 5 times in its overexpression strain AGB1235 in comparison to the wild type (wt) strain AGB552.

Then, SMs were extracted after three and five days of sexual growth and subjected to a TLC (Fig. 11). Two pure commercial compounds were used as markers: emodin and chrysophanol. All deletion strains exhibited SM production changes in comparison to wild type except the *mdpG* overexpression strain. Deletion of the genes *mdpG* and *mdpF* resulted in the loss of several wild type products as well as deletion of the genes *mdpC, mdpL, mdpD, xptA, xptB* and *xptC*, but these deletions led to various products accumulation. Emodin could be identified in the deletion strain Δ*mdpC* after three days of sexual growth but the amount of emodin was lower after five days of sexual growth. In the case of Δ*mdpL*, both emodin and chrysophanol were identified after three days, whereas emodin was decreased and chrysophanol was increased after five days.

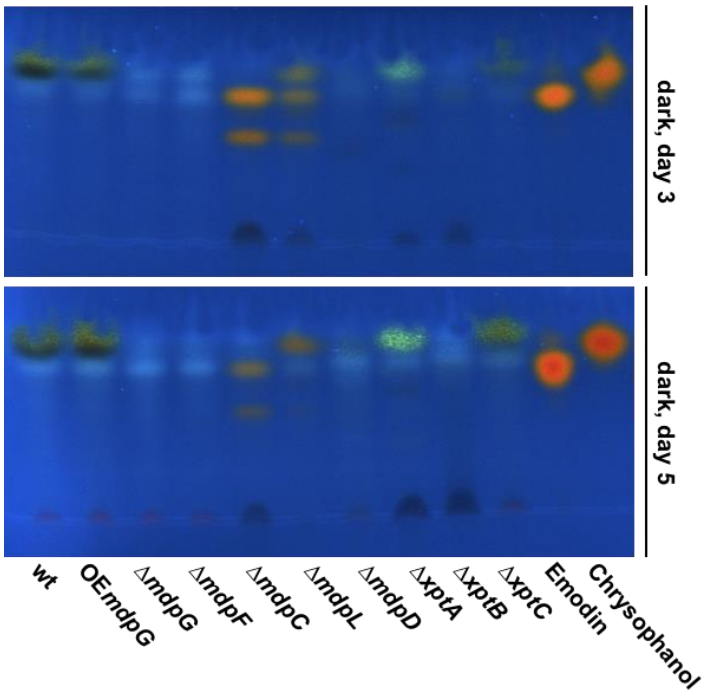

Figure 11. Deletion of genes of *mdp/xpt* clusters resulted in the accumulation of various compounds including emodin and chrysophanol in *A. nidulans*.

Approximately 1000 conidiospores of *A. nidulans* wild type and *mdp/xpt* mutant strains were point-inoculated on minimal medium (MM) agar plate and cultivated for three and five days at 37°C in dark. Agar pieces containing the colony were extracted with ethyl acetate. Extracted SMs were dissolved in methanol and separated by chloroform/methanol 9:1 (v/v) with trifluoroacetic acid (0.1% (v/v)), and pure emodin and chrysophanol were used as markers. TLC plates were visualized under UV light (λ = 366 nm). wt = wild type, OE = overexpression, Δ = deletion.

To identify the SMs observed on the TLC, high performance liquid chromatography coupled to mass spectrometry was used (Fig. 12-13). Wild type (wt) of *A. nidulans* produced the final products, shamixanthone (**2**) and epishamixanthone (**3**) (Fig. 12-13, table 6) as well as the intermediates emericellin (**1**) and arugosin A (**18**). Deletion of the first two genes encoding enzymes in the biosynthetic pathway, *mdpG* and *mdpF*, resulted in complete loss of the final products shamixanthone (**2**) and epishamixanthone (**3**). Deletion of the genes *mdpC*, *mdpL*, *mdpD*, *xptA*, *xptB* and *xptC* also resulted in the abolishment of the final products but the strains accumulated various intermediates during sexual development (Fig. 12-13, table 6).

Deletion of the gene *mdpC* resulted in the accumulation of 2, ω-dihydroxyemodin (**4**), ω-hydroxyemodin (**5**) and emodin (**6**) during sexual development. Deletion of the gene *mdpL* accumulated the same compounds observed in Δ*mdpC* in addition to chrysophanol (**7**). Deletion of the gene *mdpD* mainly accumulated benzophenone alcohol (**8**), paeciloxanthone (**9**) and traces of monodictyphenone (**12**) and three unidentified compounds, **14** ($C_{30}H_{26}O_9$), **15** ($C_{20}H_{22}O_5$) and **19** ($C_{15}H_{12}O_5$) at the early stage of sexual development. Secondary metabolites extracted from five days-old surface cultures grown in the dark, revealed two new products in the deletion mutant strain *mdpD*, **10** ($C_{15}H_{14}O_5$) and compound **13**, while compound **14** was lost. Compound **13** is 3-(2,6-dihydroxyphenyl)-4-hydroxy-6-methyl-1(3H)-isobenzofuranone, which is a derivative of monodictyphenone. In this study, this compound was named "post-monodictyphenone".

The *xptA* deletion strain accumulated a high amount of variecoxanthone A (**11**) as well as a trace of compound **10**, **12**, **15** ($C_{20}H_{22}O_5$), **16** ($C_{15}H_{12}O_5$) and **17** ($C_{22}H_{25}NO_6$). The compound **16** was absent after five days. Deletion of the gene *xptB* accumulated compound **4** and trace amounts of compound **10**, **12** and **13** after three days-old sexual growth. Therein, the compound **4** was decreased after five days of sexual growth. Deletion of the last enzyme encoding gene of the biosynthetic pathway, *xptC*, accumulated compound **12**, arugosin A (**18**) and emericellin (**1**). The latter two were also present in the SMs extracted from the wild type. Arugosin A (**18**) was detected in high amounts in wild type but was decreased in the Δ *xptC* strain.

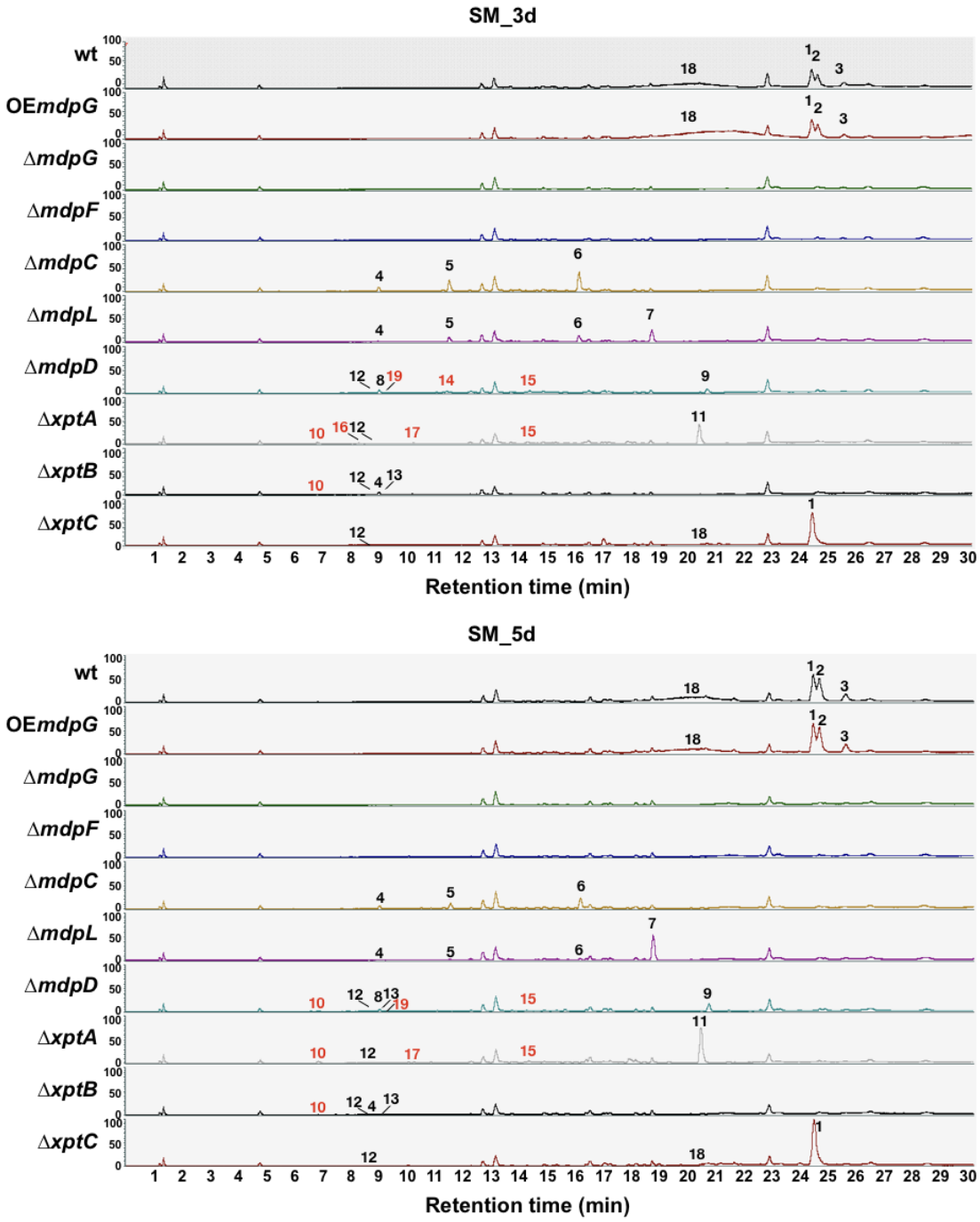

Figure 12. Deletion of genes of *mdp/xpt* clusters resulted in the accumulation of various intermediates of epi-/shamixanthone in *A. nidulans*.

Chromatogram of extracellular and intracellular secondary metabolites (SMs) of each *mdp/xpt* mutant strain was detected by LC-MS with a charged aerosol detector (CAD). Y-axis means Abs (absorbance units). SMs were harvested from point-inoculated cultures after three days (SM_3d) and five days (SM_5d) of sexual growth. wt = wild type, OE = overexpression, Δ = deletion. **1**) emericellin; **2**) shamixanthone; **3**) epishamixanthone; **4**) 2, ω-dihydroxyemodin; **5**) ω-hydroxyemodin; **6**) emodin; **7**) chrysophanol; **8**) benzophenone alcohol; **9**) paeciloxanthone; **10**) $C_{15}H_{14}O_5$; **11**) variecoxanthone A; **12**) monodictyphenone; **13**) post-monodictyphenone; **14**) $C_{30}H_{26}O_9$; **15**) $C_{20}H_{22}O_5$; **16**) $C_{15}H_{12}O_5$; **17**) $C_{22}H_{25}NO_6$; **18**) arugosin A; **19**) $C_{15}H_{12}O_5$. Red numbers: unidentified compounds.

Taken together, the backbone PKS protein MdpG is the first enzyme in the biosynthetic pathway of epi-/shamixanthone. A strain that overexpressed the PKS encoding gene *mdpG* (OE*mdpG*) under the constitutive promoter of *gpdA* exhibited gene up-regulation in mRNA level (Fig. 10) but no difference in secondary metabolite production in comparison to the wild type (Fig. 11-13). As seen in the figure 12 and 13, by deleting genes of *mdp/xpt* clusters, the respective mutant strains did not produce the final products any more but accumulated various intermediates of epi-/shamixanthone during sexual development. In particular, the deletion mutant strains of *mdpC*, *mdpL*, *mdpD*, *xptA* and *xptB* exhibited a high diversity of the accumulated intermediates. Moreover, there were dynamic changes of components when comparing the compound composition after three or five days of sexual growth.

To further investigate the component changes produced by the deletion strains of *mdpC*, *mdpL*, *mdpD*, *xptA* and *xptB* during sexual development, a relative quantification of the compounds was performed, which was based on the internal standard PABA (peak area was set to 100%). As shown in figure 14, after grown three days in dark, SMs of Δ*mdpC* contained 90% of 2, ω-dihydroxyemodin (**4**), 394% of ω-hydroxyemodin (**5**) and 851% of emodin (**6**), which were decreased to 83%, 230% and 543% respectively after five days of sexual growth. SMs of Δ*mdpL* contained 8% of **4**, 127% of **5**, 218% of **6** and 349% of chrysophanol (**7**) after three days of sexual growth. After five days, the relative quantity of the former three compounds (**4**-**6**) decreased to 0.01 %, 11% and 25%, respectively, while a 2.5-fold increase was observed for compound **7** (860%). A decrease in benzophenone alcohol (**8**) was observed in Δ*mdpD* from 116% after three days to 40% after five days of sexual growth. On the contrary, an increase in paeciloxanthone (**9**) was observed in Δ*mdpD* from 173% after three days to 312% after five days. Variecoxanthone A (**11**) increased in Δ*xptA* from 872% after three days to 1893% after five days. No difference in compound **10** was observed in Δ*xptA*. Δ*xptB* contained trace amounts of compound **4** (1.1%), compound **10** (0.4%) and monodictyphenone (**12**) (8.6%) as well as 55.3% of its derivative (**13**) after three days of sexual growth. After five days of sexual growth, the former three compounds (**4**, **10** and **12**) decreased below limit of detection whereas the relative quantity of compound **13** decreased 14-fold (4%) after five days. Compounds **14**, **15**, **16**, **17** and **19** were only present in trace amounts and were below the limit of quantification.

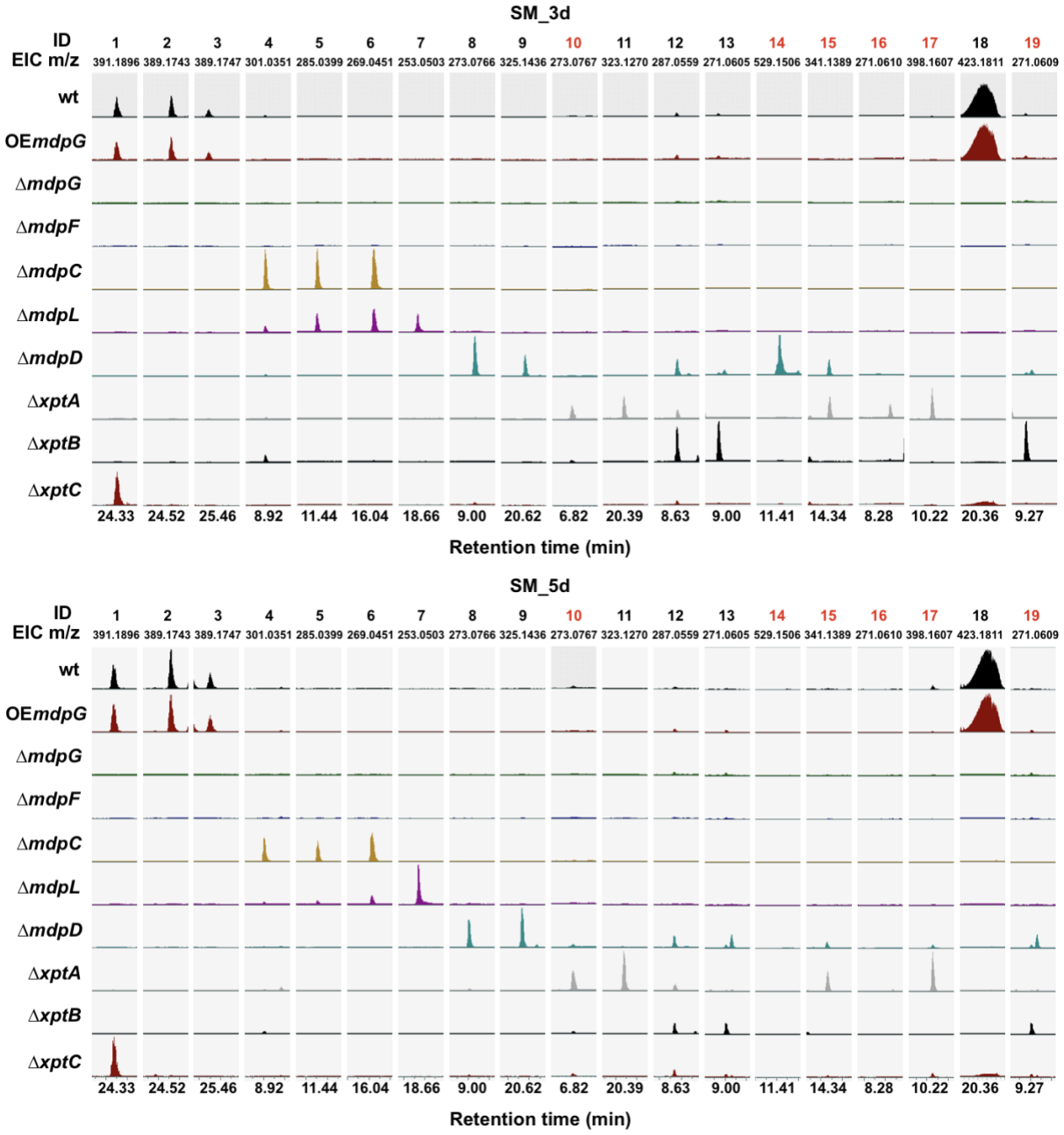

Figure 13. Deletion of genes of *mdp/xpt* clusters resulted in the accumulation of various emodin, benzophenone and xanthone derivatives in *A. nidulans*.

EICs (extracted ion chromatogram) of the accumulated compounds in SM_3d and SM_5d of *mdp/xpt* mutant strains were analyzed in positive and negative modes. wt = wild type, OE = overexpression, Δ = deletion. ID: compound number used in this study. m/z of **1**, **2**, **3**, **9** and **11** were detected in positive mode, the rest were detected in negative mode. **1**) emericellin; **2**) shamixanthone; **3**) epishamixanthone; **4**) 2, ω-dihydroxyemodin; **5**) ω-hydroxyemodin; **6**) emodin; **7**) chrysophanol; **8**) benzophenone alcohol; **9**) paeciloxanthone; **10**) $C_{15}H_{14}O_5$; **11**) variecoxanthone A; **12**) monodictyphenone; **13**) post-monodictyphenone; **14**) $C_{30}H_{26}O_9$; **15**) $C_{20}H_{22}O_5$; **16**) $C_{15}H_{12}O_5$; **17**) $C_{22}H_{25}NO_6$; **18**) arugosin A; **19**) $C_{15}H_{12}O_5$. Red numbers: unidentified compounds.

Table 6. Metabolite markers identified by HPLC-MS

UN: Unidentifiied compound; A: Exact mass measurement; B: UV/VIS spectra; C: MS/MS fragment information from commercial standard; D: MS/MS fragment information from literature.

ID	Metabolite marker	Retention time(min)	Detected as	Sum formula	Exact mass measured	Exact mass calculated	Confirmed by	Reference
1	emericellin	24.33	[M-H2O+H]+	C25H28O5	408.0005	408.1937	A,B	James F. Sanchez et al. 2011
2	shamixanthone	24.52	[M-H2O+H]+	C25H26O5	406.1743	406.1780	A,B	James F. Sanchez et al. 2011
3	epishamixanthone	25.46	[M-H2O+H]+	C25H26O5	406.1747	406.1780	A,B	James F. Sanchez et al. 2011
4	2,ω-dihydroxyemodin	8.96	[M-H]-	C15H10O7	302.0351	302.0348	A,B	James F. Sanchez et al. 2011
5	ω-hydroxyemodin	11.48	[M-H]-	C15H10O6	286.0399	286.0477	A,B	James F. Sanchez et al. 2011
6	emodin	16.09	[M-H]-	C15H10O5	270.0451	270.0528	A,B,C	James F. Sanchez et al. 2011
7	chrysophanol	18.66	[M-H]-	C15H10O4	254.0503	254.0579	A,B	James F. Sanchez et al. 2011
8	benzophenone alcohol	9.00	[M-H]-	C15H14O5	274.0766	274.0841	A	Daniel Pockrandt et al. 2012
9	paeciloxanthone	20.62	[M+H]+	C20H20O4	324.1435	324.1362	A	James F. Sanchez et al. 2011
10	UN	6.82	[M-H]-	C15H14O5	274.0767	274.0841	A	—
11	variecoxanthone A	20.39	[M-H2O+H]+	C20H20O5	340.1270	340.1311	A,B	James F. Sanchez et al. 2011
12	monodictyphenone	8.63	[M-H]-	C15H12O6	288.0558	288.0634	A	James F. Sanchez et al. 2011
13	post-monodictyphenone	9.00	[M-H]-	C15H12O5	272.0605	272.0685	A	James F. Sanchez et al. 2011
14	UN	11.41	[M-H]-	C30H26O9	530.1506	530.1577	A	—
15	UN	14.34	[M-H]-	C20H22O5	342.1389	342.1467	A	—
16	UN	8.28	[M-H]-	C15H12O5	272.0610	272.0685	A	—
17	UN	10.22	[M-H]-	C22H25O6N	399.1607	399.1682	A	—
18	arugosin A	20.36	[M-H]-	C25H28O6	424.1811	424.1964	A,D	Daniel Pockrandt et al. 2012 JC Albright et al. 2015
19	UN	9.27	[M-H]-	C15H12O5	272.0609	272.0685	A	—
20	austinol	12.68	[M+H]+	C25H30O8	458.2013	458.1941	A,B	Szewczyk et al., 2008
21	dehydroaustinol	13.15	[M+H]+	C25H28O8	456.1859	456.1857	A,B	Szewczyk et al., 2008
22	UN	22.61	[M+H]+	C18H35NO	281.2791	281.2719	A	—

Taken together, the *mdp/xpt* clusters produced epi-/shamixanthone as final products during fungal sexual development in *A. nidulans*. Deletion of the genes in *mdp/xpt* clusters interrupted the biosynthetic pathway resulting in the accumulation of emodin, benzophenone and their various derivatives (Fig. 12 and 13), and the amount of these intermediates changed along with the fungal development process (Fig. 14). 2, ω-dihydroxyemodin (**4**), ω-hydroxyemodin (**5**),

emodin (**6**), benzophenone alcohol (**8**), monodictyphenone (**12**) and compound **13** were decresed but chrysophanol (**7**), paeciloxanthone (**9**) and variecoxanthone A (**11**) were increased after five days of sexual growth.

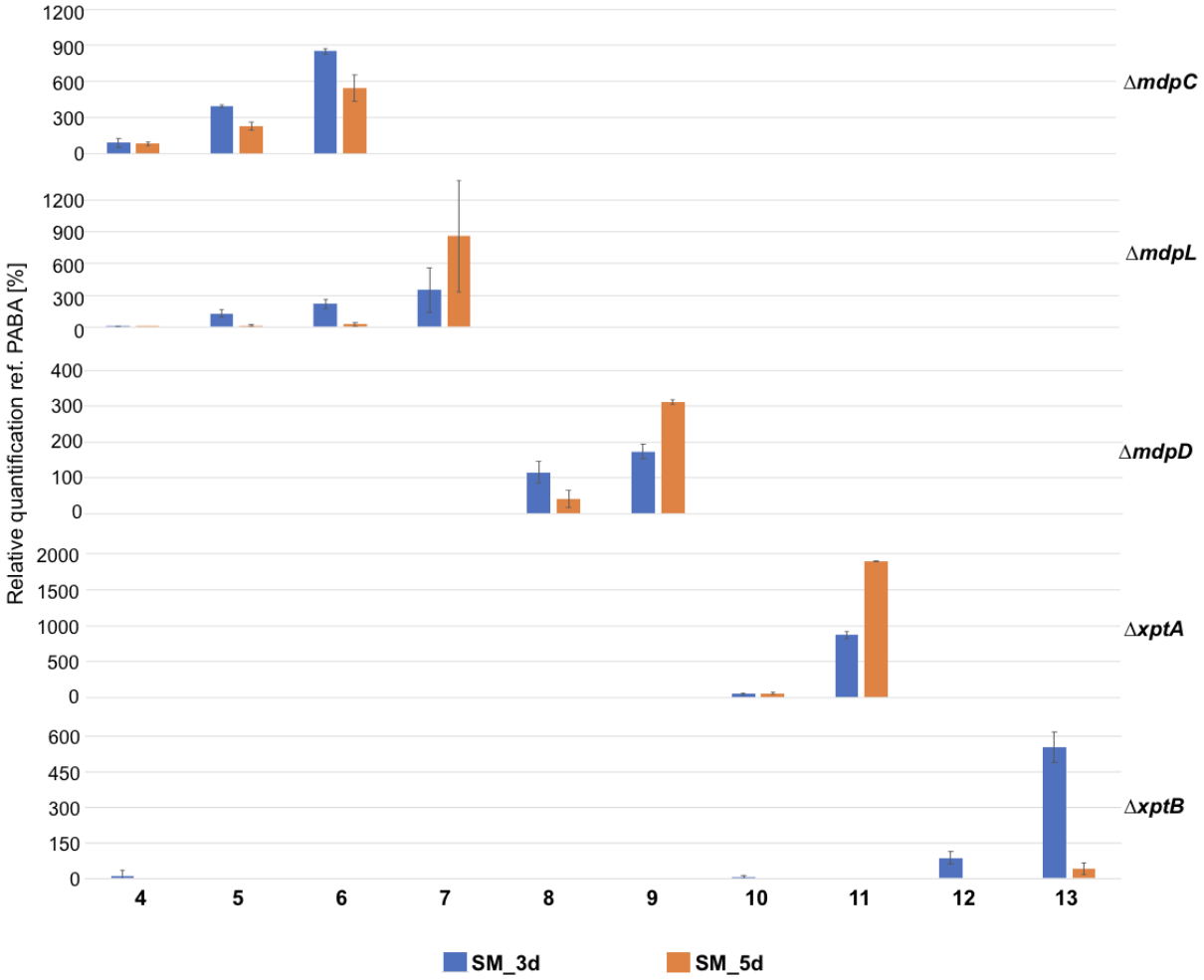

Figure 14. A dynamic change of accumulated compounds in *A. nidulans mdp/xpt* deletion strains was observed after three or five days of sexual growth.

Extracellular and intracellular secondary metabolites of each *mdp/xpt* mutant strain were harvested from the surface of point-inoculated cultures. SMs from three days (SM_3d) and five days (SM_5d) were measured by LC-MS with a charged aerosol detector (CAD). PABA was used as the internal standard and its peak area was set to 100%. Relative quantification of each component was based on PABA. Error bar indicates standard deviation with two biological replicates, Δ = deletion, **4**) 2, ω-dihydroxyemodin; **5**) ω-hydroxyemodin; **6**) emodin; **7**) chrysophanol; **8**) benzophenone alcohol; **9**) paeciloxanthone; **10**) $C_{15}H_{14}O_5$; **11**) variecoxanthone A; **12**) monodictyphenone; **13**) post-monodictyphenone.

3.1.2 The *mdp/xpt* clusters derived metabolites are localized in Hülle cells

The *mdp/xpt* clusters are especially expressed during fungal sexual development in *A. nidulans*, and four out of 15 encoded enzymes were confirmed to be localized in sexual mycelia and Hülle cells (Bayram *et al.*, 2016, Dirnberger, 2018). *A. nidulans* wild type produced the final products shamixanthone (**2**) and epishamixanthone (**3**) derived by the *mdp/xpt* gene clusters. Deletion strains lacking different genes of *mdp/xpt* clusters did not produce the final products. These mutant strains, however, accumulated various intermediates including emodin, chrysophanol and monodictyphenone and their derivatives (Fig. 12-13). These compounds are yellow in color when they are in powder form (Sanchez *et al.*, 2011).

To further characterize the roles of these products, their localizations were investigated during asexual and sexual development in *A. nidulans*. *A. nidulans* prefers asexual development in the light and forms conidiophores with green spores but preferentially undergoes sexual development in the dark with low oxygen levels and produces mainly sexual fruiting bodies surrounded by Hülle cells. As seen in Figure 15A, after three days of growth in the light, the wild type formed a colony with an overall green conidiation. Overexpressing the gene *mdpG* and deleting the genes of *mdp/xpt* clusters had no obvious conidiation difference but deleting the genes *mdpC* and *mdpL* resulted in a yellowish colony in the light. After three days of growth in the dark, the wild type formed an overall yellow colony with less green conidiation. The deletion strains Δ*mdpG* and Δ*mdpF* showed overall less yellow color compared to wild type, while the mutant strains Δ*mdpC* and Δ*mdpL* showed more overall yellow color compared to wild type (Fig. 15A). OE*mdpG* and the deletion strains Δ*mdpD*, Δ*xptA* Δ*xptB* and Δ*xptC* showed the same colony phenotype with wild type in the dark. Moreover, an accumulation of reddish pigments was observed on the back side of the colony of Δ*mdpC* and Δ*mdpL* strains in the light and dark.

When zooming in, the color of single Hülle cell could be determined (Fig. 15B). The color of the colony was derived from the Hülle cells "nest". Hülle cells of wt, OE*mdpG*, Δ*mdpD*, Δ*xptA*, Δ*xptB* and Δ*xptC* had a similar color. Hülle cells of Δ*mdpG* and Δ*mdpF* were pale, and Δ*mdpC* and Δ*mdpL* were reddish. This finding indicates that secondary metabolites derived by the

mdp/xpt clusters are localized in Hülle cells. Deletion of genes of the *mdp/xpt* clusters changed the metabolites production, which led to the accumulation of different metabolites in Hülle cells.

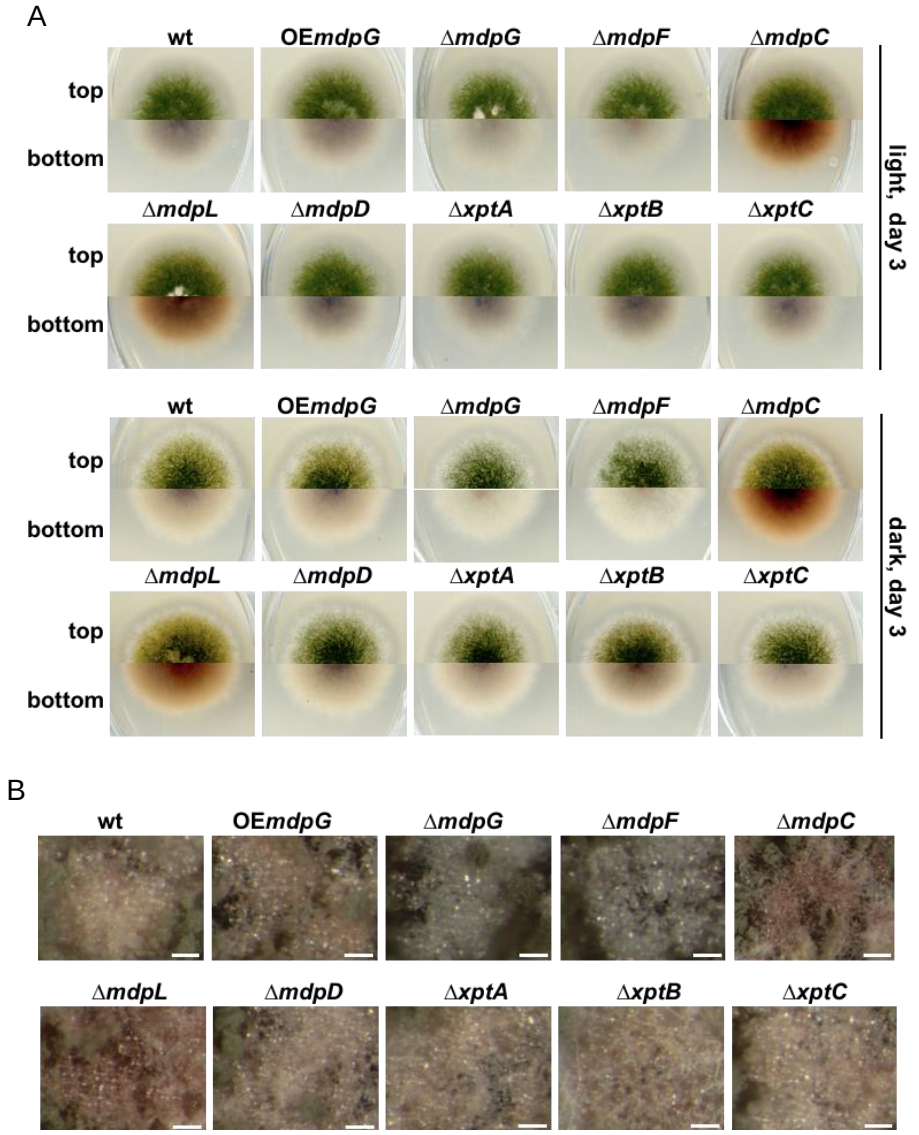

Figure 15. Secondary metabolites produced by *mdp/xpt* clusters were accumulated in Hülle cells. A) Phenotypical analysis of *mdp/xpt* mutant strains of *A. nidulans*. Approximately 1000 conidiospores of each strain were point-inoculated on minimal medium (MM) and grown for three days in light (upper panel) and dark (lower panel) at 37°C. B) Deletion of genes of the *mdp/xpt* clusters changed the color of Hülle cells. Photomicrographs of Hülle cells after five days of sexual growth. White bars = 50 µm.

The backbone gene *mdpG* encodes the PKS protein as the first enzyme in the biosynthetic pathway of epi-/shamixanthone. Deletion of the gene *mdpG* resulted in the abolishment of all products of *mdp/xpt* clusters (Fig. 11-13) and the formation of colorless Hülle cells (Fig. 15B). In order to verify the role of the gene *mdpG* in the secondary metabolites production and coloring of Hülle cells, the reintroduction of *mdpG* in its deletion strain was performed. The

phenotype of *mdpG* complementation can be restored to wild type with yellow Hülle cells (Fig. 16A) and its secondary metabolites production can be restored completely with the production of emericellin (**1**), shamixanthone (**2**), epishamixanthone (**3**) and arugosin A (**18**), which were present in wild type but lost in the Δ*mdpG* strain (Fig. 16B).

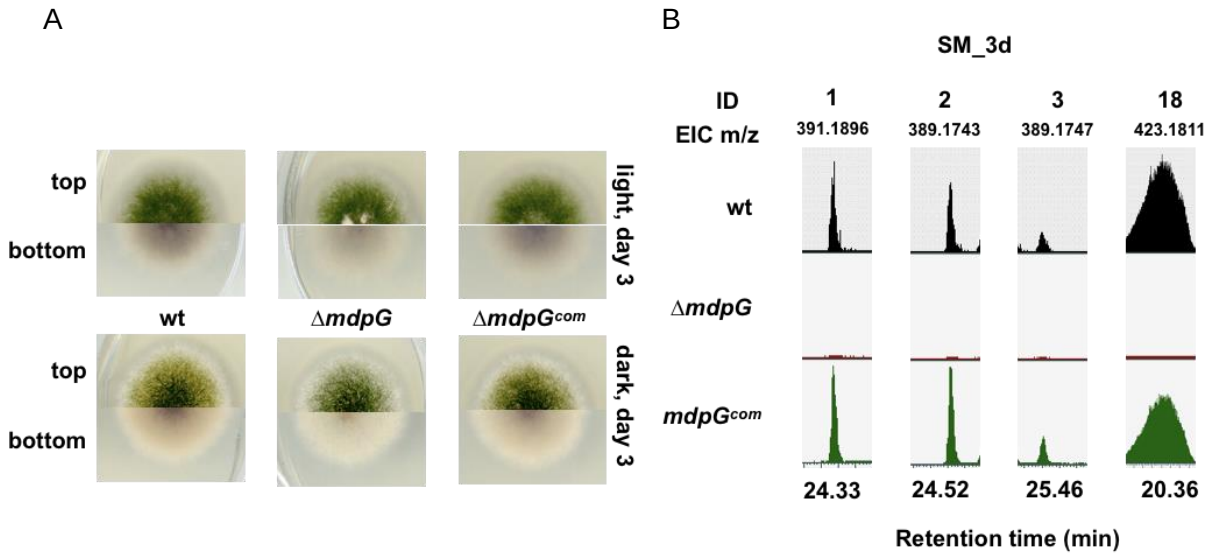

Figure 16. The complementation of *mdpG* was restored to wild type.
A) Phenotypical analysis of *mdpG* strains. Approximately 1000 conidiospores of each strain were point-inoculated on minimal medium (MM) grown for three days in light (upper panel) and dark (lower panel) at 37°C. B) EICs (extracted ion chromatogram) of the accumulated compounds in SM_3d of *mdpG* strains in the dark. wt = wild type, Δ = deletion, com = complementation strain. ID: compound number used in this study. m/z of **1**, **2** and **3** were detected in positive mode, **18** was detected in negative mode. **1**) emericellin; **2**) shamixanthone; **3**) epishamixanthone; **18**) arugosin A.

The gene *mdpC* encodes a ketoreductase converting emodin and its derivatives to downstream products in epi-/shamixanthone biosynthetic pathway. Deletion of the gene *mdpC* resulted in the accumulation of 2, ω-dihydroxyemodin (**4**), ω-hydroxyemodin (**5**) and emodin (**6**) in Hülle cells and further reddish pigmented colony in comparison to wild type. In order to verify the role of the gene *mdpC* in the secondary metabolites production and coloring of Hülle cells, the reintroduction of *mdpC* in its deletion strain was performed. The phenotype of *mdpC* complementation was restored to wild type with yellow Hülle cells (Fig. 17A) and its secondary metabolites production was partly restored (Fig. 17B). The complementation strain produced the final shamixanthone (**2**), epishamixanthone (**3**), and emericellin (**1**) and arugosin A (**18**) presented in wild type and lost the accumulation of emodins (**4**, **5**, **6**), but all of its peaks were

higher than that presented in wild type including austinol (**20**), dehydroaustinol (**21**) (Szewczyk *et al.*, 2008), and an unidentified compound **22** ($C_{18}H_{35}NO$) (Table 6) as well.

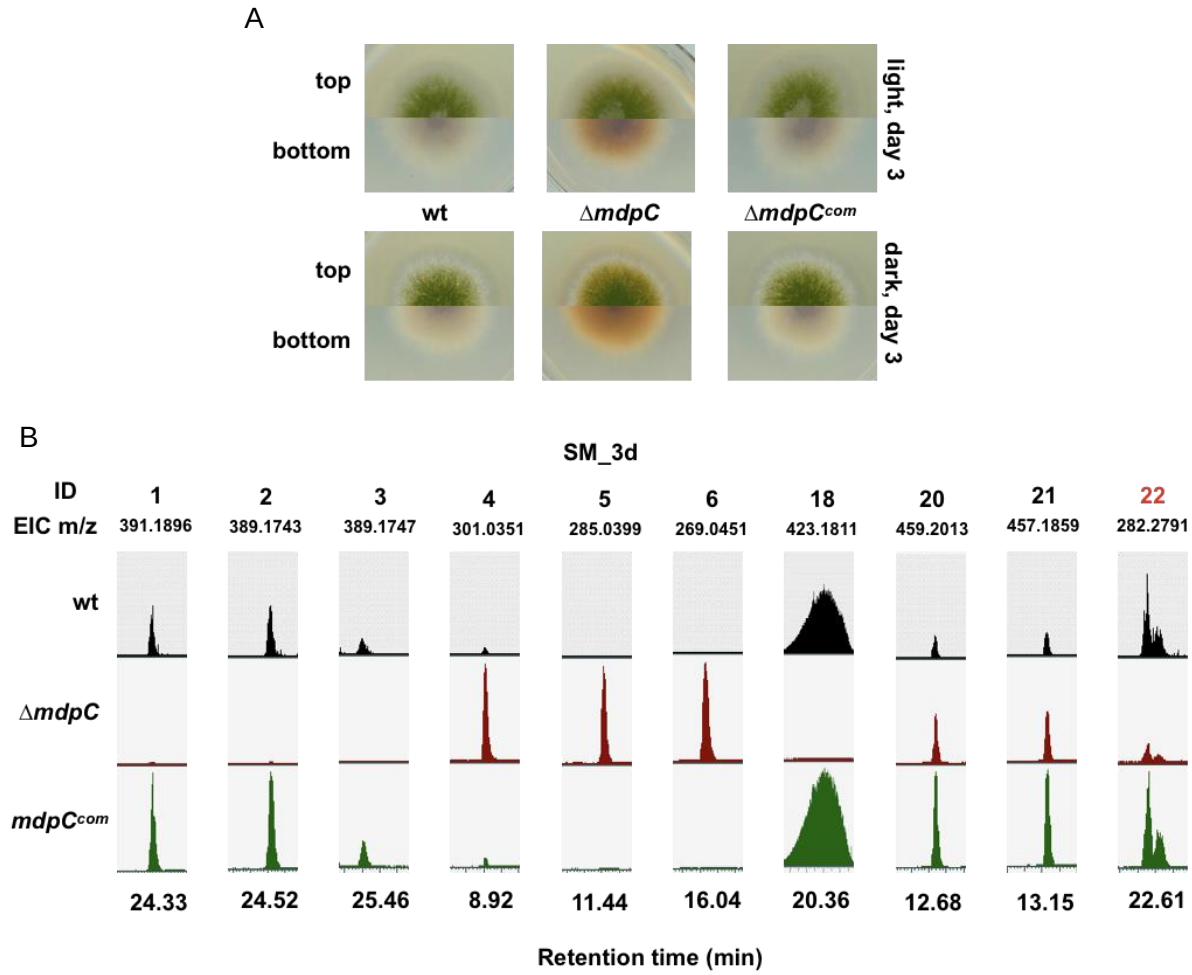

Figure 17. The SM production of the complementation of *mdpC* was partially restored to wild type. A) Phenotypical analysis of *mdpC* strains. Approximately 1000 conidiospores of each strain point-inoculated on minimal medium (MM) and grown for three days in light (upper panel) and dark (lower panel) at 37°C. B) EICs (extracted ion chromatogram) of the accumulated compounds in SM_3d of *mdpC* strains in the dark. wt = wild type, Δ = deletion, com = complementation strain. ID: compound number used in this study. m/z of **1**, **2**, **3, 20, 21** and **22** were detected in positive mode, **4**, **5**, **6** and **18** were detected in negative mode. **1**) emericellin; **2**) shamixanthone; **3**) epishamixanthone; **4**) 2, ω-dihydroxyemodin; **5**) ω-hydroxyemodin; **6**) emodin; **18**) arugosin A; **20**) austinol; **21**) dehydroaustinol; 22) $C_{18}H_{35}NO$ (unidentified).

In summary, the *mdp/xpt* gene clusters are expressed during fungal sexual development to produce epi-/shamixanthone, arugosin A and emericellin. The products are localized in the special cell type Hülle cells. Deletion of genes of the *mdp/xpt* clusters interrupted the epi-/shamixanthone biosynthetic pathway and resulted in the accumulation of various intermediates

in Hülle cells, which led to the color changes of Hülle cells and phenotypical changes of colonies.

3.2 Precursors of epi-/shamixanthone repress sexual but not asexual development initially independent of the MAPK pheromone pathway or the velvet complex.

3.2.1 Precursors of epi-/shamixanthone mediated specific repression of sexual development in *A. nidulans* without an impact on vegetative growth or asexual development.

Deletion strains of the *mdp/xpt* gene clusters cannot produce the final epi-/shamixanthone but accumulated various precursors of epi-/shamixanthone in Hülle cells during sexual development. In an effort to decipher the biological functions of the metabolites derived by the *mdp/xpt* clusters in sexual development of *A. nidulans*, the sexual development of *mdp/xpt* mutant strains were monitored over time and phenotypical changes of sexual tissues were assayed from two to 10 days.

A. nidulans can undergo sexual development in dark with low oxygen levels to form the sexual fruiting bodies cleistothecia as overwintering structures. In this study, *A. nidulans* strains were cultivated on minimal medium (MM) agar plates sealed with parafilm and aluminium foil at 37°C to induce sexual development. After two days, the colony of *A. nidulans* wild type showed the first sexual structures (Hülle cells), then formed young unmatured cleistothecia with a transparent shell after three days. After five days, these cleistothecia got mature with a dark pigmented shell containing thousands of ascospores inside. Deletion of the genes *mdpC*, *mdpL*, *mdpD*, *xptA* and *xptB* of the *mdp/xpt* clusters resulted in a delay of cleistothecium development in different degrees (Fig. 18A). After three days, these five mutant strains showed a delay in primordium (young cleistothecium) formation in comparison to wild type and the other four mutant strains, OE*mdpG*, Δ*mdpG*, Δ*mdpF* and Δ*xptC*. Δ*mdpC* and Δ*mdpL* strains, in particular formed a few smaller primordia than other strians. After four days, these five mutants showed a remarkable delay of cleistothecia maturation with a soft and less pigmented shell. After five days, Δ*mdpD* and Δ*xptA* strains released the delay and formed mature and dark pigmented cleistothecia similar to wild type. Δ*mdpC*, Δ*mdpL* and Δ*xptB* strains still showed unmatured cleistothecia. After seven days, all *A. nidulans* strains formed smooth and dark pigmented

cleistothecia except the deletion of the *mdpC* strain, which showed the strongest delay of cleistothecia maturation. Δ*mdpC* got matured cleistothecia after 10 days finally.

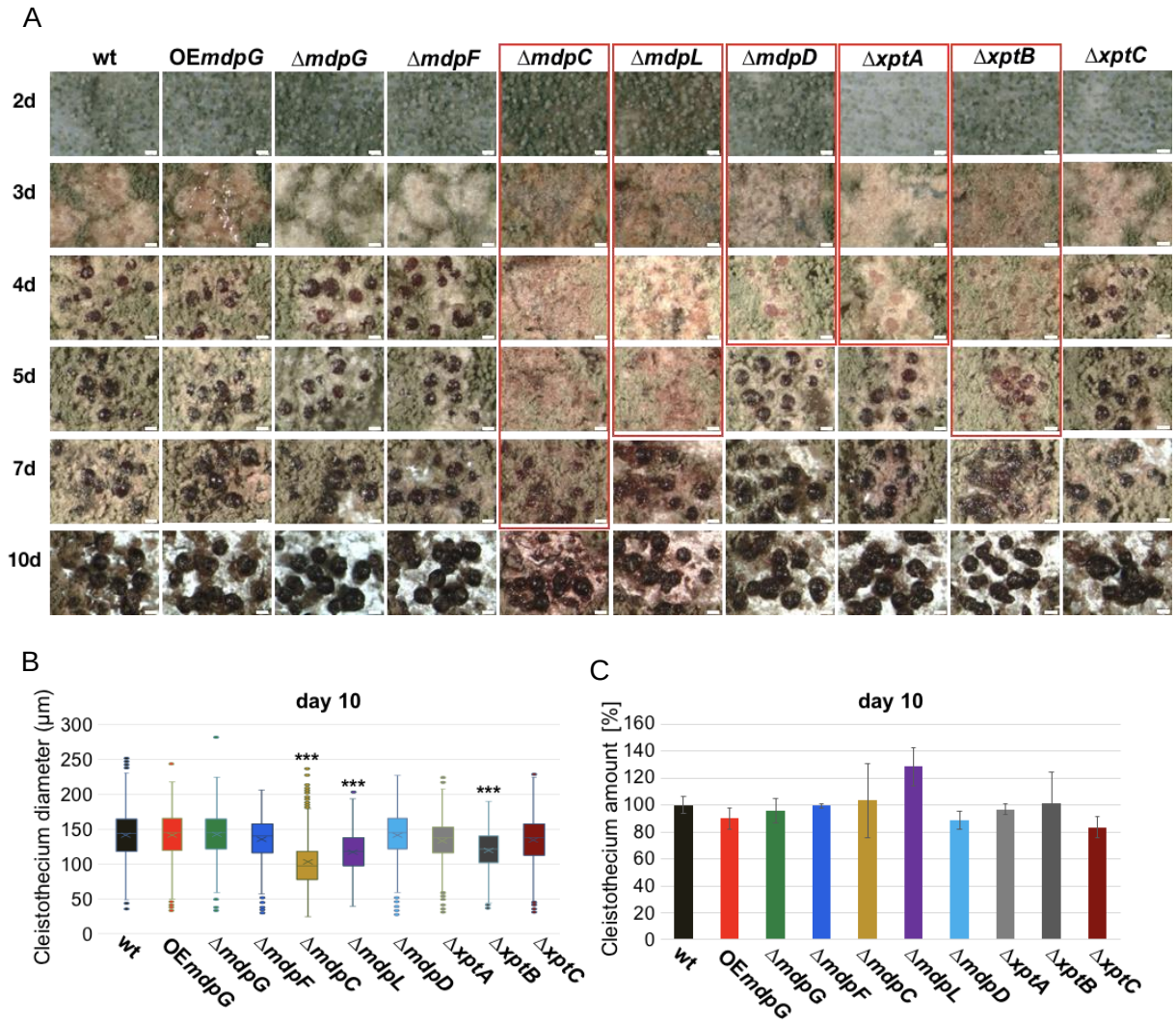

Figure 18. Deletion of genes of the *mdp/xpt* clusters led to a repression of sexual development of *A. nidulans*.

A) Δ*mdpC*, Δ*mdpL*, Δ*mdpD*, Δ*xptA* and Δ*xptB* strains showed a delayed maturation of cleistothecia. Approximately 1000 conidiospores were point-inoculated for sexual growth on minimal medium (MM) at 37°C. Microphotographs of the sexual structures at the colony center after two, three, four, five, seven and 10 days (d = day, wt = wild type, OE = overexpression, Δ = deletion, white bars = 100 µm). The delayed processes are highlighted in red frames. B) Box plot of cleistothecia size after 10 days (n = 650 (± 50), taken wild type (wt) as reference, ***$P < 0.005$). Data were collected from two biological replicates. C) Cleistothecia production of *A. nidulans* strains. Cleistothecia were collected after 10 days and counted (referenced to wild type (wt), error bar indicates standard deviation calculated from two technical and biological replicates).

Among these five mutant strains, Δ*mdpC*, Δ*mdpL* and Δ*xptB* strains exhibited a strong delay of cleistothecia maturation and produced smaller cleistothecia in comparison to the wild type (Fig.

18B). Deleting the genes of *mdp/xpt* clusters had no significant impact on the amount of cleistothecia in *A. nidulans* (Fig. 18C).

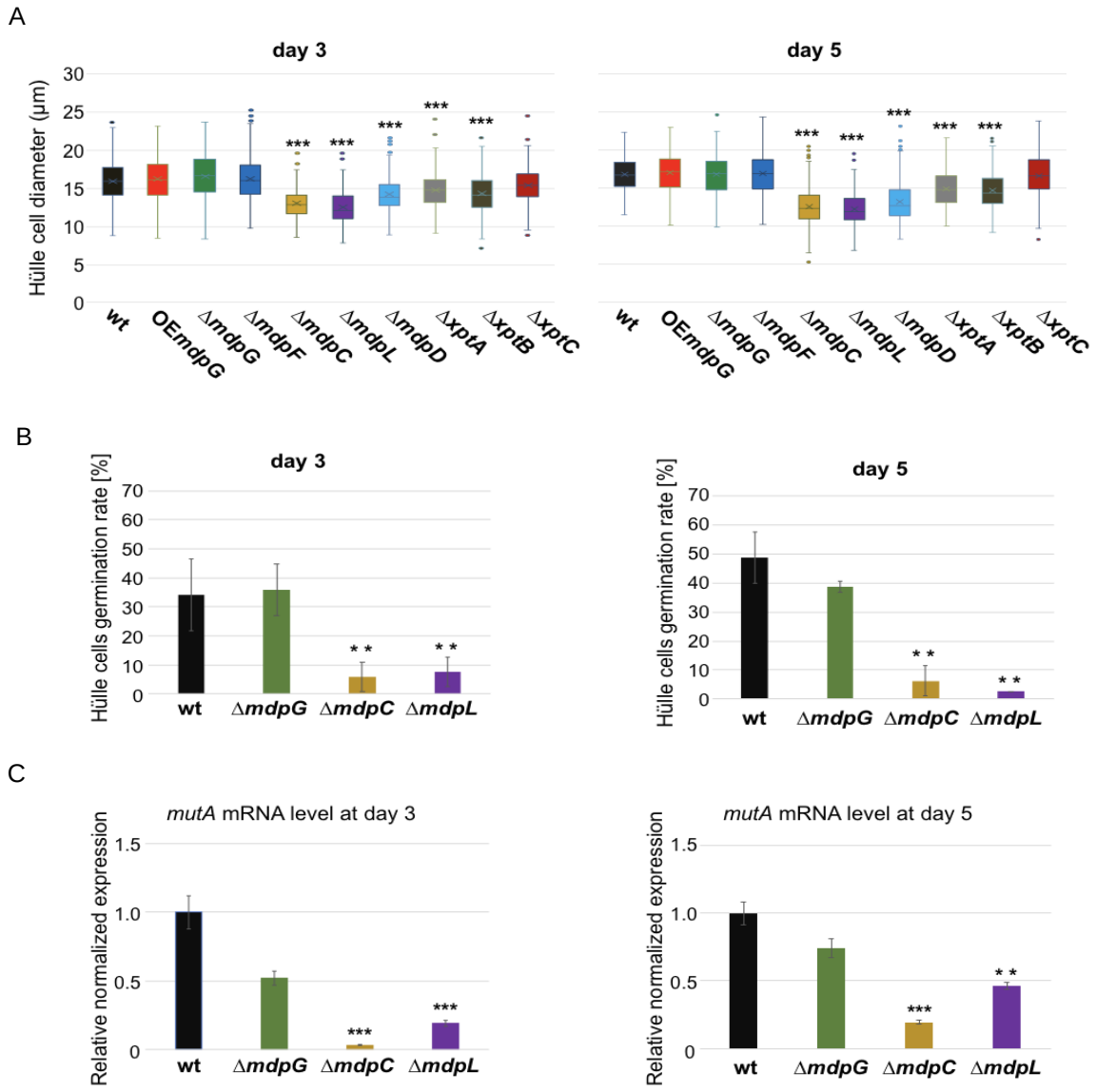

Figure 19. Deletion of genes of *mdp/xpt* clusters produced smaller Hülle cells with reduced activity. A) Box plot of Hülle cell size grown for three and five days. Hülle cells were collected from three and five days of sexual growth and measured the diameters via the microscope with software cellSens Dimension. This was repeated with two biological relicates (n ≥ 150, referenced to wt, ***$P < 0.005$). B) Hülle cell germination rate was decreased in Δ*mdpC* and Δ*mdpL*. Detached Hülle cells were collected from cleistothecia after three and five days and placed on fresh minimal medium (MM) agar plates. The germination was monitored after 48 hours at 37°C. n = 40 (± 1) with three biological replicates (**$P < 0.05$). C) *mutA* expression levels were decreased in Δ*mdpC* and Δ*mdpL* in comparison to wild type (wt) after three and five days of sexual growth. Gene expression of *mutA* was measured with qRT-PCR and *h2A* (AN3468) and *S15* (AN5997) served as house-keeping genes. Data were collected from three biological and three technical replicates (*** / ** indicates $P < 0.005$ / < 0.05).

Deletion of the genes *mdpC*, *mdpL*, *mdpD*, *xptA* and *xptB* of *mdp/xpt* clusters resulted in not only the delay of cleistothecia maturation, but also the formation of smaller Hülle cells (Fig. 19A). Therein, deletion of genes *mdpC* and *mdpL* showed the strongest impact on Hülle cell size.

In an effort to furtherly characterize the impacts of deletion of genes of the *mdp/xpt* clusters on Hülle cells, the activity of Hülle cells from Δ*mdpC* and Δ*mdpL* strains were analyzed. Hülle cells have the possibility of germinating and growing a novel branch in the life cycle of *A. nidulans* (Ellis *et al.*, 1973). Detached Hülle cells from Δ*mdpC* and Δ*mdpL* strains exhibited a low germination rate compared to wild type and the deletion strain of backbone PKS encoding gene *mdpG* (Fig. 19B). One of the proposed functions of Hülle cells is providing nutrition for the developing cleistothecia. Mutanase of *A. nidulans* degrades polysaccharides into monosaccharides, which are cell wall components and consumed for fungal growth and development (Bull, 1970, Fuglsang *et al.*, 2000). The mutanase encoding gene *mutA* is specifically and highly expressed in Hülle cells when cleistothecia are developing (Wei *et al.*, 2001). Deletion of genes *mdpC* and *mdpL* resulted in a significantly decreased expression level of *mutA* during sexual development as shown in figure 19C.

Deletion of genes of *mdp/xpt* clusters resulted in the accumulation of various epi-/shamixanthone precursors in Hülle cells and the relevant mutant strains exhibited a repression of sexual development in *A. nidulans*. In order to further verify the impacts of epi-/shamixanthone precursors on the growth and development of *A. nidulans*, SMs of *mdp/xpt* mutant strains and *A. nidulans* wild type were extracted and their bioactivities on *A. nidulans* wild type were analyzed.

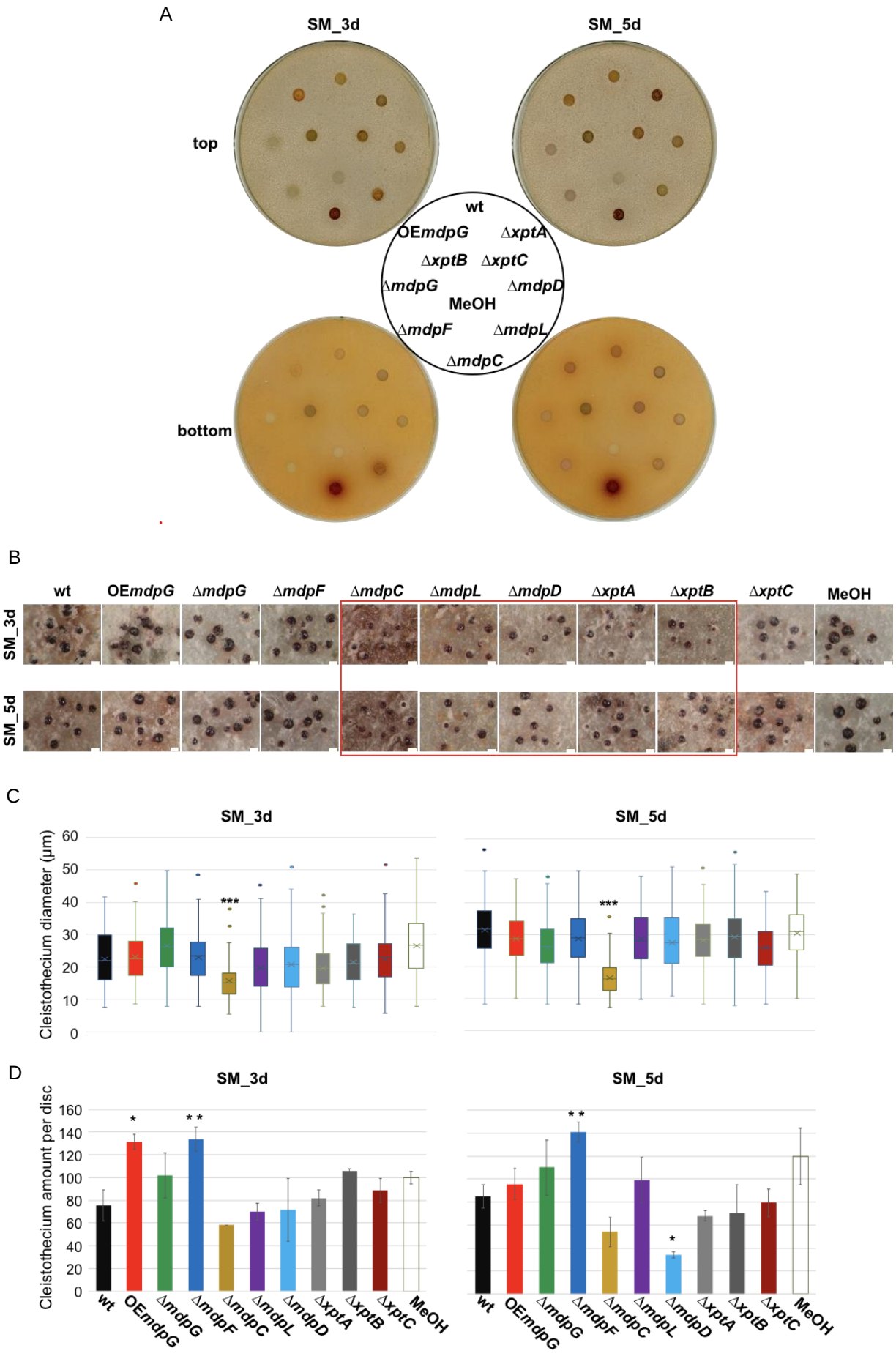
A
SM_3d
SM_5d
top
bottom
wt
OEmdpG
ΔxptA
ΔxptB
ΔxptC
ΔmdpG
ΔmdpD
MeOH
ΔmdpF
ΔmdpL
ΔmdpC
B
wt
OEmdpG
ΔmdpG
ΔmdpF
ΔmdpC
ΔmdpL
ΔmdpD
ΔxptA
ΔxptB
ΔxptC
MeOH
SM_3d
SM_5d
C
SM_3d
SM_5d
Cleistothecium diameter (µm)
***
D
SM_3d
SM_5d
Cleistothecium amount per disc
wt
OEmdpG
ΔmdpG
ΔmdpF
ΔmdpC
ΔmdpL
ΔmdpD
ΔxptA
ΔxptB
ΔxptC
MeOH

Figure 20. SMs of Δ*mdpC* repressed the sexual fruiting body development of *A. nidulans* wild type. A) The growth of *A. nidulans* wild type under the extracted SMs stress of wild type (wt) and *mdp/xpt* mutant strains. SM extracts were dissolved in methanol (MeOH) and loaded onto sterile paper discs, and pure MeOH as blank control (SM_3d: SMs were extracted from three days of sexual growth, SM_5d: SMs were extracted from five days of sexual growth). Discs were dried in sterile bench with air flow 30 min to evaporate methanol completely, and then placed on the minimal medium agar plate inoculated with 1 x 10_5 *A. nidulans* wild type conidiospores, and sexual grown for five days at 37°C. B) Microphotograph of cleistothecia on each paper disc. The repressed processes are highlighted in red frames (white bars = 100 µm). C) Size of cleistothecia from each paper disc. D) Production of cleistothecia from each paper disc. (wt - Δ*xptC*: extracted SMs of the wild type and *mdp/xpt* mutant strains, methanol (MeOH) as blank control. Error bar indicates standard deviation with two technical and biological replicates. Referenced to that under the SMs stress of wild type (wt). ***/ **/ * indicates $P < 0.005$ / < 0.05 / < 0.5.

SMs extracted from *mdp/xpt* deletion strains after three and five days of sexual growth were loaded on paper discs and placed on minimal medium agar plates, which were pre-inoculated with conidiospores of *A. nidulans* wild type. SMs extracted from *A. nidulans* wild type and the solvent methanol were used as control. As shown in figure 20A, all of the treatments exhibited no impact on the growth of *A. nidulans* wild type, but there was a change in developmental structure formation (Fig. 20B). After five days of sexual growth, *A. nidulans* wild type can form mature sexual fruiting bodies with a smooth and pigmented shell. SMs extracted from the deletion strains Δ*mdpC*, Δ*mdpL*, Δ*mdpD*, Δ*xptA* and Δ*xptB* after three and five days of sexual growth decelerate the cleistothecia development of *A. nidulans* wild type (Fig. 20B).

Extracted SMs of Δ*mdpC* contains abundant 2, ω-dihydroxyemodin (**4**), ω-hydroxyemodin (**5**) and emodin (**6**) as detected by LC-MS, and it also led to the significantly smaller cleistothecia formation in *A. nidulans* wild type (Fig. 20C) in comparison to that under the SMs stress of other *mdp/xpt* mutant strains and control.

For the cleistothecia production, *A. nidulans* wild type produced more cleistothecia under the SMs stress of Δ*mdpF* from three and five days and OE*mdpG* from three days, but fewer cleistothecia under the SMs stress of Δ*mdpD* from five days (Fig. 20D).

A. nidulans undergoes asexual or sexual development coordinated by regulatory complexes, which response to the environmental stimuli and decide fungal development (Park *et al.*, 2019). These two fungal development ways are coexisting. Light accelerates asexual and decreases sexual development to form conidiophores with conidiospores. Darkness accelerates sexual but

delays asexual development, whereas, many light-induced genes are expressed with a delay up to two days to form asexual tissues (Bayram *et al.*, 2016). Deletion of genes of *mdp/xpt* clusters resulted in the accumulation of various bioactive epi-/shamixanthone precursors in Hülle cells and the repression of sexual development. In order to check whether the accumulation of epi-/shamixanthone precursors also has impact on asexual development of *A. nidulans*, the production, viability and germination of conidiospores from *A. nidulans* wild type and *mdp/xpt* mutant strains were quantified.

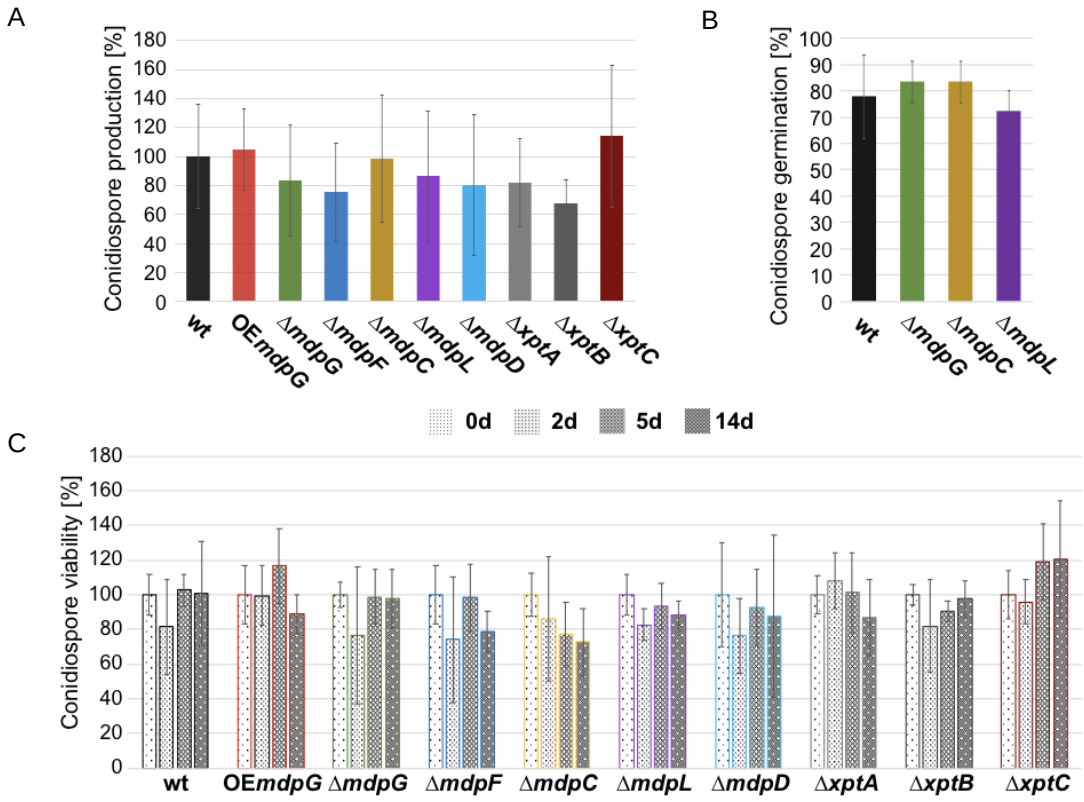

Figure 21. Deletion strains of *mdp/xpt* clusters exhibited no effect on the asexual development of *A. nidulans*.

A) Conidiospore production of *mdp/xpt* mutant strains and *A. nidulans* wild type (wt). Approximately 1000 conidiospores per strain were point-inoculated on minimal medium (MM) agar plates and incubated three days in light at 37°C. Conidiospore amounts formed by wt were set to 100%. Error bar indicates standard deviation with three technical and two biological replicates. B) Conidiospore germination of three *mdp* deletion mutant strains and the wild type (wt) of *A. nidulans*. 20 (±1) conidiospores were picked with a micromanipulator and placed on fresh agar plates in a matrix to germinate two days in light at 37°C, and the visible colonies were counted. Error bar indicates standard deviation with two technical and two biological replicates. C) Conidiospore viability of *mdp/xpt* mutant strains and wild type (wt) of *A. nidulans*. 4°C stored 200 spores per strain were plated on MM plates after zero, two, five and 14 d of storage and germinated for two days at 37°C. Initial spore-forming units of each strain were set to 100%. Data were collected from three technical and three biological replicates.

As shown in figure 21A, deletion of the genes of *mdp/xpt* clusters exhibited no effect on the production of conidiospores. No difference in germination of the conidiospores from *A. nidulans* wild type and *mdp/xpt* mutant strains, Δ*mdpG*, Δ*mdpC* and Δ*mdpL*, was observed (Fig. 21B). Furthermore, there was no difference in the viability of conidiospores from *mdp/xpt* mutant strains and *A. nidulans* wild type. These results indicate that the precursors of epi-/shamixanthone derived by *mdp/xpt* clusters specifically repress sexual development but without impact on asexual development of *A. nidulans*.

3.2.2 Repression of fruiting body maturation by epi-/shamixanthone precursors is independent of velvet gene expression and MAP kinase protein expression

A. nidulans sexual development is a complex process controlled by various signalling pathways. The classical pathways are mitogen activated protein kinases (MAPKs) pheromone pathways and their downstream targets, the velvet complex as shown in figure 7. MAPKs SakA and MpkC are physically interacting involved in stress signal transduction. SakA has cross-talking interaction with another MAPK member MpkB by reducing the activity of SteA to regulate the sexual development of *A. nidulans* (Aguirre *et al.*, 2018, Kawasaki *et al.*, 2002, Manfiolli *et al.*, 2019). The downstream target of the MpkB pathway is the heterotrimeric velvet complex VeA-VelB-LaeA, which plays an important role in both the production of secondary metabolites and sexual development of *A. nidulans* (Bayram *et al.*, 2008). As described above, precursors of epi-/shamixanthone were localized in Hülle cells and repressed the sexual development of *A. nidulans*. In an effort to identify the working targets of epi-/shamixanthone precursors in sexual development and elucidate the mechanisms of the repression of sexual development, genes and proteins from the MAPK pathways and velvet complex were analyzed in the mutant strains, Δ*mdpC* and Δ*mdpL*. They exhibited the strongest effect on Hülle cells and sexual fruiting bodies in this study. At the same time, Δ*mdpG* was used as a control strain, which exhibited no accumulation of epi-/shamixanthone precursors and no effect on sexual development.

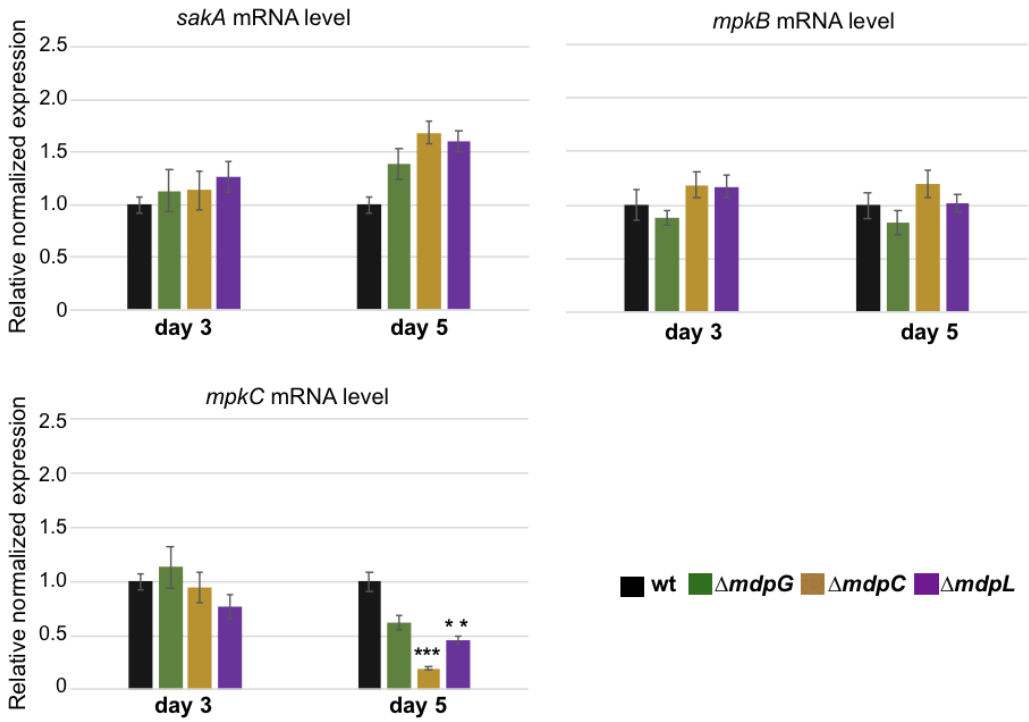

Figure 22. Deletion of genes *mdpC* and *mdpL* had no effect on the gene expression of *sakA*.
Gene expression was measured with qRT-PCR and *h2A* (AN3468) and *S15* (AN5997) served as house-keeping genes. *mpkC* was down-regulated in Δ*mdpC* and Δ*mdpL* after five days during sexual development. Error bar indicates standard deviation with three biological and technical replicates, ***/ ** indicates $P < 0.005$ / < 0.05.

As shown in figure 22, the gene expression of sexual regulators from MAPK pheromone pathways, namely *sakA*, *mpkB* and *mpkC*, showed no changes in Δ*mdpC*, Δ*mdpL* and Δ*mdpG* strains compared to the wild type in the early stage of sexual development. But the gene *mpkC* showed down-regulation in Δ*mdpC* and Δ*mdpL* strains after five days.

The gene expression of velvet complex and another two sexual regulators, *nsdD* and *stuA*, also showed no change in Δ*mdpC* in comparison to wild type in the early stage of sexual development (Fig. 23). Therein, the sexual regulator encoding gene *veA* showed a slight up-regulation (no statistical significance) in Δ*mdpC*. After five days, the gene *velB* was down-regulated while *stuA* was up-regulated in Δ*mdpC*.

The repression of sexual development was observed in the early stage after three days of sexual growth. However, the gene expression changes of *mpkC*, *velB* and *stuA* were only detected in the late stage of sexual development. These results suggest that precursors of epi/shamixanthone

repress the sexual development of *A. nidulans* not initially through the MAPK pheromone pathways or velvet complex.

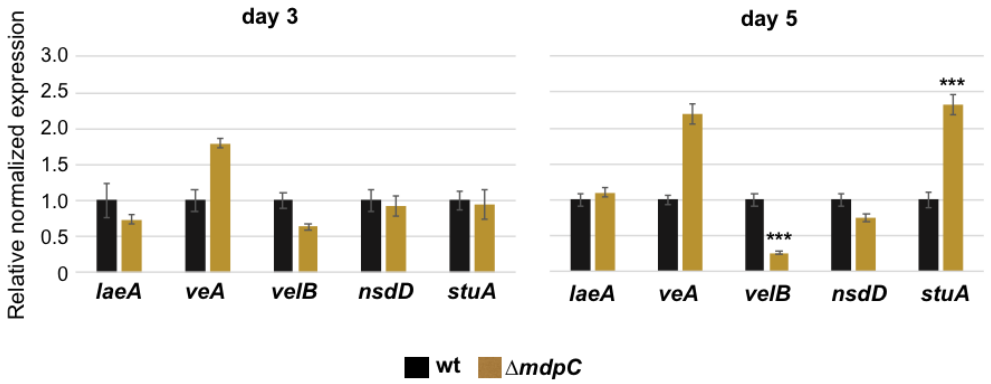

Figure 23. Deletion of the gene *mdpC* changed the expression of *velB* and *stuA* in the late stage of sexual development.

Gene expression was measured with qRT-PCR and *h2A* (AN3468) and *S15* (AN5997) served as house-keeping genes. Error bar indicates standard deviation with three biological and technical replicates, *** $P < 0.005$. *veA* mRNA level of day 5 was significantly up-regulated once in three biological replicates.

SakA is a member of the Hog1/Spc1/p38 MAPK family, a central component of stress signal transduction pathway in *A. nidulans*, and also regulates fungal sexual development and spore viability (Furukawa *et al.*, 2005, Kawasaki *et al.*, 2002, Lara-Ortíz *et al.*, 2003). SakA is activated by phosphorylation in response to oxidative and osmotic stress signals and represses the transcription of genes needed for cleistothecia formation. Deletion strains of *mdp/xpt* clusters accumulated various precursors of epi-/shamixanthone including emodin and its derivatives. Emodin is involved in the ROS/p38/p53/Puma signaling pathway in mammalian cells to regulate transcription regulators and protein, DNA and RNA degradation (Lin *et al.*, 2019, Liu *et al.*, 2015). In order to check whether the precursors of epi-/shamixanthone accumulated in Δ*mdpC* and Δ*mdpL* strains have impact on the sexual repressor SakA, the protein level of phosphorylated SakA and the total amount of SakA were detected. Δ*mdpG* was also used as a control strain as described above.

As shown in figure 24, the protein level of phosphorylated SakA and the total amount of SakA-GFP showed no difference in Δ*mdpC*, Δ*mdpL* and Δ*mdpG* strains in comparison to *A. nidulans* wild type after three or five days of sexual growth. This result suggests that the accumulated precursors of epi-/shamixanthone act independently of SakA.

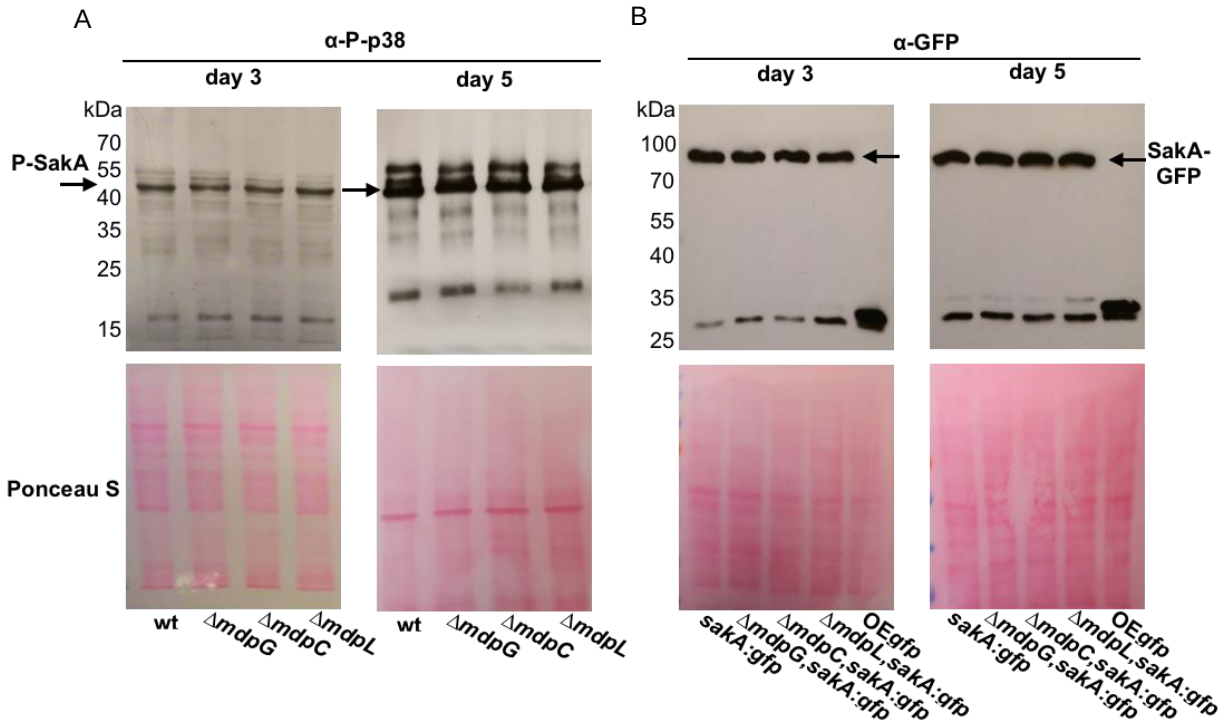

Figure 24. Deletion of genes *mdpC* and *mdpL* exhibited no impact on the protein level of SakA or phosphorylated SakA.

A) Protein levels of phosphorylated SakA in wild type (wt), Δ*mdpG*, Δ*mdpC* and Δ*mdpL* from three and five days of sexual growth. The target protein was detected with P-p38 antibody. Arrow indicates the position of SakA in 43.2 kDa. B) Total SakA in wild type (wt), Δ*mdpG*, Δ*mdpC* and Δ*mdpL* from three days and five days of sexual growth. SakA was tagged with GFP and detected with anti-GFP antibody, and free GFP (26.9 kDa) as positive control. Arrow indicates the position of SakA-GFP in 70.1 kDa. Ponceau stained membranes were shown as a loading control.

3.3 Precursors of epi-/shamixanthone cause oxidative and weak acidic stress sensitivity and disturb reproduction of other fungi and flies.

3.3.1 Increased amounts of epi-/shamixanthone precursors cause oxidative and weak acidic stress sensitivity

In fungal survival niche, UV radiation is one of the environmental stresses that can reduce spore germination or even kill conidia of most fungal species with direct exposure (Braga *et al.*, 2015). Fungal derived pigments can be a strategy to resist UV damage (Allam *et al.*, 2012, Beck *et al.*, 2014). As shown in figure 15, *A. nidulans* produces yellowish xanthone pigments derived by the *mdp/xpt* clusters enriched in Hülle cells. Deletion of the genes *mdpG* and *mdpF* resulted in the loss of these pigments while deletion of the genes *mdpC*, *mdpL*, *mdpD*, *xptA*, *xptB* and *xptC* resulted in the accumulation of various precursors of epi-/shamixanthone. Some of these pigments possess bioactivity and can increase intracellular reactive oxygen species (ROS),

which can damage all kinds of biomolecules to reduce fungal growth and development (Halliwell *et al.*, 2015, Moreira *et al.*, 2018). In order to investigate whether the increased amounts of epi-/shamixanthone precursors play roles in fungal stress response, *A. nidulans* wild type and *mdp/xpt* mutant strains were tested with UV (λ = 366 nm) and the oxidizers menadione sodium bisulfite (MSB), diamide and potassium sorbate (KSB), which is a weak acid and can lead to oxidative stress as well (Taghavi *et al.*, 2013).

Under laboratory sexual growth conditions (Control), colony growth of *mdp/xpt* mutant strains had no difference in comparison to the wild type (Fig. 25A). Under UV radiation, colonies exhibited more green spores in comparison to the control condition, but colony size showed no difference. Fungal growth was observed in the presence of MSB, KSB and diamide and a negative effect of these stress generating agents on the fungal growth (colony size) and conidiation was observed. All of them led to less conidiospore production, and KSB and diamide led to smaller colonies. In the same stress condition, however, colony size and conidiation of *mdp/xpt* mutant strains and wild type had no difference.

A. nidulans wild type got matured cleistothecia with a dark pigmented shell after five days of sexual growth. Deletion of genes of *mdp/xpt* clusters led to the accumulations of precursors of epi-/shamixanthone and exhibited a delayed maturation of cleistothecia during sexual development. The further finding was that these deletion mutant strains of *mdp/xpt* clusters were more sensitive to oxidative and weak acidic stresses.

Under KSB, diamide and MSB caused oxidative and weak acidic stress conditions, *A. nidulans* wild type showed a slight influence on cleistothecia maturation, but Δ*mdpC*, Δ*mdpL*, Δ*mdpD*, Δ*xptA* and Δ*xptB* mutant strains showed a strong delay of cleistothecium development and maturation (Fig. 25B). The delayed maturation was released after up to 10 days.

This finding suggests that accumulated epi-/shamixanthone precursors in *mdp/xpt* mutant strains cause oxidative and weak acidic stress sensitivity, which results in a strongly delayed sexual fruiting body development.

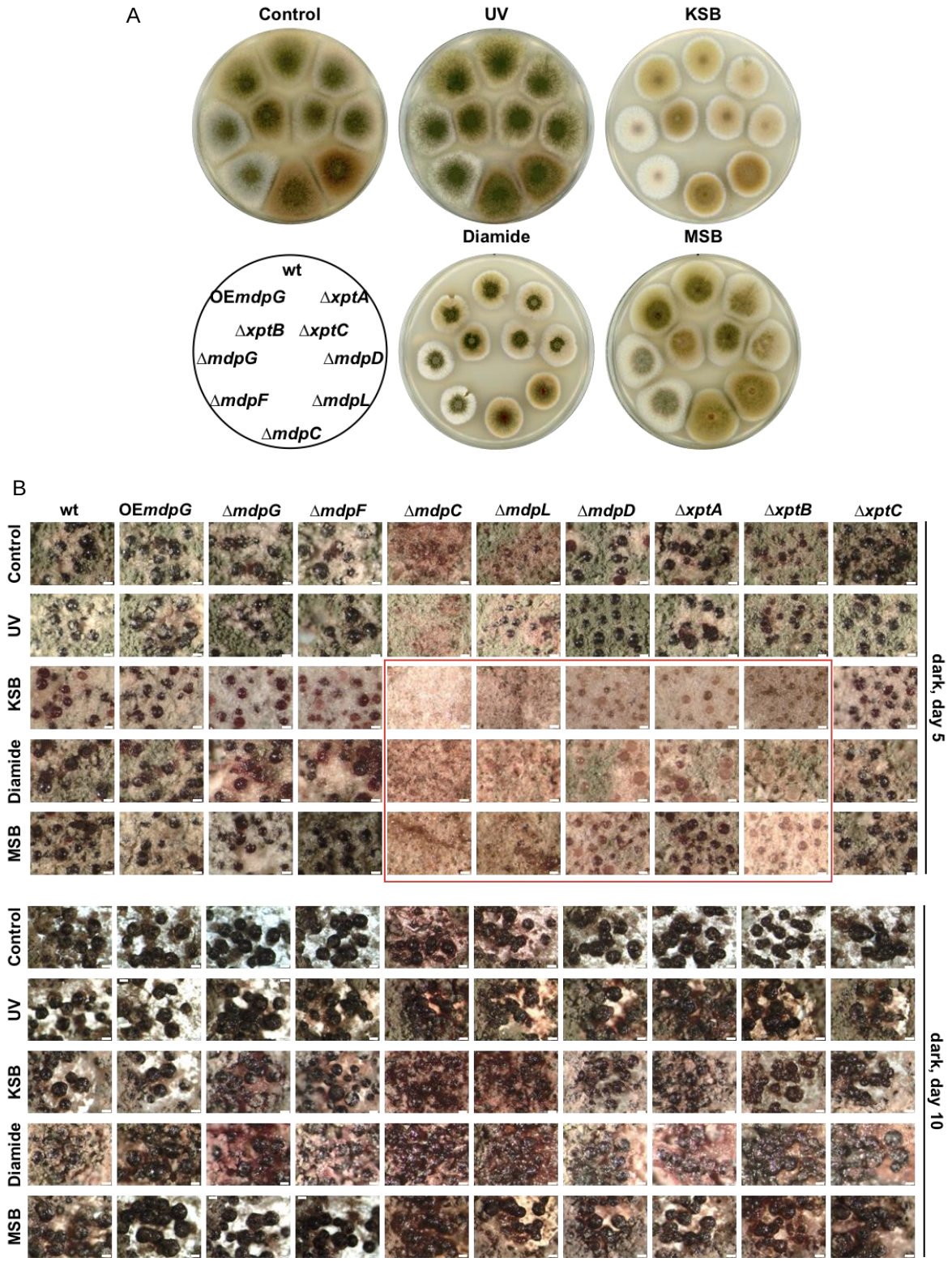

Figure 25. Deletion of genes *mdpC, mdpL, mdpD, xptA* and *xptB* of *mdp/xpt* clusters caused *A. nidulans* oxidative and acidic stress sensitivity.

A) Colony growth of *A. nidulans* wild type and *mdp/xpt* mutant strains exhibited no remarkable difference under a same stress condition. Approximately 1000 conidiospores were point-inoculated on minimal medium (MM) and were grown under UV light and stress agents contained MM agar plates, sexual grown for five days (Control: MM medium; UV: λ = 366 nm, 5 µW; KSB: 1 mM Potassium Sorbate; Diamide: 1 mM Diamide; MSB: 0.01mM Menadione Sodium Bisulfite). B) Cleistothecia

development of wild type (wt) and *mdp/xpt* mutant strains under stress conditions. Microphotographs of the sexual structures at the colony center after five (upper panel) and 10 (lower panel) days. The delayed processes of sexual development are highlighted in red frames. This experiment was carried out in three biological replicates. White bars = 100 µm.

3.3.2 Precursors of epi-/shamixanthone have a broad bioactivity on development of different fungi and fly egg depositing behavior.

Interspecies interactions are complex relationships of microbes, fungi, insects and plants. Antagonistic and beneficial interactions are commonly present in the natural niche between microbe and eukaryotic organisms. Studies of interactions mainly focus on growth-inhibitory and phenotypic outcomes including sporulation, biofilm formation and secondary metabolite production (Shank *et al.*, 2009). Small molecular secondary metabolites play crucial roles in interspecies interactions as communication signals or chemical weapons. The receptor organisms change metabolism, morphology and development to response the "guest" signals.

A. nidulans can exert inhibitory activity against the mycelial growth and spore production of *Fusarium oxysporum* f. sp. *lycopersici* (Sibounnavong *et al.*, 2009). In fungal-insect antagonisms, *A. nidulans* induced the insecticide production of juvenile hormone by feeding to *Drosophila melanogaster* larvae (Nielsen *et al.*, 2013a).

A. nidulans wild type produces emericellin, shamixanthone, epishamixanthone and arugosin A derived by the *mdp/xpt* clusters. Deletion mutant strains of *mdp/xpt* clusters produced emodins, benzophenones and various xanthone derivatives. These compounds vary in molecular structures and biofunction in the regulation of *A. nidulans* sexual development. To obtain a broader perspective on the role of *mdp/xpt* clusters derived metabolites in fungal-fungal and fungal-insect interactions, the bioactivity of secondary metabolites extracted from *A. nidulans* wild type and *mdp/xpt* clusters mutant strains on other organisms were tested.

The plant pathogenic fungi *Verticillum dahliae*, *Verticillium longisporum* and *Colletotrichum graminicola*, the model organsim *Sordaria macrospora*, and the insect *Drosophila melanogaster* were chosen as the testees. SMs were extracted from the *mdp/xpt* mutant strains and *A. nidulans* wild type after three and five days of sexual growth. Extracted SMs were dissolved in methanol and loaded onto sterile paper discs, and pure methanol as a blank control.

The discs were dried to evaporate the methanol completely, and then placed on the agar plates inoculated with tested fungal spores.

Wild type of *Verticillum dahliae* and *Verticillum longisporum* can produce the scattered black resting structures (microsclerotia) on agar plate cultivation. Tested on *V. dahliae*, SMs extracted after three days (SM_3d) of *A. nidulans* wild type and *mdp/xpt* mutant strains showed no obvious effect on the formation of microsclerotia in comparison to the blank control (MeOH). Five days of SMs (SM_5d) of Δ*mdpC* and Δ*mdpL* strains repressed the formation of microsclerotia (Fig. 26A). Tested on *V. longisporum,* SMs extracted after three and five days of Δ*mdpC* and Δ*mdpL* repressed the formation of microsclerotia. SM_3d of Δ*mdpC* exhibited slight repression on the formation of microsclerotia. On the contrary, SM_5d of Δ*mdpC* exhibited a strong repression. SMs extracted after three days of Δ*mdpD* repressed the formation of microsclerotia obviously but SMs extracted after five days did not (Fig. 26A).

Colletotrichum graminicola can form the blister-like fruiting structures (conidiomata) on agar plate cultivation. Tested on *C. graminicola,* SMs extracted from *A. nidulans* wild type and *mdp/xpt* deletion strains repressed the hyphal growth in comparison to the blank control (MeOH) but showed no obvious effect on the conidiomata development of *C. graminicola* (Fig. 26B). This indicates that the repression of hyphal growth is a cluster independent effect.

The fungus *Sordaria macrospora* can produce flask-shaped sexual fruiting bodies (perithecia) after seven days cultivation on agar plate. SMs extracted after three days (SM_3d) of *A. nidulans* wild type and *mdp/xpt* deletion strains exhibited remarkable repression on the formation of perithecia in comparison to the blank control (Fig. 26C). Five days of SMs (SM_5d) of Δ*mdpC*, Δ*mdpL* and Δ*mdpD* also showed the repression on the formation of perithecia. A perithecia-repression halo of *S. macrospora* was formed around the SMs loaded paper discs but was not present around the blank control (MeOH). Furthermore, SMs extracted after three days of *A. nidulans* wild type and *mdp/xpt* deletion strains exhibited a strong perithecia-repression on *S. macrospora* forming bigger halos in comparison to SMs extracted after five days except Δ*mdpC*, Δ*mdpL* and Δ*mdpD* strains. This indicates that SMs have cluster independent perithecia repression. But SMs of Δ*mdpC*, Δ*mdpL* and Δ*mdpD* strains have cluster-specific effect showed

stronger repression. Therein, SMs of Δ*mdpC* exhibited the strongest repression on the perithecium of *S. macrospora* (Fig. 26D).

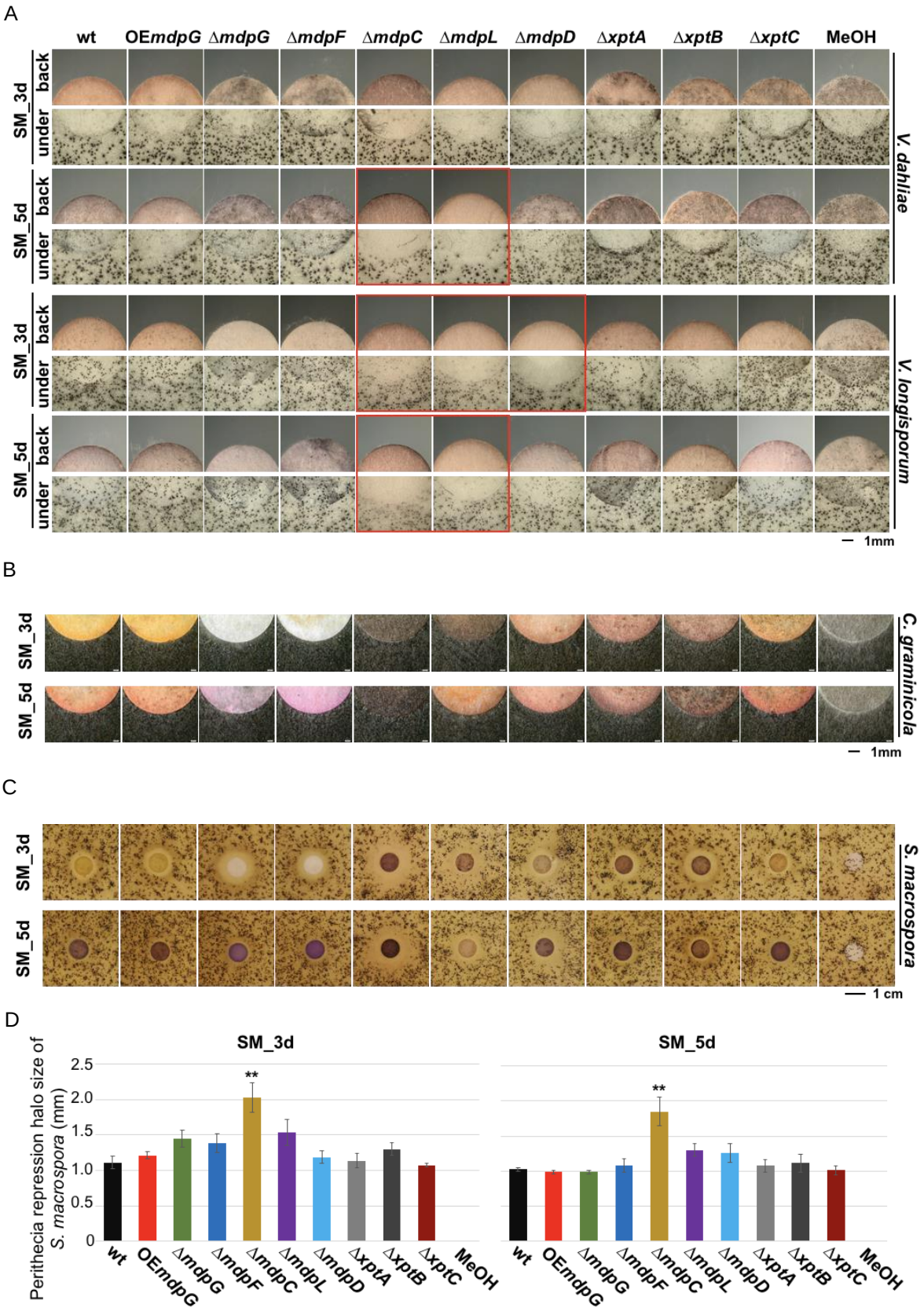

Figure 26. Precursors of epi-/shamixanthone repressed the resting and reproductive structure development of different fungi.

A), B) and C) Photomicrographs of *V. dahliae*, *V. longisporum*, *C. graminicola* and *S. macrospora* under the SM stress of *A. nidulans*. SM extracts of *A. nidulans* wild type and the mutant strains of *mdp/xpt* clusters were dissolved in methanol and loaded onto sterile paper discs, and pure methanol as blank control. The discs were dried in sterile bench with air flow 30 min to evaporate the methanol completely, and then placed on spores-inoculated plates. For *Verticillium* sp., the simulated xylem medium (SXM) agar plates were inoculated with 1 x 10^5 *V. dahliae* or *V. longisporum* spores, 10 days at 25°C. For *C. graminicola*, the complete medium (CM) agar plates were inoculated with 5 x 10^6 spores, 7 days at room temperature under continuous fluorescent light. For *S. macrospora*, the cornmeal malt fructification medium (BMM) agar plates were inoculated with 2 x 10^5 spores, seven days at 27°C. wt = wild type; OE = overexpression; Δ = deletion; MeOH = methanol; back = the back side of paper disc; under = under the paper disc in situ. Impacted processes are highlighted in red frames. D) Perithecia repression halo diameter of *S. macrospora* after five days. Blank control methanol showed no repression halo. Error bar indicates standard deviation with two technical and biological replicates. Referenced to wild type (wt), $^{**}P < 0.05$.

Taken together, SMs derived by the *mdp/xpt* clusters of *A. nidulans* possess a broad bioactivity on development of different fungi. Especially SMs of Δ*mdpC* and Δ*mdpL* showed a general bioactivity, which contain abundant emodin and its derivatives and SMs of Δ*mdpL* contain abundant chrysophanol as well. To verify the main active components of SMs, the bioactivity of the pure chemicals of emodin and chrysophanol was tested.

As described above, pure emodin and chrysophanol were also dissolved in methanol and loaded on paper discs. The final amount of pure emodin and chrysophanol was 0.075 mg per disc. This was based on the amount of emodin in SM_5d of Δ*mdpC* loaded on each paper disc. As shown in figure 27A, pure emodin and chrysophanol had no effect on the cleistothecia development of *A. nidulans* wild type. Pure emodin exhibited an obvious repression on the formation of microsclerotia of *V. longisporum* and of perithecia of *S. macrospora* but no remarkable effect on *V. dahliae*. Chrysophanol showed a moderate repression on the production of *V. longisporum* microsclerotia but no obvious effect on *V. dahliae* and *S. macrospora* (Fig. 27A). When tested on the insect *Drosophila melanogaster*, emodin reduced the amount of deposited eggs significantly in comparison to the blank control ethanol (EtOH) (Fig. 27B).

In summary, emodin as one of the active components of *A. nidulans* secondary metabolites derived by the *mdp/xpt* clusters plays an important role in fungal-fungal and fungal-insect antagonism.

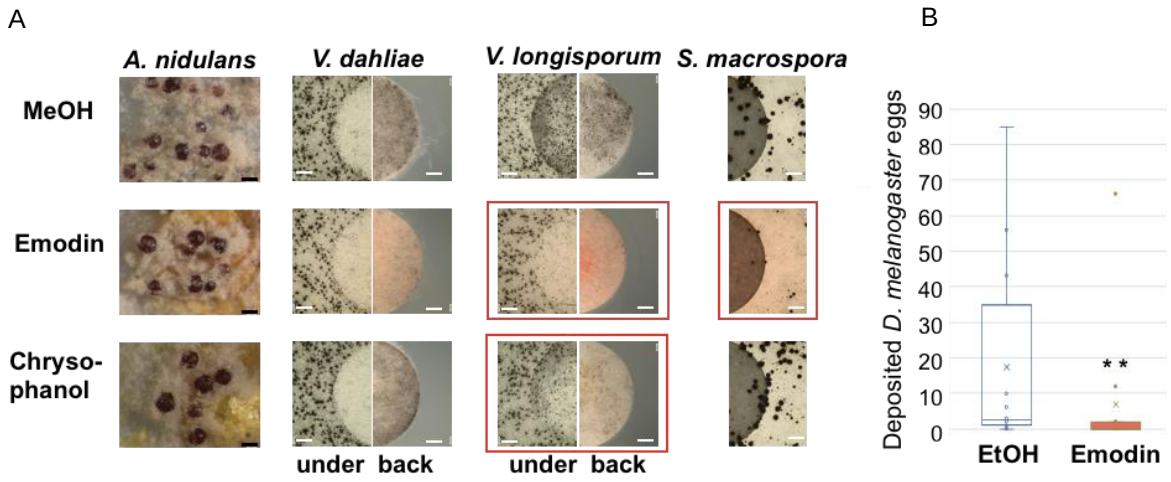

Figure 27. Emodin, a precursor of epi-/shamixanthone, is one of the key factors for repression of development of different fungi and the egg depositing behavior of flies.

A) Photomicrographs of *A. nidulans*, *V. dahliae*, *V. longisporum* and *S. macrospora* in the presence of pure chemicals. 0.075 mg pure emodin and chrysophanol were dissolved in methanol and loaded on the paper disc, and pure methanol as blank control. The discs were dried to evaporate the methanol completely, and then placed on spores-inoculated plates. For *A. nidulans*, 1 x 10_5 conidiospores were inoculated on minimal medium (MM) agar plates sexual grown for five days. For *Verticillium* sp., the simulated xylem medium (SXM) agar plates were inoculated with 1 x 10_5 *V. dahliae* or *V. longisporum* spores, 10 days at 25°C. For *S. macrospora*, the cornmeal malt fructification medium (BMM) agar plates were inoculated with 2 x 10_5 spores, seven days at 27°C. under = under the paper disc; back = the back side of paper disc; black bars = 200 µm; white bars = 1 mm. Impacted processes are highlighted in red frames. B) Egg laying of *Drosophila melanogaster* under the stress of emodin. On the ordinate, the distribution of the number of eggs in each well is shown. 12 wells of 24-well-plates were filled with 2 ml of a combination of Drosophila corn meal medium and fungal glucose minimal medium (DPM/GMM). 0.04 mg/ml of emodin was mixed in medium and pure ethanol as control. One fertilized female *Drosophila melanogaster* of the same generation was added in each well. After three days at 30°C in darkness, the flies were removed and the deposited eggs were enumerated (** $P < 0.05$).

4 Discussion

Disrupting the intact epi-/shamixanthone biosynthetic pathway by deleting the genes *mdpC*, *mdpL*, *mdpD*, *xptA* and *xptB* separately resulted in the accumulation of various precursors of epi-/shamixanthone. The negative effects of epi-/shamixanthone precursors on sexual development of *A. nidulans* were leading to smaller Hülle cells with reduced activity and a delayed maturation of sexual fruiting bodies. The most abundant and active epi-/shamixanthone precursors are emodin and its derivatives resulting in the strongest effect on Hülle cells and sexual fruiting bodies and exhibiting a broad bioactivity on other organisms, suppressing the formation of resting and reproductive structures of other fungi and insects.

Xanthones represent a structurally diverse class of natural products and are commonly present in plants, fungi, lichens and bacteria (Anderson *et al.*, 1988, Chiang *et al.*, 2010, Krick *et al.*, 2007, Luo *et al.*, 2014). Xanthone formation has been proposed to proceed by a complex sequence of rearrangement, deoxygenation, epoxidation, and Baeyer-Villiger oxidation (Chiang *et al.*, 2010). In *A. nidulans*, xanthone skeletal rearrangement is mainly genarated in two ways. The first way is the conversion of emodin to a benzophenone intermediate, known as monodictyphenone, which is subsequently cyclized to xanthones (Chiang *et al.*, 2010, Nielsen *et al.*, 2011). The second way is the conversion of emodin to its derivative, chrysophanol, which is continuously converted to xanthones via multistep reactions (Ahmed *et al.*, 1992, Pockrandt *et al.*, 2012). These pathways are commonly conserved in filamentous fungi (Fig. 28), *e.g.*, the cladofulvin biosynthesis in *Cladosporium fulvum* (Griffiths *et al.*, 2016); the biosynthesis of dihydroxy-xanthone, agnestins A and B in *Paecilomyces variotii* (Szwalbe *et al.*, 2019); geodin of *Aspergillus terreus* heterologously reconstituted in *A. nidulans* (Nielsen *et al.*, 2013b); the biosynthesis of ravenelin and shamixanthone in *Aspergillus variecolor* (Ahmed *et al.*, 1992, Ahmed *et al.*, 1987); the biosynthesis of ergochrome EE in *Penicillium oxalicum* (Franck *et al.*, 1980); the biosynthesis of cryptosporioptide in the endophytic fungus *Cryptosporiopsis* sp. 8999 (Greco *et al.*, 2019). These pathways are also conserved in lichen xanthone biosynthesis (Le Pogam *et al.*, 2016). Plants produce 80% of natural xanthones in a simpler way. They synthesize the xanthone skeleton without the anthraquinone emodin as

intermediate. The xanthone scaffold origins from an acetate-derived A-ring and a 3-hydroxybenzoic acid-derived C-ring (El-Seedi *et al.*, 2010).

The epi/shamixanthone-producing gene clusters *mdp/xpt* of *A. nidulans* consist of 15 genes, which produce approximately 30 xanthone precursors via the above mentioned chrysophanol and monodictyphenone pathways. These epi-/shamixanthone precursors are mainly based on anthraquinone and benzophenone skeletons.

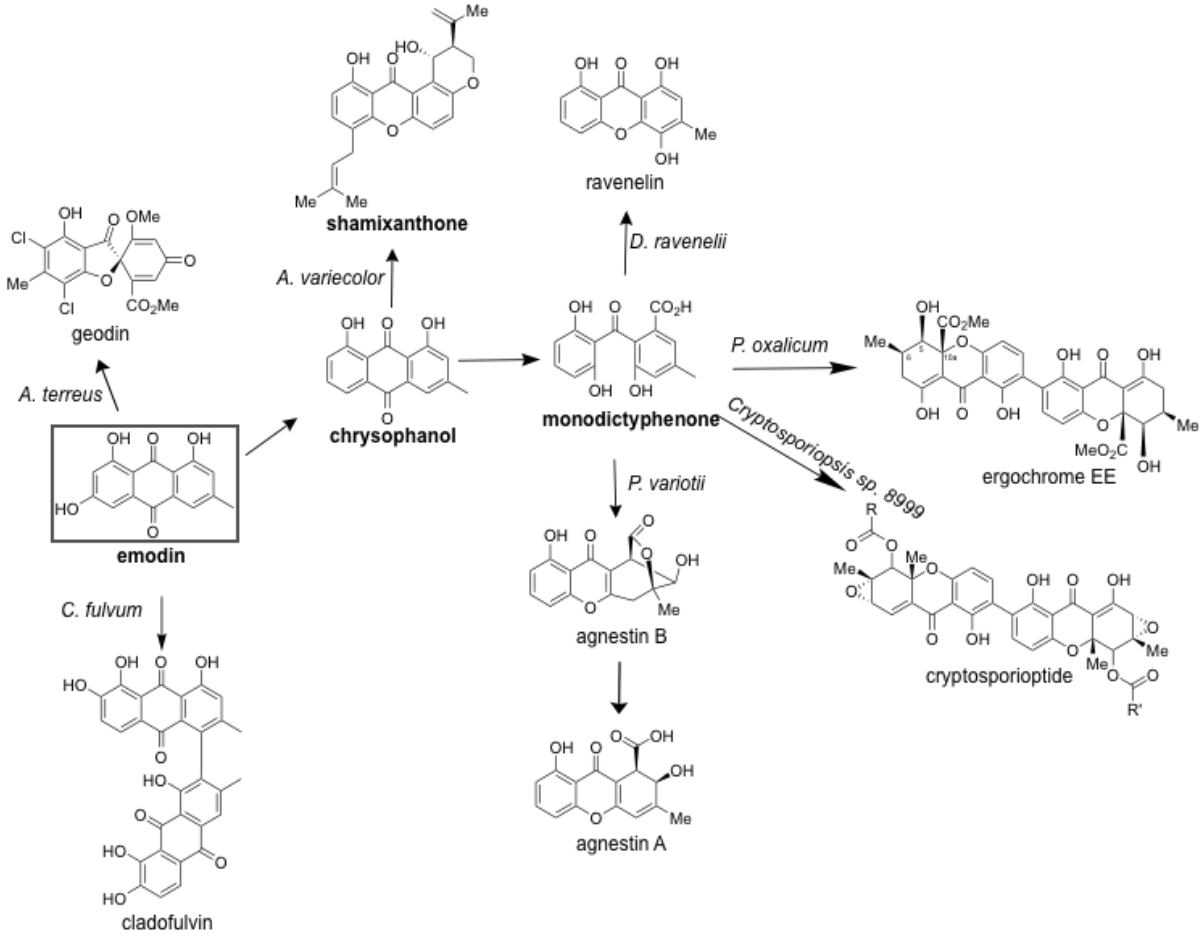

Figure 28. Typical fungal xanthone metabolites derived from emodin skeleton.
Emodin as the original skeleton forms diverse xanthones in different fungi. Highlighted compunds are also produced in *A. nidulans*. Summarized from Griffiths *et al.*, 2016, Szwalbe *et al.*, 2019, Nielsen *et al.*, 2013b, Ahmed *et al.*, 1992, Ahmed *et al.*, 1987, Franck *et al.*, 1980 and Greco *et al.*, 2019.

In this study, 8 genes of epi/shamixanthone biosynthetic pathway in *A. nidulans* were deleted, namely: the backbone PKS encoding gene *mdpG*, the Zn-dependent hydrolase encoding gene *mdpF*, the ketoreductase encoding gene *mdpC*, the Baeyer-Villiger oxidase encoding gene *mdpL*, the monooxygenase encoding gene *mdpD*, the prenyltransferase encoding genes *xptA*

and *xptB* and the GMC oxidoreductase encoding gene *xptC*. 11 known epi-/shamixanthone precursors and 6 unknown compounds from *mdp/xpt* deletion mutant strains were detected (Fig. 12-13, table 6). Among the known epi-/shamixanthone precursors, there are the anthraquinone skeleton based 2, ω-dihydroxyemodin (**4**), ω-hydroxyemodin (**5**), emodin (**6**) and chrysophanol (**7**) (Fig. 29). Benzophenone alcohol (**8**), paeciloxanthone (**9**), variecoxanthone A (**11**), monodictyphenone (**12**), post-monodictyphenone (**13**) and arugosin A (**18**) are the benzophenone skeleton based.

The compound **10** ($C_{15}H_{14}O_5$) detected in the SMs of Δ*mdpD*, Δ*xptA* and Δ*xptB* strains might be the emodin analog (atrochrysone) presented in the epi/shamixanthone biosynthetic pathway (Fig. 29). Compounds **16** ($C_{15}H_{12}O_5$) and **19** ($C_{15}H_{12}O_5$) were detected in the SMs of Δ*xptA* and Δ*mdpD* respectively. This suggests that compound **16** might be the precursor of variecoxanthone A and **19** might be arugosin F. The compound **15** ($C_{20}H_{22}O_5$) detected in the SMs of Δ*mdpD* and Δ*xptA* might be a paeciloxanthone analog. Compound **14** ($C_{30}H_{26}O_9$) and **17** ($C_{22}H_{25}NO_6$) were also detected in the SMs of Δ*mdpD* and Δ*xptA* but might be not derived directly by the *mdp/xpt* clusters. Compound **14** has more carbon atoms even than the final products epi/shamixanthone. Compound **17** contains a nitrogen atom, which is impossible coming from the epi/shamixanthone biosynthetic pathway.

In addition, the PKS encoding gene *mdpG* overexpression mutant strain (OE*mdpG*) showed no difference at all in the production of secondary metabolites in comparison to wild type (Fig. 11-13) and it also showed no impact on the sexual development of *A. nidulans*. Although the gene expression of *mdpG* was up-regulated more than 5-fold compared to the wild type (Fig. 10), it was not enough to drive the whole gene clusters. Another possible reason is that the up-regulation was just present on the gene expression level but not on the protein level.

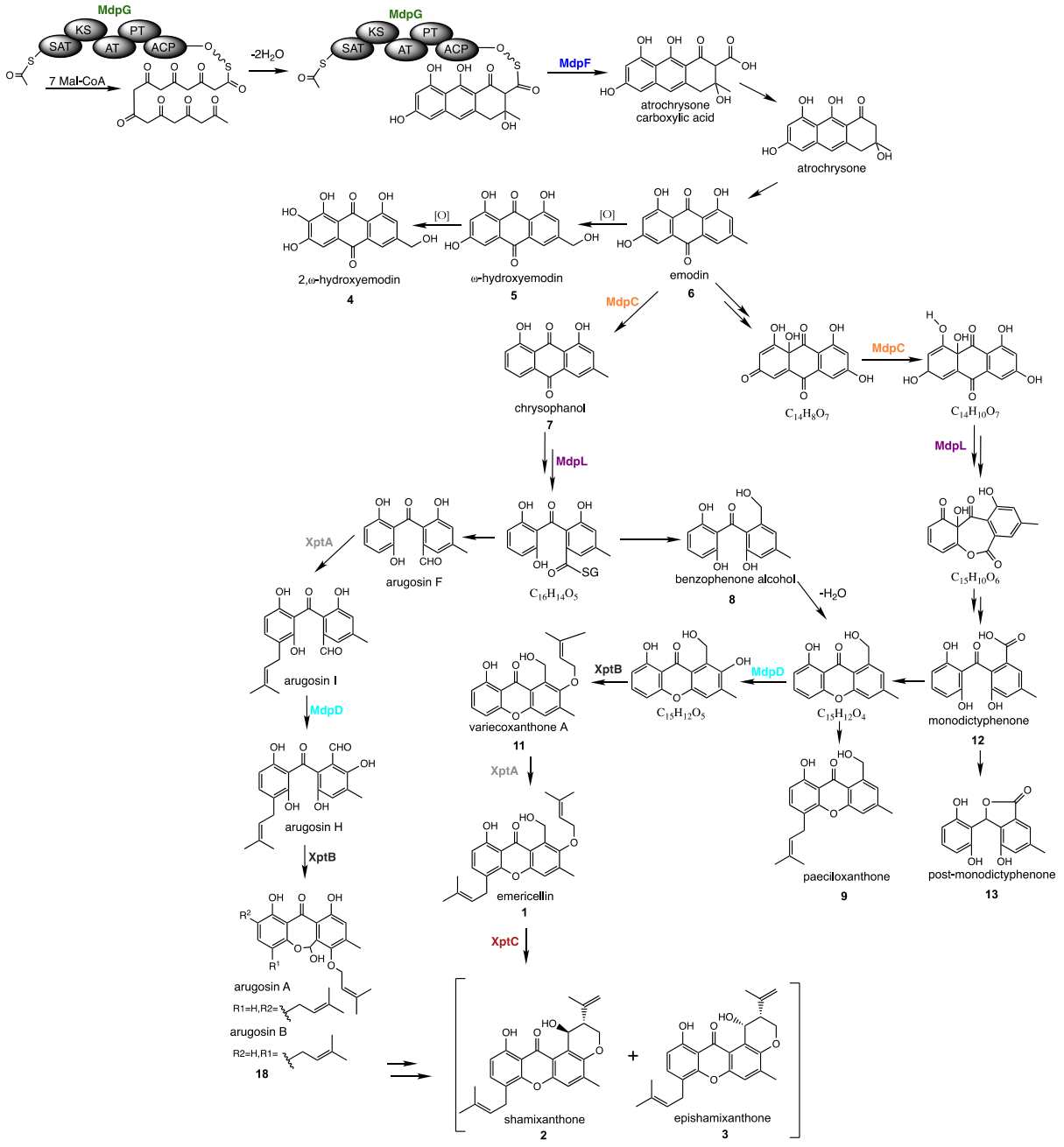

Figure 29. Simplified biosynthetic pathway of epi/shamixanthone in this study.

MdpG as the PKS backbone is localized at the first palce of the epi/shamixanthone biosynthetic pathway and catalyzes the starter units to form the octaketide. The hydrolase MdpF catalyzes polyketide and releases it from MdpG. Further spontaneous reactions lead to the formation of the crucial intermediate emodin. MdpC and MdpL are involved in the biotransformation from emodin to chrysophanol or monodictyphenone. The following processes are performed by the monooxygenase MdpD and prenyltransferases and oxidoreductase Xpt enzymes via benzophenone or arugosin pathway to form the final products shamixanthone and epishamixanthone. Modified from Chiang *et al.*, 2010, Pockrandt *et al.*, 2012 and Sanchez *et al.*, 2011. Analyzed enzymes are marked in the same color code as their encoding gene deletions in the Results part as shown in figure 12-13.

4.1 Products of *mdp/xpt* clusters are localized in Hülle cells.

As previously demonstrated by Bayram *et al*., the *mdp/xpt* clusters were up-regulated during sexual development in *A. nidulans* (Bayram *et al.*, 2016). Furthermore, four of Mdp/Xpt enzymes were localized in sexual mycelia and Hülle cells (Dirnberger, 2018). Normally, *A. nidulans* forms a yellowish colony on surface cultivation during sexual development. The yellow color originates from the aggregation of Hülle cells which was confirmed by microscopy. When deleting the backbone PKS encoding gene *mdpG* and the Zn-dependent hydrolase encoding gene *mdpF*, which are the first two steps in the epi/shamixanthone biosynthetic pathway (Fig. 29), the mutant strains did not produce any products of the *mdp/xpt* clusters. This result was confirmed by LC-MS, where the compounds emericellin (**1**), shamixanthone (**2**), epishamixanthone (**3**) and arugosin A (**18**) were not detected (Fig. 12). Furthermore, these two mutant strains produced colorless Hülle cells, which resulted in pale-looking colonies. In 2010, Chiang *et al*. showed that the most of the products of *mdp/xpt* clusters are yellow colors in powder forms (Chiang *et al.*, 2010). This indicates that the yellow color of *A. nidulans* colony is because of the products of *mdp/xpt* clusters which are enriched in Hülle cells. This was further confirmed by the deletion of the ketoreductase encoding gene *mdpC* and the Baeyer-Villiger oxidase encoding gene *mdpL*, which resulted in the accumulation of abundant reddish emodin and its derivatives resulting in reddish Hülle cells and colonies.

One of the proposed functions of Hülle cells is coping with biotic and/or abiotic stresses during sexual development. For instance, Hülle cells could be one strategy to cope with oxidative stress in *A. nidulans*. CpeA (Catalase-Peroxidase Gene) and the laccase II are localized to the Hülle cells (Hermann *et al.*, 1983, Scherer *et al.*, 2002). Both of them are dealing with the reactive oxygen species (ROS) during fungal development. The products of *mdp/xpt* clusters, emodins and xanthones, possess antioxidant bioactivity. They are localized in Hülle cells, which further support the antioxidative role of Hülle cells. Emodins and xanthones also possess antimicrobial and antifungal bioactivity. During cleistothecium development, it was demonstrated that surrounding Hülle cells accumulated emodins and xanthones (Fig. 15B). They can possibly act as the chemical weapons against other competitors in the growing niche. This ecological point of view is also supported by the distribution of emodin among plant organs. Normally, the

unripe fruits, seeds and roots of plants contain higher emodin concentration than leaves and other organs to fight against potential enemies (Izhaki, 2002).

4.2 Precursors of epi-/shamixanthone repress sexual development of *A. nidulans*.

4.2.1 Emodins are the main factors of sexual development repression.

A different degree of delay in sexual development was observed upon deleting different genes of *mdp/xpt* clusters due to the accumulation of the precursors of epi-/shamixanthone in the mutant strains (Fig. 18A). The Δ*mdpC* strain accumulated high amounts of 2, ω-dihydroxyemodin (**4**), ω-hydroxyemodin (**5**) and emodin (**6**) and exhibited the strongest delay of sexual fruiting body maturation among the tested *mdp/xpt* mutant strains (Fig. 14 and 18-19). The Δ*mdpL* and Δ*xptB* strains accumulated less emodin and its derivatives in comparison to Δ*mdpC* strain and therefore exhibited only a moderate delay of sexual fruiting body maturation, as expected. Δ*mdpD* and Δ*xptA* strains accumulated various benzophenone compounds and several unidentified compounds without emodins and exhibited a slightly delay in maturation of sexual fruiting bodies.

All of these five mutant strains produced smaller Hülle cells (Fig. 19A). Therein, Δ*mdpC*, Δ*mdpL* and Δ*xptB* strains showed a stronger delay in sexual fruiting body maturation and produced smaller cleistothecia (Fig. 18B). This might be because of the accumulation of emodin and its derivatives.

Hülle cells differentiate from hyphae in the early stage of sexual development forming a nest-like structure around the developing cleistothecium (Sohn *et al.,* 2002). The functions of Hülle cells are protection and nourishment of the maturating cleistothecium (Braus *et al*., 2002, Bayram *et al*., 2010) and they have the possibility of germinating and developing a novel branch in the life cycle of *A. nidulans* (Ellis *et al.,* 1973). Hülle cells contain various enzymes required for cleistothecia development and coping with abiotic stresses (Hermann *et al.*, 1983, Scherer *et al.*, 2002, Wei *et al.*, 2001). The control and regulation of Hülle cell formation and cleistothecia development are correlated but not completely dependent on each other. The COP9 signalosome (CSN) in *A. nidulans* is a key regulator of sexual development and the Δ*csn* mutant strains are capable of initiating the sexual cycle to develop thick Hülle cells- nests and

primordia, but maturation to cleistothecia is blocked (Busch *et al.*, 2003). The global regulator of fungal development and secondary metabolism *laeA* deletion strain cannot produce normal amounts of Hülle cells as wild type, which results in the formation of significantly smaller cleistothecia compared to wild type (Bayram *et al.*, 2010). This information suggests that Hülle cells is crucial for the sexual fruiting body development.

In this study, two fungal activities supported by Hülle cells were analyzed. One is the germination ability of Hülle cells and another is *mutA* expression control. Hülle cells can germinate and form vegetative hyphae to start a new life cycle (Ellis *et al.*, 1973). In this work, Hülle cells from Δ*mdpC* and Δ*mdpL* strains exhibited reduced germination activity as well as reduced *mutA* expression levels compared to wild type and Δ*mdpG* (Fig. 19). The reason might be that the accumulated emodins are harmful to the Hülle cells. It was shown that the gene *mutA* was particularly expressed in Hülle cells during sexual development probably to provide polysaccharides for the developing cleistothecium (Wei *et al*., 2001). The gene *mutA* is expressed normally in "healthy" Hülle cells and providing materials for cleistothecia. If Hülle cells are not "healthy" and cannot perform their functions accordingly, the expression of *mutA* also will be influenced. Namely, the expression of *mutA* can be one indicator of Hülle cells activity (Bayram *et al.*, 2010, Vienken *et al.*, 2005, Wei *et al.*, 2001). This further supports that Hülle cells act as the nursing cells, protect and provide nutrients for the developing cleistothecia (Bayram *et al.*, 2010, Hermann *et al.*, 1983).

Taken together, precursors of epi-/shamixanthone (Fig. 14) accumulated in Hülle cells might have weakened the activity of Hülle cells, which in turn weakened the support for cleistothecia development, and resulted in the maturation delay of the cleistothecia. Therein, accumulated emodins play crucial roles in repressing the development of Hülle cells. This is in agreements with the profile of the extracted SMs from *A. nidulans* strains. In particular, the SMs of Δ*mdpC* showed significant repression on cleistothecia development (Fig. 20). Although SM extracts from Δ*mdpL* and Δ*xptB* also contained emodin and its derivatives, their concentration was too low (Fig. 14) to repress the cleistothecia development though extracellular in comparison to SMs of Δ*mdpC*. This also implies that the effect of emodins is concentration dependent.

Pure emodin alone, however, has no impact on the cleistothecia development of *A. nidulans* (Fig. 27A). This does not contradict the results of this study, because the extracted SMs are a mixture of compounds and in many cases it was shown that these active secondary metabolites do not work alone (Izhaki, 2002). The SM extracts from Δ*mdpC* mutant strain contain not only abundant emodin but also emodin-derived compounds, such as 2, ω-dihydroxyemodin and ω-hydroxyemodin. This mixture might have chemical interaction exhibiting the activity on the cleistothecia development of Δ*mdpC*. For example, dehydroaustinol can rescue the non-sporulation only in conjunction with the orsellinic acid derivative diorcinol (Rodríguez-Urra *et al.*, 2012). This case can help to understand that the pure emodin alone did not repress the cleistothecia development of *A. nidulans*.

4.2.2 The repression of sexual development is independent of MAPK pheromone pathways or the velvet complex

Sexual development of *A. nidulans* is controlled and regulated by multiple transcription regulators and signaling pathways. In this study, interruption of the xanthone biosynthetic pathway resulted in accumulation of emodins and its derivatives in Hülle cells. As a result, Hülle cell development was further repressed showing reduced activity and delayed cleistothecium development.

The global regulator of secondary metabolism LaeA is involved in the production of sterigmatocystin, penicillin and many other compounds in *A. nidulans*, which might confer a certain advantage to the fungus during growth under competition environment. As LaeA also partly controls the formation of Hülle cells, loss of LaeA function resulted in almost no Hülle cell formation, as demonstrated by Bayram *et al.* (Bayram *et al.*, 2010). In this study, the repression of Hülle cells development due to the accumulation of emodins and its derivatives, showed no change in the expression levels of *laeA* gene (Fig. 23).

In the dark, LaeA interacts with the velvet family members VeA and VelB to form the VelB-VeA-LaeA (velvet) complex, which controls the fungal sexual development and secondary metabolism of *A. nidulans*. VeA is a positive regulator in sexual development (Kim *et al.*, 2002), whereas VelB is a positive regulator of asexual development, interacting with VosA to regulate conidiospore maturation and germination (Park *et al.*, 2012). VelB can also interact with VeA

to control sexual development (Bayram *et al.*, 2008). In this study, no change in the expression of *veA* was observed when deleting *mdpC* in comparison to wild type (no statistically significant difference). The gene expression of *velB* on the other hand, exhibited significant difference in the deletion of the *mdpC* strain only in late stage of sexual development. While no change was observed in the early stage of sexual development, significant down-regulated was observed in the late stage of sexual development in Δ*mdpC* mutant strain in compared to wild type. However, the sexual development delay in the deletion of the *mdpC* mutant strain was observed in the early stage of development (Fig. 18A). The gene expression of velvet complex cannot explain the reason of delayed sexual development. The down-regulation of *velB* might just reflect the feedback of delayed sexual development.

Another possibility is that emodins affect the velvet complex at protein level. The emodin derivatives aloe-emodin, chrysophanol, rhein and physcion characterized in other organisms were described have binding affinities to proteins in NF-κB pathways (Panigrahi *et al.*, 2015b, Quan *et al.*, 2019). NF-κB proteins are transcription factors commonly present in mammalian cells possessing a central role in coordinating the expression of a wide variety of genes that control immune responses (Li *et al.*, 2002). They are structurally similar to velvet proteins (Ahmed *et al.*, 2013). The velvet family member VeA can be activated in phosphorylation and enters into the nucleus to form the velvet complex with VelB and LaeA (Bayram *et al.*, 2008, Frawley *et al.*, 2018), and regulates the formation of Hülle cells and cleistothecia (Kim *et al.*, 2002). Stefan Rauscher and co-workers confirmed that dephosphorylated VeA reduced the velvet complex formation, induced the *veA* gene expression and also delayed the cleistothecia development (Rauscher *et al.*, 2016). Emodins might bind to VeA preventing its proper phosphorylation which reduces the velvet complex formation, and thereby delays sexual development in early stage. Then, the feedback of the requirement of more VeA was transduced to the gene expression. This might be the reason why *veA* exhibited moderate up-regulation in the deletion of the *mdpC* strain (Fig. 23). The delayed sexual development was released after 7-10 days (Fig. 18A). The possible reason is the concentration of emodins reduced along with the development process (Fig. 14). The phosphorylation of VeA is not inhibited any longer and the velvet complex can be formed like normal.

StuA is a morphological modifier required for the very earliest events of asexual reproduction but also required for inducing the expression of the catalase-peroxidase gene (*cpeA*) during sexual development (Miller *et al.*, 1991, Scherer *et al.*, 2002). The coding gene *stuA* showed no change in the early stage of sexual development but significant up-regulation in Δ*mdpC* after five days (Fig. 23). One possible explanation is that emodins accumulation resulted in ROS increase (Lin *et al.*, 2019), which then induced the expression of catalase-peroxidase genes via the developmental regulator StuA as the detoxification mechanism.

The MAPK pheromone pathways have evolved to transduce environmental and developmental signals (growth factors, stress) into adaptive and programmed responses (Peti *et al.*, 2013). Four MAPK pheromone pathways are present in *A. nidulans*. Two of them have the stress-activated protein kinases (SAPKs) SakA and MpkC as key players and are involved in stress signal transduction and repression of sexual development. The third pathway harbors MpkB as key player, which interacts with the conserved nuclear transcription factor SteA to initiate sexual development and also phosphorylates the sexual regulator VeA (Bayram *et al.*, 2012a). The fourth pathway with MpkA regulates cell wall signaling, oxidative stress response and secondary metabolism (Valiante *et al.*, 2008, Chelius *et al.*, 2019). In mammalian cells, emodin induces tumor cell apoptosis and protects against hepatitis through inhibiting activation of the MAPK signaling pathways (He *et al.*, 2018, Jiang *et al.*, 2018, Xue *et al.*, 2015). Emodin has chemical groups that can bind to the dewatering groups of p38 MAPK analyzed via a molecular designing software (Wang *et al.*, 2006). *A. nidulans sakA* gene encodes a member of the Hog1/Spc1/p38 MAPK family, and SakA is activated by phosphorylation in response to oxidative stress (Kawasaki *et al.*, 2002). However, *sakA* expression level showed no changes in the deletion of *mdpG*, *mdpC* and *mdpL* strains and *A. nidulans* wild type. Also, no change in expression level was observed for the *mpkB* gene. The SakA ortholog MpkC shows 62% identity to SkaA and physically interacts with SakA, playing major, distinct and sometimes opposing roles in conidiation and in response to stress (Aguirre *et al.*, 2018). The encoding gene *mpkC* showed no changes in the deletion of *mdpG*, *mdpC* and *mdpL* strains and *A. nidulans* wild type in the early stage of sexual development but was significantly down-regulated in the sexual development delayed mutant strains after five days. The reason can also be that emodins

accumulation increased the oxidative stress in cells, which induced the MpkC nuclear accumulation (Aguirre *et al.*, 2018). The down-regulation of *mpkC* expression might be because of the negative feedback of MpkC nuclear accumulation.

On the protein level, active phosphorylated SakA and MpkC can be detected by the same antibody anti-phospho-p38 through western immunoblotting. Both of them showed no difference in the deletion of *mdpG*, *mdpC* and *mdpL* strains and *A. nidulans* wild type (Fig. 24A). Also total SakA detected by a GFP-tagged version and a GFP antibody was not changed by deletion of the genes *mdpG*, *mdpC* and *mdpL* (Fig. 24B). One possibility is that small molecular emodins just bind to the target proteins by forming hydrogen bonds changing the protein conformation and affecting the protein activity but not the protein level (Wink *et al.*, 2018). Since these interactions are possible with a lot of target proteins, we would expect that emodin has multiple targets in cells and multifunctional activities.

In summary, the accumulation of epi-/shamixanthone precursors resulted in the repression of sexual development in *A. nidulans* had no connection been found with the MAPK pheromone pathways or the velvet complex, although it resulted in some regulator genes expression change in the late stage of sexual development as the by-effects. This might be elucidated by further experiments.

4.3 Increased amounts of epi-/shamixanthone precursors cause oxidative and weak acidic stress sensitivity.

Many filamentous fungi produce red, bluish green or black polyketide-derived pigments, which can play a protective role against environmental stresses such as UV irradiation and oxidation (Durán *et al.*, 2002). *A. nidulans* produces yellowish xanthones derived by the *mdp/xpt* clusters during sexual development. Deletion of genes of the *mdp/xpt* clusters localized at the downstream of the epi-/shamixanthone biosynthetic pathway resulted in the accumulation of xanthone precursors. These accumulated pigments exhibited no effect on the resistance of UV irradiation but caused oxidative and weak acidic stress sensitivity that led to repressed development of cleistothecia in *A. nidulans* (Fig. 25B). Although the repression also happened in these xanthone precursors accumulated strains under normal growth conditions, after five days, the repression was enhanced dramatically in the presence of the oxidative and weak acidic

stress. This result suggests that accumulated xanthone precursors already weakened the cell ability in some degree. Extracellular oxidative and weak acidic stresses can induce further intracellular oxidative stress (Sugihara *et al.*, 1998, Taghavi *et al.*, 2013). This might be strongly repressed the sexual development.

4.4 Precursors of epi-/shamixanthone have a broad bioactivity on other organisms.

4.4.1 Repression of *Verticillium* spp. resting structure formation.

SMs extracted from Δ*mdpC* and Δ*mdpL* mutant strains were rich in 2, ω-dihydroxyemodin (**4**), ω-hydroxyemodin (**5**), emodin (**6**) and chrysophanol (**7**) (Fig. 12-14), which exhibited strong repression on the microsclerotia formation of *V. longisporum* (Fig. 26A). Emodin as the crucial intermediate of xanthone possesses a broad spectrum of bioactivities. It displays antifungal activity against 6 plant pathogenic fungi by affecting colony morphology and protein synthesis, and destroying cell membrane (Luo *et al.*, 2019). Chrysophanol, derives from emodin by losing the 3-hydroxy group, exhibited fungicidal effects against powdery mildew caused by *Blumeria graminis* f. sp. *hordei* and *Podosphaera xanthii* (Choi *et al.*, 2004, Hildebrandt *et al.*, 2018), against ring worm caused by dermatophytes, and against *Candida albicans*, *Cryptococus neoformans*, *Trichophyton mentagrophytes* and *Aspergillus fumigatus* (Malik *et al.*, 2016). This is further confirmed by the fact that pure chemical emodin repressed the microsclerotia formation of *V. longisporum*, and pure chrysophanol moderately repressed the microsclerotia formation of *V. longisporum* (Fig. 27A). However, pure emodin and chrysophanol had no obvious effect on *V. dahliae*. SMs of Δ*mdpC* and Δ*mdpL* after five days repressed the formation of microsclerotia of *V. dahliae* (Fig. 26A). This might not be because of 2, ω-dihydroxyemodin (**4**), ω-hydroxyemodin (**5**) and emodin (**6**) but because of secondary metabolites from other gene clusters.

Although SMs extracted from Δ*mdpD* did not contain emodins and chrysophanol, it still repressed the microsclerotia formation of *V. longisporum*. SMs of Δ*mdpD* contained various benzophenones, such as benzophenone alcohol (**8)**, monodictyphenone (**12)** and post-monodictyphenone **(13)**, and paeciloxanthone (**9**) as well as some unidentified compounds, $C_{30}H_{26}O_9$ (**14**), $C_{20}H_{22}O_5$ (**15**) and $C_{15}H_{12}O_5$ (**19**) (Fig. 12). These compounds might be the

factors of repression of the microsclerotia. Although there is no direct evidence to support this speculation, several cases shows that benzophenone-related compounds have been found to be antifungal agents against *Candida parapsilosis* and *Candida glabrata* (Pippi *et al.*, 2015). Monodictyphenone was firstly isolated from the fungus *Monodictys putredinis* (Krick *et al.*, 2007) and showed a moderate inhibition of the phase I enzyme Cyp1A of carcinogens. *iso*-monodictyphenone was identified from the marine mangrove-derived fungus *Penicillium* sp. MA-37 (Luo *et al.*, 2014) and exhibited brine shrimp lethality and showed activity against the aqua-bacterium *Aeromonas hydrophilia*. Moreover, paeciloxanthone exhibited cytotoxicity against hepG2, acetylcholineesterase (AChE) inhibitory and antimicrobial activities (Wen *et al.*, 2008).

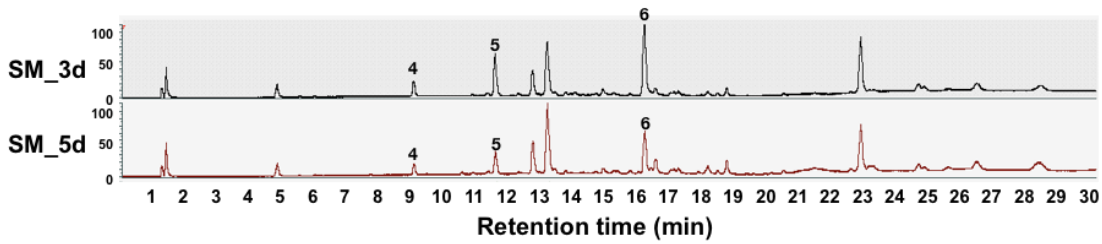

Figure 30. Comparison of secondary metabolites of Δ*mdpC* strain from three and five days of sexual growth.

Y-axis means Abs (absorbance units). **4**) 2, ω-dihydroxyemodin; **5**) ω-hydroxyemodin; **6**) emodin. SM_3d contains 90% of **4**, 394% of **5** and 851% of **6**. SM_5d contains 83% of **4**, 230% of **5** and 543% of **6**. The relative quantification was based on PABA (peak area was set to 100%) as described in the Method part.

The inhibition of microsclerotia formation of *V. longisporum* varies between SMs extracted from Δ*mdpD* after three days or five days of sexual growth. SMs extracted after three days showed stronger inhibition than SMs extracted after five days. This can be due to the reduced amounts of benzophenone alcohol (**8**) and compound **14** ($C_{30}H_{26}O_9$) in SMs extracted after five days. However, SMs extracted from Δ*mdpC* mutant strain after three days showed weaker inhibition on the microscrotia formation of *V. longisporum* compared SMs extracted after five days. This cannot be explained by the *mdp/xpt* clusters products because SMs extracted from Δ*mdpC* mutant strain after three days contain more emodins than after five days (Fig. 30). Therefore, the inhibition effect observed by SMs extracted from Δ*mdpC* might be because of other bioactive SMs of *A. nidulans*. For example, the *mdp/xpt* clusters also involved in

sterigmatocystin production (Simpson, 2012, Szwalbe *et al.*, 2019). Disturbed epi-/shamixanthone biosynthesis by deleting gene *mdpC* might also influence other SMs production. However, the changes have not been found from current measurements.

4.4.2 Repression of *S. macrospora* reproduction

S. macrospora is a homothallic fungus. Protoperithecia can develop directly into sexual fruiting bodies (perithecia), and conidia and trichogynes are absent (Lord *et al.*, 2011). Perithecium formation begins with ascogonial coils. Along with ascogonial coil growing, the spherical protoperithecium is formed and matures to form a pigmented, flask-shaped perithecium within seven days. Esser and co-workers identified 22 genes involved in different stages of perithecial morphogenesis (Esser *et al.*, 1958) and lately Lord and coworkers analyzed eight of these genes in the life cycle of *S. macrospora* and proposed a detailed developmental pathway of perithecial morphogenesis (Lord *et al.*, 2011).

In the present study, we provide evidence that the extracellular stimuli regulate perithecium formation of *S. macrospora*. SMs extracted after three days of sexual growth of *A. nidulans* wild type and *mdp/xpt* deletion strains repressed the perithecium formation of *S. macrospora* strongly, as well as SMs extracted after five days from mutant strains Δ*mdpC*, Δ*mdpL* and Δ*mdpD* (Fig. 26C). Since all SMs of after three days from *A. nidulans* wild type and *mdp/xpt* deletion strains repressed perithecium formation, the effect is not only from the *mdp/xpt* clusters, an effect that comes from other gene clusters. For example, SMs extracted from Δ*mdpG* and Δ*mdpF* after three days of sexual growth without any metabolites derived by the *mdp/xpt* clusters (Fig. 11-12), which repressed the perithecia formation of *S. macrospora*. SMs of five days from mutant strains Δ*mdpC*, Δ*mdpL* and Δ*mdpD* exhibited a strong repression on the formation of perithecia. This might be because of emodins and benzophenones containing. Whereas, SMs of *A. nidulans* wild type, OE*mdpG* and deletion of *mdpG*, *mdpF*, *xptA*, *xptB* and *xptC* after five days exhibited less repression on the formation of perithecia (Fig. 26C). This might be because of the concentration changes of other secondary metabolites. For example, compound **22** was decreased in SMs of *A. nidulans* wild type after five days (Fig. 31). The compound **22** was identified in positive mode with $[M+H]^+$: 282.2791(table 6). This compound

might be an oleamide analog (https://www.smitherspira.com/SmithersPira/media/Food-Contact/HR-LCMS-and-GC-MSMS-Analyses-of-NIAS-Smithers-Pira.pdf). Oleamide as an endogenous bioactive lipid signaling molecule has been well characterized in mammalian nervous system (Mendelson *et al*., 2001) and possesses the antiallergic activity by suppressing p38 mitogen-activated protein kinases (p38-MAPKs) in mammalian cells (Yang *et al*., 2016). This information suggests that the compound **22** might also possesses bioactivity repressing the the perithecia formation of *S. macrospora*.

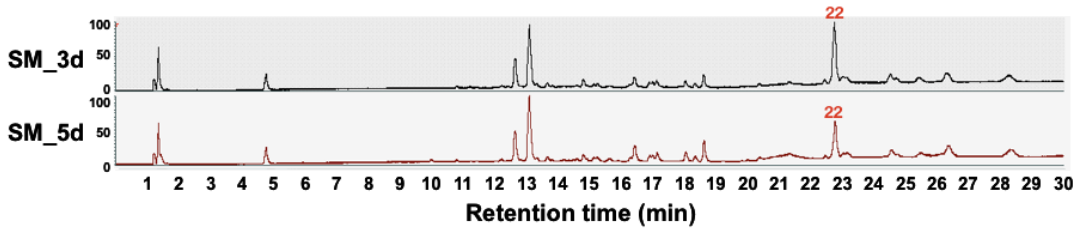

Figure 31. Comparison of secondary metabolites of *A. nidulans* wild type from three and five days of sexual growth.
Y-axis means Abs (absorbance units). **22**) $[M+H]^+$: 282.2791.

The SMs extracted from *A. nidulans* strains repressed the perithecia formation of *S. macrospora* resulting in the formation of repression halos surrounding the paper discs, especially that from the mutant strain Δ*mdpC*, which contains abundant amounts of emodins. Furthermore, pure emodin tested on *S. macrospora* verified that emodin is one of the key factors of *A. nidulans* SMs that repress the perithecia formation of *S. macrospora*. But its effect is less than the SM extracts of Δ*mdpC* (Fig. 27). In the future, it is worth to elucidate the repression machansims of emodin on the perithecia formation.

4.4.4 Repression of fly egg laying activity

Secondary metabolites play important roles in fungal-insect antagonism including communication, developmental control and defense. *Drosophila melanogaster* and species of the fungus *Aspergillus* (*A. nidulans*, *A. fumigatus* and *A. flavus*) are a well-studied model of animal-microbe competition. Juvenile hormone is a distinct animal hormone that affects insect development and reproduction (Wyatt *et al.*, 1996). In 2013, Nielsen *et al*. induced the production of juvenile hormone-III in *A. nidulans* by feeding *A. nidulans* to *D. melanogaster* larvae (Nielsen *et al.*, 2013a).

LaeA is a global secondary metabolites regulator in *Aspergillus*. A *laeA* deletion strain reduced or even blocked the production of several secondary metabolites, including insecticidal mycotoxins, such as sterigmatocystin from *A. nidulans*, aflatoxin from *A. flavus* and gliotoxin from *A. fumigatus* (Bok *et al.*, 2004, Kale *et al.*, 2008, Perrin *et al.*, 2007). *A. nidulans laeA* deletion strain was more fit for the fungivorous springtail *Folsomia candida* and larvae survival of *Drosophila melanogaster* and suffered more fungivory than *A. nidulans* wild type (Rohlfs *et al.*, 2007, Trienens *et al.*, 2010). Disruption of the production of some secondary metabolites directly affects insect survival and behavior. Deletion of the PKS encoding gene *mdpG* increased the adult *Drosophila melanogaster* egg laying activity (Regulin *et al.*, 2018). This indicates that the products related to *mdpG* and its gene clusters must have influences on the *D. melanogaster* egg laying behavior. In line with previous results, we tested the effect of pure emodin on female *D. melanogaster* with same concentration of the emodin produced in a single colony of Δ*mdpC* after five days of sexual growth. The pure emodin exhibited significant repression on the amount of deposited *D. melanogaster* eggs (Fig. 27B). Emodin is one of the anthraquinone derivatives, which are commonly found in dyes and pigments, and many plants and other organisms. Anthraquinones are promising candidates for many contexts of insecticidal pest management in ecosystem-friendly ways (DeLiberto *et al.*, 2016). Emodin was identified as the crucial chemical in *Cassia obtusifolia* seeds extract against mosquito larvae (Yang *et al.*, 2003). Kambou Georges and co-worker also identified emodin as the most abundant and active anthraquinone in *Cassia nigricans* exhibiting approximately 85% mortality on adult *Bemisia tabaci* and larvae *Anopheles gambiaea* (Georges *et al.*, 2008). It was also reported that some plant seeds were toxic to poultry and wild birds as the plant seeds contained emodins (Damron *et al.*, 2001). These findings suggest that anthraquinone emodins can be widely used in organic pest managements.

4.5 Conclusion and outlook

The diversity of secondary metabolite function and structure is still perplexing and needs to be further elucidated. This study demonstrated the *in vivo* roles of secondary metabolites in fungal development and their broad bioactivity on other organisms. The PKS encoding *mdp/xpt* gene

clusters produced emodins and benzophenones and their derivatives as intermediates, which were finally conversed into epi-/shamixanthone. Most of the products of the *mdp/xpt* gene clusters have an anthraquinone skeleton and the others have a benzophenone skeleton. Emodins were the most abundant and active compounds accumulated in *mdp/xpt* cluster deletion strains during sexual development in *A. nidulans*. Emodins were localized in Hülle cells, which are a special cell type required for sexual fruiting body development. We could demonstrate that abundant amounts of emodins repressed the development of Hülle cells, leading to smaller size Hülle cells with reduced activity. Emodins also repressed the development of cleistothecia, which were smaller in size and showed delayed maturation. Furthermore, we observed that emodins accumulation also caused oxidative and weak acidic stress sensitivity in *A. nidulans* resulting in strongly delayed cleistothecia maturation. Emodins, however, exhibited no influence on asexual development and vegetative growth. These small molecules have an anthraquinone backbone with -OH and -CH_2OH groups and exhibited broad bioactivity on other fungi and insects (Fig. 32). They inhibited the resting structure formation of the plant pathogenic fungus *Verticillium longisporum* and the fruiting body formation of the model fungus *Sordaria macrospora*. Among these anthraquinone metabolites, emodin is one of the crucial active ingredients which also was verified to reduce the fly egg laying activity.

Although xanthones derived from the anthraquinone emodin are widely present in fungi (Fig. 28), the intact *mdp/xpt* clusters of *A. nidulans* are reasonably unique within the analyzed 18 *Aspergillus* species. The *mdp/xpt* clusters of *A. nidulans* have partly synteny in *A. sydowii* and *A. versicolor* (de Vries *et al.*, 2017). *A. nidulans* and *A. versicolor* are capable of forming dark cleistothecia with walls composed of flattened cells and red ascospores inside. These cleistothecia were surrounded by a stromatic layer of Hülle cells (Geiser, 2009). The speculation of actual significance of this mode of reproduction is acting as overwintering structures for survival in the soil or other harsh niches. The *mdp/xpt* clusters were specifically expressed during cleistothecia formation and produced various active products in Hülle cells. This implies that the metabolites derived by *mdp/xpt* clusters play protective roles in cleistothecia development against surrounding competitors and/or predators.

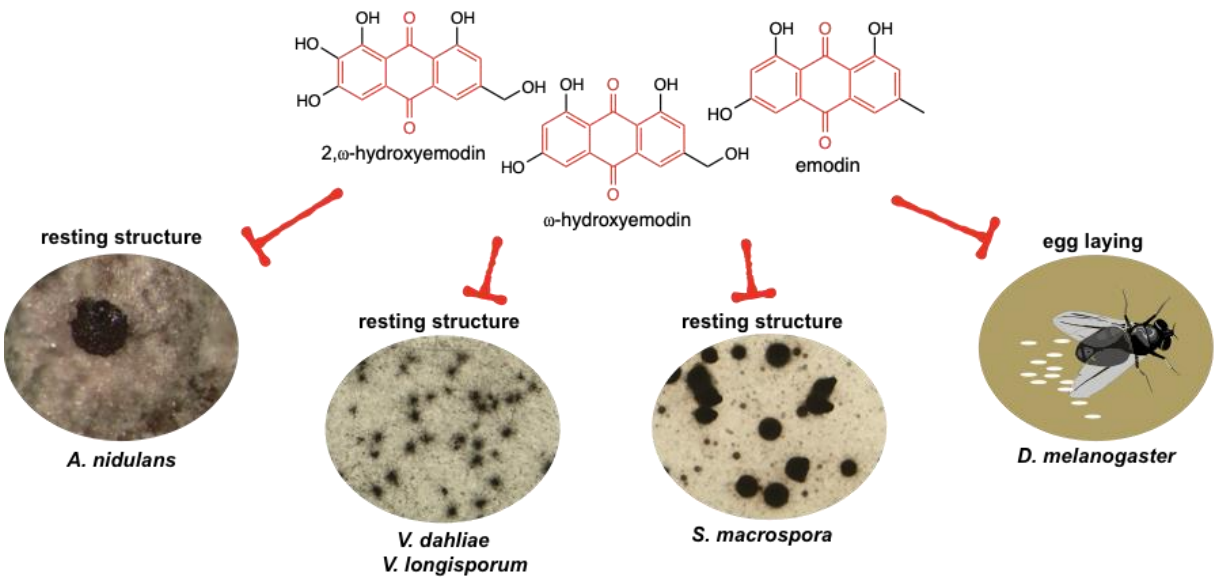

Figure 32. Emodins exhibited a broad bioactivity on fungal and insect reproduction and survival structures.
Emodins are the most abundant and active precursors of epi-/shamixanthone accumulated in *A. nidulans*, which repress the development of sexual fruiting body and Hülle cell of *A. nidulans*. Extracted emodins from *A. nidulans* repress the formation of resting structure of *Verticillium* sp. and the fruiting body of *S. macrospora*. This was furtherly confirmed by testing pure emodin on these fungi as well as on the egg laying activity of *D. melanogaster*.

Emodin and its derivatives have aroused great interest among researchers due to their functional diversity and their high potential for pharmaceutical implications. The mode of action of emodin described in the literature include emodin as a proteinase inhibitor binding to the active center of proteins, down-regulating signals or developmental regulator genes, and /or provoking oxidative stress, triggering cell membrane scrambling and disturbing ion channels (Dong *et al.*, 2016, Koerner *et al.*, 2017, Mischitelli *et al.*, 2016). All of these effects can induce cell apoptosis and death. Researches mainly focus on mammalian cells to elucidate the regulatory mechanisms of antitumor and anti-inflammatory activities.

Emodin possesses antioxidant activity but also increases intracellular oxidative stress (Moreira *et al.*, 2018). Emodin possesses $O_2^{\bullet-}$ and $^{\bullet}NO$ capture capacity and can also increase the thiobarbituric acid reactive species (TBARS) in tested tumor cells. Under normal physiological conditions, cells can keep a balance between oxidative species and antioxidants. ROS can regulate cell proliferation, differentiation and metabolism, and can also activate healthy immune responses in low concentration. On the contrary, a high amount of ROS leads to DNA

damage and lipid oxidation. In a similar way, the effects of emodin on ROS can vary depending on its cellular concentration. In the case of *A. nidulans*, *mdp/xpt* mutant strains accumulated abundant amount of emodin and its derivatives in the early stage of sexual development while decreased amount of emodin and its derivatives was observed in the late stage. Meanwhile, the repression of sexual fruiting body development was observed in the early stage of development while it was released in the late stage of development. The underlying mechanism might be that the abundant emodins increased the ROS in cells and caused the cytotoxic effects in cell proliferation and differentiation, which are frequently happening in the early stage of sexual fruiting body formation (Sohn *et al.*, 2002). The amount of emodin decreased with fungal growth process might indicate the connection with catalase, superoxide dismutase (SOD) and NADPH oxidase (NOX) which act on ROS metabolism. The following events illustrate how a proper level of ROS might rescue the delayed maturation of sexual fruiting bodies (Fig. 33).

This hypothesis might also apply to the mode of action of SMs extracted from *A. nidulans* strains tested on other organisms. In plant-fungal interactions, oxidative burst induced by biological inducers of plant defense system is a peculiar example of the participation of ROS (Gessler *et al.*, 2007). Some of the inducers are linked to the fungal cell wall, while the receptors are located on the plant plasma membrane. When fungal infection is recognized by the plant, a defense reaction is initiated and fungal cells are subjected to the oxidative stress from the plant. Emodin and its derivatives originated from *A. nidulans* might have triggered the defense reaction of the tested organisms and promoted ROS burst, which is also susceptible and harmful to the producers. The results suggest that emodins are chemical weapons against other competitors and also indicate the biological functions of emodin production in *A. nidulans*. Emodins widely found in planta and fungi possess high potential in pharmaceutical industry. Emodins can be used as fungicides and insecticides to allow organic defense in the agriculture.

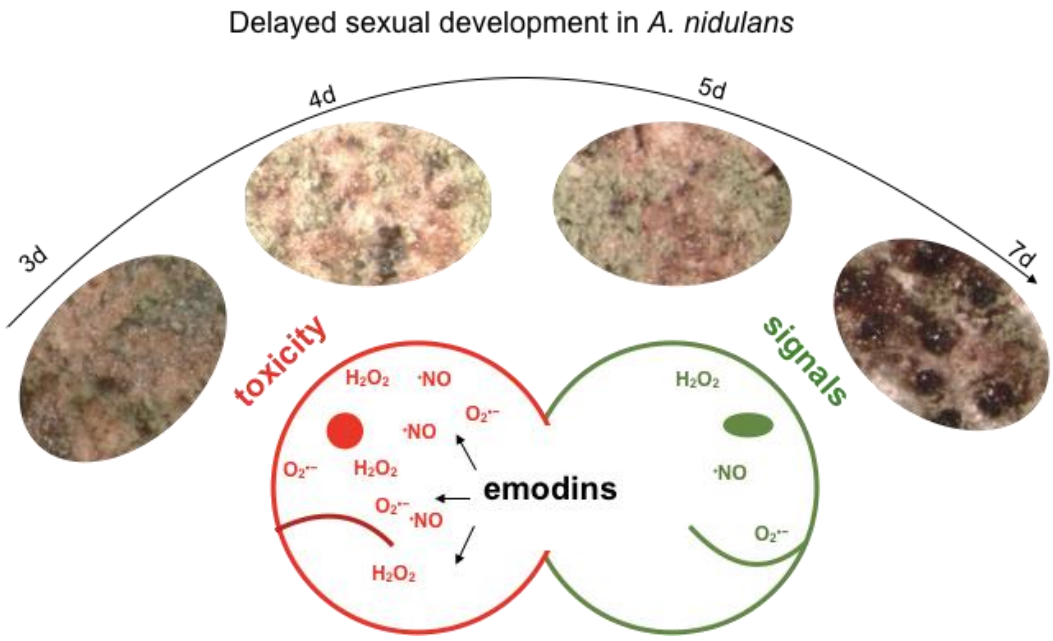

Figure 33. Emodins disturbed the intracellular ROS balance resulting in the repressed sexual development of *A. nidulans*.
Disruption of epi-/shamixanthone biosynthesis led to the accumulation of emodins in the early stage of sexual development, which increased the toxicity of ROS in cells. Cells either consumed the emodins for downstream production or transported emodin out of the cells. Both ways might resulte in decreased ROS concentrations to the proper level which was required in the late stage of sexual development. Reduced ROS concentration released the delay in sexual development and matured cleistothecia were formed. The arrow represents the sexual fruiting body developmental process and different stages of oxidative stress initiated by ROS.

Taken together, disruption of epi-/shamixanthone biosynthesis in *A. nidulans* resulted in the accumulation of various xanthone precursors. Among them, emodin and its derivatives are the most active ingredients exhibiting broad activities: 1) repression of sexual development in *A. nidulans*, 2) repression of development in other fungi and insects. However, there are many gaps in our understanding of the mechanism of the repression of sexual development in the producer, including their targets in the cells and their regulation pathways in sexual development. Furthermore, their costs and benefits in fungal survival and development, *e.g.* in fungal-fungal and fungal-insect antagonism, are also fascinating. Although the proposed ROS model seen in figure 33 can explain some of the observation, more evidence is needed to decode the mechanism. It is also not clear how emodins increase intracellular concentration of ROS

and repress the sexual development process, and how emodins act as extracellular stimuli and activate the ROS burst in receptor organisms.

References

Aguirre J, Garrido-Bazán V, Jaimes-Arroyo R, Sánchez O & Lara-Rojas F (2018). SakA and MpkC stress MAPKs show opposite and common functions during stress responses and development in *Aspergillus nidulans*. Frontiers in Microbiology 9: 2518

Ahmed S, Bardshiri E, McIntyre C & Simpson T (1992). Biosynthetic-studies on tajixanthone and shamixanthone, polyketide hemiterpenoid metabolites of *Aspergillus variecolor*. Australian Journal of Chemistry 45: 249-274

Ahmed SA, Bardshiri E & Simpson TJ (1987). A convenient synthesis of isotopically labelled anthraquinones, chrysophanol, islandicin, and emodin. Incorporation of [methyl-2 H 3] chrysophanol into tajixanthone in *Aspergillus variecolor*. Journal of the Chemical Society, Chemical Communications: 883-884

Ahmed YL, Gerke J, Park H-S, Bayram Ö, Neumann P, Ni M, Dickmanns A, Kim SC, Yu J-H & Braus GH (2013). The velvet family of fungal regulators contains a DNA-binding domain structurally similar to NF-κB. PLoS biology 11: e1001750

Allam NG & El-Zaher EA (2012). Protective role of *Aspergillus fumigatus* melanin against ultraviolet (UV) irradiation and Bjerkandera adusta melanin as a candidate vaccine against systemic candidiasis. African Journal of Biotechnology 11: 6566-6577

Allen P (1976). Spore germination and its regulation. Encyclopedia of Plant Physiology 4: 51-85

Andersen MR, Nielsen JB, Klitgaard A, Petersen LM, Zachariasen M, Hansen TJ, Blicher LH, Gotfredsen CH, Larsen TO & Nielsen KF (2013). Accurate prediction of secondary metabolite gene clusters in filamentous fungi. Proceedings of the National Academy of Sciences 110: 99-107

Anderson JA, Lin BK, Williams HJ & Scott AI (1988). Deoxygenation of phenolic natural products. Enzymic conversion of emodin to chrysophanol. Journal of the American Chemical Society 110: 1623-1624

Andrianopoulos A & Timberlake WE (1994). The *Aspergillus nidulans abaA* gene encodes a transcriptional activator that acts as a genetic switch to control development. Molecular and Cellular Biology 14: 2503-2515

Ariede MB, Candido TM, Jacome ALM, Velasco MVR, de Carvalho JCM & Baby AR (2017). Cosmetic attributes of algae-A review. Algal Research 25: 483-487

Arnaud M, Cerqueira G, Inglis D, Skrzypek M, Binkley J, Chibucos M, Crabtree J, Howarth C, Orvis J & Shah P (2012). The *Aspergillus* Genome Database (AspGD). Nucleic Acids Research 40

Baidya S, Cary JW, Grayburn WS & Calvo A (2011). Role of nitric oxide and flavohemoglobin homolog genes in *Aspergillus nidulans* sexual development and mycotoxin production. Applied and Environmental Microbiology 77: 5524-5528

Bainbridge J (1989). Frogs that sweat-not bullets but a poison for darts. Smithsonian 19: 70-76

Barber J, Chapman AC, Howard TD & Tebb G (1988). Recycling of polyketides by fungi: the degradation of citrinin by *Penicillium citrinum*. Applied Microbiology and Biotechnology 29: 387-391

Barbulova A, Colucci G & Apone F (2015). New Trends in Cosmetics: By-Products of Plant Origin and Their Potential Use as Cosmetic Active Ingredients. Cosmetics 2: 82-92

Bayram Ö, Bayram ÖS, Ahmed YL, Maruyama J-i, Valerius O, Rizzoli SO, Ficner R, Irniger S & Braus GH (2012a). The *Aspergillus nidulans* MAPK module AnSte11-Ste50-Ste7-Fus3 controls development and secondary metabolism. PLoS genetics 8: e1002816

Bayram Ö & Braus GH (2012b). Coordination of secondary metabolism and development in fungi: the velvet familyof regulatory proteins. FEMS Microbiology reviews 36: 1-24

Bayram Ö, Feussner K, Dumkow M, Herrfurth C, Feussner I & Braus GH (2016). Changes of global gene expression and secondary metabolite accumulation during light-dependent *Aspergillus nidulans* development. Fungal Genetics and Biology 87: 30-53

Bayram Ö, Krappmann S, Ni M, Bok JW, Helmstaedt K, Valerius O, Braus-Stromeyer S, Kwon N-J, Keller NP & Yu J-H (2008). VelB/VeA/LaeA complex coordinates light signal with fungal development and secondary metabolism. Science 320: 1504-1506

Bayram ÖS, Bayram Ö, Valerius O, Park HS, Irniger S, Gerke J, Ni M, Han K-H, Yu J-H & Braus GH (2010). LaeA control of velvet family regulatory proteins for light-dependent development and fungal cell-type specificity. PLoS genetics 6: e1001226

Bebber DP, Holmes T & Gurr SJ (2014). The global spread of crop pests and pathogens. Global Ecology and Biogeography 23: 1398-1407

Beck H, Freitas S, Weber G, Robinson S & Morrell J (2014). Resistance of fungal derived pigments to ultraviolet light exposure. International Research Group in Wood Protection; International Research Group/Wood Protection: St George, UT, USA

Bergmann S, Schümann J, Scherlach K, Lange C, Brakhage AA & Hertweck C (2007). Genomics-driven discovery of PKS-NRPS hybrid metabolites from *Aspergillus nidulans*. Nature Chemical Biology 3: 213-217

Bertani G (1951). Studies on lysogenesis I.: the mode of phage liberation by lysogenic *Escherichia coli*. Journal of Bacteriology 62: 293-300

Bills GF & Gloer JB (2016). Biologically active secondary metabolites from the fungi. Microbiology Spectrum 4: 1087-1119

Bloemendal S, Bernhards Y, Bartho K, Dettmann A, Voigt O, Teichert I, Seiler S, Wolters DA, Pöggeler S & Kück U (2012). A homologue of the human STRIPAK complex controls sexual development in fungi. Molecular Microbiology 84: 310-323

Bok JW, Chiang Y-M, Szewczyk E, Reyes-Domingez Y, Davidson AD, Sanchez JF, Lo H-C, Watanabe K, Strauss J & Oakley BR (2009). Chromatin-level regulation of biosynthetic gene clusters. Nature Chemical Biology 5: 462-464

Bok JW, Hoffmeister D, Maggio-Hall LA, Murillo R, Glasner JD & Keller NP (2006). Genomic mining for *Aspergillus* natural products. Chemistry & Biology 13: 31-37

Bok JW & Keller NP (2004). LaeA, a regulator of secondary metabolism in *Aspergillus* spp. Eukaryotic Cell 3: 527-535

Bokor E, Ámon J, Keisham K, Karácsony Z, Vágvölgyi C & Hamari Z (2019). HMGB proteins are required for sexual development in *Aspergillus nidulans*. PLoS one 14: e0216094

Bouhired S, Weber M, Kempf-Sontag A, Keller NP & Hoffmeister D (2007). Accurate prediction of the *Aspergillus nidulans* terrequinone gene cluster boundaries using the transcriptional regulator LaeA. Fungal Genetics and Biology 44: 1134-1145

Braga GU, Rangel DE, Fernandes ÉK, Flint SD & Roberts DW (2015). Molecular and physiological effects of environmental UV radiation on fungal conidia. Current Genetics 61: 405-425

Brakhage AA (2013). Regulation of fungal secondary metabolism. Nature Reviews Microbiology 11: 21-32

Brown D, Yu J, Kelkar H, Fernandes M, Nesbitt T, Keller N, Adams T & Leonard T (1996). Twenty-five coregulated transcripts define a sterigmatocystin gene cluster in *Aspergillus nidulans*. Proceedings of the National Academy of Sciences 93: 1418-1422

Bu'lock JD (1967). Essays in biosynthesis and microbial development.

Bull A (1970). Chemical composition of wild-type and mutant *Aspergillus nidulans* cell walls. The nature of polysaccharide and melanin constituents. Microbiology 63: 75-94

Busch S & Braus GH (2007). How to build a fungal fruit body: from uniform cells to specialized tissue. Molecular Microbiology 64: 873-876

Busch S, Eckert SE, Krappmann S & Braus GH (2003). The COP9 signalosome is an essential regulator of development in the filamentous fungus *Aspergillus nidulans*. Molecular Microbiology 49: 717-730

Bussink HJ & Osmani SA (1998). A cyclin-dependent kinase family member (PHOA) is required to link developmental fate to environmental conditions in *Aspergillus nidulans*. The EMBO journal 17: 3990-4003

Calvo AM & Cary JW (2015). Association of fungal secondary metabolism and sclerotial biology. Frontiers in Microbiology 6: 62

Calvo AM, Gardner HW & Keller NP (2001). Genetic connection between fatty acid metabolism and sporulation in *Aspergillus nidulans*. Journal of Biological Chemistry 276: 25766-25774

Calvo AM, Wilson RA, Bok JW & Keller NP (2002). Relationship between secondary metabolism and fungal development. Microbiol Mol Biol Rev 66: 447-459

Canosa I, Rojo F & Alonso JC (1996). Site-specific recombination by the β protein from the streptococcal plasmid pSM19035: minimal recombination sequences and crossing over site. Nucleic Acids Research 24: 2712-2717

Caputi L & Aprea E (2011). Use of terpenoids as natural flavouring compounds in food industry. Recent patents on food, Nutrition & Agriculture 3: 9-16

Cerqueira GC, Arnaud MB, Inglis DO, Skrzypek MS, Binkley G, Simison M, Miyasato SR, Binkley J, Orvis J & Shah P (2013). The *Aspergillus* Genome Database: multispecies curation and incorporation of RNA-Seq data to improve structural gene annotations. Nucleic Acids Research 42: 705-710

Chang C-H, Lin C-C, Yang J-J, Namba T & Hattori M (1996). Anti-inflammatory effects of emodin from *Ventilago leiocarpa*. The American Journal of Chinese Medicine 24: 139-142

Chen H, Hsieh W, Chang W & Chung J (2004). Aloe-emodin induced in vitro G2/M arrest of cell cycle in human promyelocytic leukemia HL-60 cells. Food and Chemical Toxicology 42: 1251-1257

Chiang Y-M, Szewczyk E, Davidson AD, Entwistle R, Keller NP, Wang CC & Oakley BR (2010). Characterization of the *Aspergillus nidulans* monodictyphenone gene cluster. Applied and Environmental Microbiology 76: 2067-2074

Chiang Y-M, Szewczyk E, Davidson AD, Keller N, Oakley BR & Wang CC (2009). A gene cluster containing two fungal polyketide synthases encodes the biosynthetic pathway for a polyketide, asperfuranone, in *Aspergillus nidulans*. Journal of the American Chemical Society 131: 2965-2970

Chiang Y-M, Szewczyk E, Nayak T, Davidson AD, Sanchez JF, Lo H-C, Ho W-Y, Simityan H, Kuo E & Praseuth A (2008). Molecular genetic mining of the *Aspergillus* secondary metabolome: discovery of the emericellamide biosynthetic pathway. Chemistry & Biology 15: 527-532

Choi GJ, Lee S-W, Jang KS, Kim J-S, Cho KY & Kim J-C (2004). Effects of chrysophanol, parietin, and nepodin of *Rumex crispus* on barley and cucumber powdery mildews. Crop Protection 23: 1215-1221

Couch RD & Gaucher GM (2004). Rational elimination of *Aspergillus terreus* sulochrin production. Journal of Biotechnology 108: 171-177

Croteau R, Kutchan TM & Lewis NG (2000). Natural products (secondary metabolites). Biochemistry and Molecular Biology of Plants 24: 1250-1319

Daly SM, Elmore BO, Kavanaugh JS, Triplett KD, Figueroa M, Raja HA, El-Elimat T, Crosby HA, Femling JK & Cech NB (2015). ω-Hydroxyemodin limits *Staphylococcus aureus* quorum sensing-mediated pathogenesis and inflammation. Antimicrobial Agents and Chemotherapy 59: 2223-2235

Damron BL & Jacob J (2001). Toxicity to poultry of common weed seeds. University of Florida Cooperative Extension Service, Institute of Food and Agricultural and Sciences

de Vries RP, Riley R, Wiebenga A, Aguilar-Osorio G, Amillis S, Uchima CA, Anderluh G, Asadollahi M, Askin M & Barry K (2017). Comparative genomics reveals high biological diversity and specific adaptations in the industrially and medically important fungal genus *Aspergillus*. Genome Biology 18: 28

DeLiberto ST & Werner SJ (2016). Review of anthraquinone applications for pest management and agricultural crop protection. Pest Management Science 72: 1813-1825

Demain AL & Fang A (2000). The natural functions of secondary metabolites. In History of Modern Biotechnology I, pp 1-39. Springer

Dettmann A, Heilig Y, Ludwig S, Schmitt K, Illgen J, Fleißner A, Valerius O & Seiler S (2013). HAM-2 and HAM-3 are central for the assembly of the Neurospora STRIPAK complex at the nuclear envelope and regulate nuclear accumulation of the MAP kinase MAK-1 in a MAK-2-dependent manner. Molecular Microbiology 90: 796-812

Dirnberger B (2018). Proteomics of (*Aspergillus nidulans*) Sexually Differentiated Cells. In Georg-August-Universität Göttingen

Dirschnabel DE, Nowrousian M, Cano-Domínguez N, Aguirre J, Teichert I & Kück U (2014). New insights into the roles of NADPH oxidases in sexual development and ascospore germination in *Sordaria macrospora*. Genetics 196: 729-744

Dong X, Fu J, Yin X, Cao S, Li X, Lin L, Huyiligeqi & Ni J (2016). Emodin: a review of its pharmacology, toxicity and pharmacokinetics. Phytotherapy Research 30: 1207-1218

Dorland WAN (2011). Dorland's Illustrated Medical Dictionary32: Dorland's Illustrated Medical Dictionary. Elsevier Health Sciences,

Drocourt D, Calmels T, Reynes J-P, Baron M & Tiraby Gr (1990). Cassettes of the *Streptoalloteichus hindustanus ble* gene for transformation of lower and higher eukaryotes to phleomycin resistance. Nucleic Acids Research 18: 4009

Durán N, Teixeira MF, De Conti R & Esposito E (2002). Ecological-friendly pigments from fungi. Critical Reviews in Food Science and Nutrition 42: 53-66

Duvoix A, Delhalle S, Blasius R, Schnekenburger M, Morceau F, Fougere M, Henry E, Galteau M-M, Dicato M & Diederich M (2004). Effect of chemopreventive agents on glutathione S-transferase P1-1 gene expression mechanisms via activating protein 1 and nuclear factor kappaB inhibition. Biochemical Pharmacology 68: 1101-1111

Dyer PS & O'gorman CM (2012). Sexual development and cryptic sexuality in fungi: insights from *Aspergillus* species. FEMS Microbiology reviews 36: 165-192

EbrahimáEl-Zayat AA (1991). Structure and synthesis of sporogenic psi factors from *Aspergillus nidulans*. Journal of the Chemical Society, Chemical Communications: 1486-1487

El Ariebi N, Hiscox J, Scriven SA, Müller CT & Boddy L (2016). Production and effects of volatile organic compounds during interspecific interactions. Fungal Ecology 20: 144-154

El-Seedi HR, El-Barbary M, El-Ghorab D, Bohlin L, Borg-Karlson A-K, Goransson U & Verpoorte R (2010). Recent insights into the biosynthesis and biological activities of natural xanthones. Current Medicinal Chemistry 17: 854-901

Ellis TT, Reynolds DR & Alexopoulos CJ (1973). Hülle cell development in *Emericella nidulans*. Mycologia 65: 1028-1035

Elramli N, Karahoda B, Sarikaya-Bayram Ö, Frawley D, Ulas M, Oakley CE, Oakley BR, Seiler S & Bayram Ö (2019). Assembly of a heptameric STRIPAK complex is required for coordination of light-dependent multicellular fungal development with secondary metabolism in *Aspergillus nidulans*. PLoS genetics 15: e1008053

Esser K & Straub J (1958). Genetische Untersuchungen an *Sordaria macrospora* Auersw., Kompensation und Induktion bei Genbedingten Entwicklungsdefekten. Molecular and General Genetics 89: 729-746

Etxebeste O, Garzia A, Espeso EA & Ugalde U (2010b). *Aspergillus nidulans* asexual development: making the most of cellular modules. Trends in Microbiology 18: 569-576

Fekete-Szücs E (2016). Investigation of secondary metabolite genes putatively involved in Hülle cell formation. In Georg-August-Universität Göttingen

Firn RD & Jones CG (2000). The evolution of secondary metabolism–a unifying model. Molecular Microbiology 37: 989-994

Foster JW & Karow EO (1945). Microbiological Aspects of Penicillin: VIII. Penicillin from Different Fungi. Journal of Bacteriology 49: 19

Fradin EF, Zhang Z, Ayala JCJ, Castroverde CD, Nazar RN, Robb J, Liu C-M & Thomma BP (2009). Genetic dissection of *Verticillium wilt* resistance mediated by tomato Ve1. Plant Physiology 150: 320-332

Franck B, Bringmann G & Flohr G (1980). Sequence Analysis of Ergochrome-Biosynthesis by Competitive Incorporation. Angewandte Chemie International Edition in English 19: 460-461

Frandsen RJ, Khorsand-Jamal P, Kongstad KT, Nafisi M, Kannangara RM, Staerk D, Okkels FT, Binderup K, Madsen B & Møller BL (2018). Heterologous production of the widely used natural food colorant carminic acid in *Aspergillus nidulans*. Scientific Reports 8: 12853

Frawley D, Karahoda B, Bayram ÖS & Bayram Ö (2018). The HamE scaffold positively regulates MpkB phosphorylation to promote development and secondary metabolism in *Aspergillus nidulans*. Scientific Reports 8: 16588

Fuglsang CC, Berka RM, Wahleithner JA, Kauppinen S, Shuster JR, Rasmussen G, Halkier T, Dalbøge H & Henrissat B (2000). Biochemical analysis of recombinant fungal mutanases a new family of α1, 3-glucanases with novel carbohydrate-binding domains. Journal of Biological Chemistry 275: 2009-2018

Furukawa K, Hoshi Y, Maeda T, Nakajima T & Abe K (2005). *Aspergillus nidulans* HOG pathway is activated only by two-component signalling pathway in response to osmotic stress. Molecular Microbiology 56: 1246-1261

Galagan JE, Calvo SE, Cuomo C, Ma L-J, Wortman JR, Batzoglou S, Lee S-I, Baştürkmen M, Spevak CC & Clutterbuck J (2005). Sequencing of *Aspergillus nidulans* and comparative analysis with *A. fumigatus* and *A. oryzae*. Nature 438: 1105-1115

García-Sosa K, Villarreal-Alvarez N, Lübben P & Peña-Rodríguez LM (2006). Chrysophanol, an antimicrobial anthraquinone from the root extract of *Colubrina greggii*. Journal of the Mexican Chemical Society 50: 76-78

Geiser DM (2009). Sexual structures in *Aspergillus*: morphology, importance and genomics. Medical Mycology 47: S21-S26

Georges K, Jayaprakasam B, Dalavoy S & Nair M (2008). Pest-managing activities of plant extracts and anthraquinones from *Cassia nigricans* from Burkina Faso. Bioresource Technology 99: 2037-2045

Gerke J, Bayram Ö & Braus GH (2012a). Fungal S-adenosylmethionine synthetase and the control of development and secondary metabolism in *Aspergillus nidulans*. Fungal Genetics and Biology 49: 443-454

Gerke J, Bayram Ö, Feussner K, Landesfeind M, Shelest E, Feussner I & Braus GH (2012b). Breaking the silence: protein stabilization uncovers silenced biosynthetic gene clusters in the fungus *Aspergillus nidulans*. Applied and Environmental Microbiology 78: 8234-8244

Gessler N, Aver'Yanov A & Belozerskaya T (2007). Reactive oxygen species in regulation of fungal development. Biochemistry (Moscow) 72: 1091-1109

Giovannini MG, Poulter L, Gibson BW & Williams DH (1987). Biosynthesis and degradation of peptides derived from *Xenopus laevis* prohormones. Biochemical Journal 243: 113-120

Goldman GH, Regulin A & Kempken F (2018). Fungal genotype determines survival of *Drosophila melanogaster* when competing with *Aspergillus nidulans*. PLoS one 13: e0190543

Gonçalves R, Lisboa H & Pombeiro-Sponchiado S (2012). Characterization of melanin pigment produced by *Aspergillus nidulans*. World Journal of Microbiology and Biotechnology 28: 1467-1474

Grau MF, Entwistle R, Oakley CE, Wang CC & Oakley BR (2019). Overexpression of an LaeA-like methyltransferase upregulates secondary metabolite production in *Aspergillus nidulans*. ACS Chemical Biology 14: 1643-1651

Greco C, de Mattos-Shipley K, Bailey AM, Mulholland NP, Vincent JL, Willis CL, Cox RJ & Simpson TJ (2019). Structure revision of cryptosporioptides and determination of the genetic basis for dimeric xanthone biosynthesis in fungi. Chemical Science 10: 2930-2939

Griffiths S, Mesarich CH, Saccomanno B, Vaisberg A, De Wit PJ, Cox R & Collemare J (2016). Elucidation of cladofulvin biosynthesis reveals a cytochrome P450 monooxygenase required for anthraquinone dimerization. Proceedings of the National Academy of Sciences 113: 6851-6856

Halliwell B & Gutteridge JM (2015). Free radicals in biology and medicine. Oxford University Press, USA,

Han K-H, Lee D-B, Kim J-H, Kim M-S, Han K-Y, Kim W-S, Park Y-S, Kim H-B & Han D-M (2003a). Environmental factors affecting development of *Aspergillus nidulans*. The Journal of Microbiology 41: 34-40

Han KH, Han K-Y, Kim M-S, Lee D-B, Kim J-H, Chae S-K, Chae K-S & Han D-M (2003b). Regulation of *nsdD* expression in *Aspergillus nidulans*. The Journal of Microbiology 41: 259-261

Han KH, Han KY, Yu JH, Chae KS, Jahng KY & Han DM (2001). The *nsdD* gene encodes a putative GATA-type transcription factor necessary for sexual development of *Aspergillus nidulans*. Molecular Microbiology 41: 299-309

Hanahan D, Jessee J & Bloom FR (1991). Plasmid transformation of *Escherichia coli* and other bacteria. In Methods in Enzymology, pp 63-113. Elsevier

Hartmann T, Dümig M, Jaber BM, Szewczyk E, Olbermann P, Morschhäuser J & Krappmann S (2010). Validation of a self-excising marker in the human pathogen *Aspergillus fumigatus* by employing the *β-rec/six* site-specific recombination system. Applied and Environmental Microbiology 76: 6313-6317

Haslam E (1986). Secondary metabolism–fact and fiction. Natural Product Reports 3: 217-249

He B, Chen J, Liu L, Wang H, Wang S, Li P & Zhou J (2018). Emodin inhibits formation of hypertrophic scars through regulating the p38/MAPK signaling pathway. International Journal of Clinical and Experimental Medicine 11: 12310-12317

Hermann TE, Kurtz MB & Champe SP (1983). Laccase localized in hulle cells and cleistothecial primordia of *Aspergillus nidulans*. Journal of Bacteriology 154: 955-964

Hildebrandt U, Marsell A & Riederer M (2018). Direct Effects of Physcion, Chrysophanol, Emodin, and Pachybasin on Germination and Appressorium Formation of the Barley (*Hordeum vulgare* L.) Powdery Mildew Fungus *Blumeria graminis* f. sp. *hordei* (DC.) Speer. Journal of Agricultural and Food Chemistry 66: 3393-3401

Hiscox J, O'Leary J & Boddy L (2018). Fungus wars: basidiomycete battles in wood decay. Studies in Mycology 89: 117-124

Holighaus G & Rohlfs M (2019). Volatile and non-volatile fungal oxylipins in fungus-invertebrate interactions. Fungal Ecology 38: 28-36

Hounsome N, Hounsome B, Tomos D & Edwards-Jones G (2008). Plant metabolites and nutritional quality of vegetables. Journal of Food Science 73: 48-65

Huang B, Guo J, Yi B, Yu X, Sun L & Chen W (2008). Heterologous production of secondary metabolites as pharmaceuticals in *Saccharomyces cerevisiae*. Biotechnology Letters 30: 1121-1137

Hussein HS & Brasel JM (2001). Toxicity, metabolism, and impact of mycotoxins on humans and animals. Toxicology 167: 101-134

Hynes J, Müller CT, Jones TH & Boddy L (2007). Changes in volatile production during the course of fungal mycelial interactions between *Hypholoma fasciculare* and *Resinicium bicolor*. Journal of Chemical Ecology 33: 43-57

Inglis DO, Binkley J, Skrzypek MS, Arnaud MB, Cerqueira GC, Shah P, Wymore F, Wortman JR & Sherlock G (2013). Comprehensive annotation of secondary metabolite biosynthetic genes and gene clusters of *Aspergillus nidulans*, *A. fumigatus*, *A. niger* and *A. oryzae*. BMC Microbiology 13: 91

Inoue H, Nojima H & Okayama H (1990). High efficiency transformation of *Escherichia coli* with plasmids. Gene 96: 23-28

Izhaki I (2002). Emodin–a secondary metabolite with multiple ecological functions in higher plants. New Phytologist 155: 205-217

Jaimes-Arroyo R, Lara-Rojas F, Bayram Ö, Valerius O, Braus GH & Aguirre J (2015). The SrkA kinase is part of the SakA mitogen-activated protein kinase interactome and regulates stress responses and development in *Aspergillus nidulans*. Eukaryotic Cell 14: 495-510

Jain S, Wiemann P, Thill E, Williams B, Keller N & Kabbage M (2018). A Bcl-2 Associated Athanogene (*bagA*) Modulates Sexual Development and Secondary Metabolism in the Filamentous Fungus *Aspergillus nidulans*. Front Microbiol 9: 1316

Jayasuriya H, Koonchanok NM, Geahlen RL, McLaughlin JL & Chang C-J (1992). Emodin, a protein tyrosine kinase inhibitor from *Polygonum cuspidatum*. Journal of Natural Products 55: 696-698

Jiang J, Zhou N, Ying P, Zhang T, Liang R & Jiang X (2018). Emodin promotes apoptosis of human endometrial cancer through regulating the MAPK and PI3K/AKT pathways. Open Life Sciences 13: 489-496

Käfer E (1977). Meiotic and mitotic recombination in *Aspergillus* and its chromosomal aberrations. In Advances in Genetics, pp 33-131. Elsevier

Kale SP, Milde L, Trapp MK, Frisvad JC, Keller NP & Bok JW (2008). Requirement of LaeA for secondary metabolism and sclerotial production in *Aspergillus flavus*. Fungal Genetics and Biology 45: 1422-1429

Kawasaki L, Sánchez O, Shiozaki K & Aguirre J (2002). SakA MAP kinase is involved in stress signal transduction, sexual development and spore viability in *Aspergillus nidulans*. Molecular Microbiology 45: 1153-1163

Keller NP (2018). Fungal secondary metabolism: regulation, function and drug discovery. Nature Reviews Microbiology 17: 167-180

Khalid S, Baccile JA, Spraker JE, Tannous J, Imran M, Schroeder FC & Keller NP (2017). NRPS-derived isoquinolines and lipopetides mediate antagonism between plant pathogenic fungi and bacteria. ACS Chemical Biology 13: 171-179

Kim H-S, Han K-Y, Kim K-J, Han D-M, Jahng K-Y & Chae K-S (2002). The *veA* gene activates sexual development in *Aspergillus nidulans*. Fungal Genetics and Biology 37: 72-80

Koerner SK, Hanai J-I, Bai S, Jernigan FE, Oki M, Komaba C, Shuto E, Sukhatme VP & Sun L (2017). Design and synthesis of emodin derivatives as novel inhibitors of ATP-citrate lyase. European Journal of Medicinal Chemistry 126: 920-928

Koide K, Bunnage ME, Paloma LG, Kanter JR, Taylor SS, Brunton LL & Nicolaou K (1995). Molecular design and biological activity of potent and selective protein kinase inhibitors related to balanol. Chemistry & Biology 2: 601-608

Koyama J, Morita I, Tagahara K, Nobukuni Y, Mukainaka T, Kuchide M, Tokuda H & Nishino H (2002). Chemopreventive effects of emodin and cassiamin B in mouse skin carcinogenesis. Cancer Letters 182: 135-139

Krappmann S, Sasse C & Braus GH (2006). Gene targeting in *Aspergillus fumigatus* by homologous recombination is facilitated in a nonhomologous end-joining-deficient genetic background. Eukaryotic Cell 5: 212-215

Krick A, Kehraus S, Gerhäuser C, Klimo K, Nieger M, Maier A, Fiebig H-H, Atodiresei I, Raabe G & Fleischhauer J (2007). Potential cancer chemopreventive in vitro activities of monomeric xanthone derivatives from the marine algicolous fungus *Monodictys putredinis*. Journal of Natural Products 70: 353-360

Krijgsheld P, Bleichrodt Rv, Van Veluw G, Wang F, Müller W, Dijksterhuis J & Wösten H (2013). Development in *Aspergillus*. Studies in Mycology 74: 1-29

Kusumawati I & Indrayanto G (2013). Natural antioxidants in cosmetics. In Studies in Natural Products Chemistry, pp 485-505. Elsevier

Kwak HJ, Park MJ, Park CM, Moon SI, Yoo DH, Lee HC, Lee SH, Kim MS, Lee HW & Shin WS (2006). Emodin inhibits vascular endothelial growth factor-A-induced angiogenesis by blocking receptor-2 (KDR/Flk-1) phosphorylation. International Journal of Cancer 118: 2711-2720

Laemmli UK (1970). Cleavage of structural proteins during the assembly of the head of bacteriophage T4. Nature 227: 680-685

Lara-Ortíz T, Riveros-Rosas H & Aguirre J (2003). Reactive oxygen species generated by microbial NADPH oxidase NoxA regulate sexual development in *Aspergillus nidulans.* Molecular Microbiology 50: 1241-1255

Le Pogam P & Boustie J (2016). Xanthones of lichen source: A 2016 update. Molecules 21: 294

Leach J, Lang B & Yoder O (1982). Methods for selection of mutants and in vitro culture of *Cochliobolus heterostrophus*. Microbiology 128: 1719-1729

Lee M-K, Kwon N-J, Choi JM, Lee I-S, Jung S & Yu J-H (2014). NsdD is a key repressor of asexual development in *Aspergillus nidulans*. Genetics 197: 159-173

Li Q & Verma IM (2002). NF-κB regulation in the immune system. Nature Reviews Immunology 2: 725-734

Lin J-G, Chen G-W, Li T-M, Chouh S-T, Tan T-W & Chung J-G (2006). Aloe-emodin induces apoptosis in T24 human bladder cancer cells through the p53 dependent apoptotic pathway. The Journal of Urology 175: 343-347

Lin L, Liu Y, Fu S, Qu C, Li H & Ni J (2019). Inhibition of Mitochondrial Complex Function-The Hepatotoxicity Mechanism of Emodin Based on Quantitative Proteomic Analyses. Cells 8: 263

Liu B, Yuan B, Zhang L, Mu W & Wang C (2015). ROS/p38/p53/Puma signaling pathway is involved in emodin-induced apoptosis of human colorectal cancer cells. International Journal of Clinical and Experimental Medicine 8: 15413-15422

Lo H-C, Entwistle R, Guo C-J, Ahuja M, Szewczyk E, Hung J-H, Chiang Y-M, Oakley BR & Wang CC (2012). Two separate gene clusters encode the biosynthetic pathway for the meroterpenoids austinol and dehydroaustinol in *Aspergillus nidulans*. Journal of the American Chemical Society 134: 4709-4720

Lord K & Read N (2011). Perithecium morphogenesis in *Sordaria macrospora*. Fungal Genetics and Biology 48: 388-399

Luo H, Li X-M, Li C-S & Wang B-G (2014). Diphenyl ether and benzophenone derivatives from the marine mangrove-derived fungus Penicillium sp. MA-37. Phytochemistry Letters 9: 22-25

Luo H, Qing Z, Deng Y, Deng Z, Tang Xa, Feng B & Lin W (2019). Two Polyketides Produced by Endophytic *Penicillium citrinum* DBR-9 From Medicinal Plant *Stephania kwangsiensis* and Their Antifungal Activity Against Plant Pathogenic Fungi. Natural Product Communications 14: 1934578X19846795

Macheleidt J, Mattern D, Fischer J, Netzker T, Weber J, Schroeckh V, Valiante V & Brakhage A (2016). Regulation and Role of Fungal Secondary Metabolites. Annual Review of Genetics 50: 371-392

Malik EM & Müller CE (2016). Anthraquinones as pharmacological tools and drugs. Medicinal Research reviews 36: 705-748

Manfiolli AO, Mattos EC, de Assis LJ, Silva LP, Ulaş M, Brown NA, Bayram Ö & Goldman GH (2019). *Aspergillus fumigatus* high osmolarity glycerol mitogen activated protein kinases SakA and MpkC physically interact during osmotic and cell wall stresses. Frontiers in Microbiology 10: 918

Manoil C & Kaiser D (1980). Purine-containing compounds, including cyclic adenosine 3', 5'-monophosphate, induce fruiting of *Myxococcus xanthus* by nutritional imbalance. Journal of Bacteriology 141: 374-377

Mapari SA, Thrane U & Meyer AS (2010). Fungal polyketide azaphilone pigments as future natural food colorants? Trends in Biotechnology 28: 300-307

Marshall CJ (1994). MAP kinase kinase kinase, MAP kinase kinase and MAP kinase. Current Opinion in Genetics & Development 4: 82-89

Martin JF (1992). Clusters of genes for the biosynthesis of antibiotics: regulatory genes and overproduction of pharmaceuticals. Journal of Industrial Microbiology 9: 73-90

Masters K-S & Bräse S (2012). Xanthones from fungi, lichens, and bacteria: the natural products and their synthesis. Chemical reviews 112: 3717-3776

McNamara S & Song XK (1996). Traditional Chinese Medicine. BasicBooks

Miller EL (2002). The penicillins: a review and update. Journal of Midwifery & Women's Health 47: 426-434

Miller KY, Toennis TM, Adams TH & Miller BL (1991). Isolation and transcriptional characterization of a morphological modifier: the *Aspergillus nidulans* stunted (*stuA*) gene. Molecular and General Genetics 227: 285-292

Mischitelli M, Jemaà M, Almasry M, Faggio C & Lang F (2016). Triggering of erythrocyte cell membrane scrambling by emodin. Cellular Physiology and Biochemistry 40: 91-103

Misiek M & Hoffmeister D (2007). Fungal genetics, genomics, and secondary metabolites in pharmaceutical sciences. Planta Medica 73: 103-115

Moreira TF, Sorbo JM, Souza FdO, Fernandes BC, Ocampos FMM, de Oliveira DMS, Arcaro CA, Assis RP, Barison A & Miguel OG (2018). Emodin, Physcion, and Crude Extract of *Rhamnus sphaerosperma* var. pubescens Induce Mixed Cell Death, Increase in Oxidative Stress, DNA Damage, and Inhibition of AKT in Cervical and Oral Squamous Carcinoma Cell Lines. Oxidative Medicine and Cellular Longevity 2018

Mueller JE, Canze M & Bryk M (2006). The requirement for COMPASS and Paf1 in transcriptional silencing and methylation of histone H3 in *Saccharomyces cerevisiae*. Genetics 173: 557-567

Mueller S, Schmitt M, Dekant W, Stopper H, Schlatter J, Schreier P & Lutz W (1999). Occurrence of emodin, chrysophanol and physcion in vegetables, herbs and liquors. Genotoxicity and anti-genotoxicity of the anthraquinones and of the whole plants. Food and Chemical Toxicology 37: 481-491

Müller SO, Eckert I, Lutz WK & Stopper H (1996). Genotoxicity of the laxative drug components emodin, aloe-emodin and danthron in mammalian cells: topoisomerase II mediated? Mutation Research/Genetic Toxicology 371: 165-173

Murrell W (1981). Biophysical studies on the molecular mechanisms of spore heat resistance and dormancy. Spores 8: 64-77

Myers CW & Daly JW (1983). Dart-poison frogs. Scientific American 248: 120-133

Nahlik K, Dumkow M, Bayram Ö, Helmstaedt K, Busch S, Valerius O, Gerke J, Hoppert M, Schwier E & Opitz L (2010). The COP9 signalosome mediates transcriptional and metabolic response to hormones, oxidative stress protection and cell wall rearrangement during fungal development. Molecular Microbiology 78: 964-979

Nayak T, Szewczyk E, Oakley CE, Osmani A, Ukil L, Murray SL, Hynes MJ, Osmani SA & Oakley BR (2006). A versatile and efficient gene-targeting system for *Aspergillus nidulans*. Genetics 172: 1557-1566

Ni M & Yu J-H (2007). A novel regulator couples sporogenesis and trehalose biogenesis in *Aspergillus nidulans*. PLoS one 2: e970

Nielsen ML, Nielsen JB, Rank C, Klejnstrup ML, Holm DK, Brogaard KH, Hansen BG, Frisvad JC, Larsen TO & Mortensen UH (2011). A genome-wide polyketide synthase deletion library uncovers novel genetic links to polyketides and meroterpenoids in *Aspergillus nidulans*. FEMS Microbiology Letters 321: 157-166

Nielsen MT, Klejnstrup ML, Rohlfs M, Anyaogu DC, Nielsen JB, Gotfredsen CH, Andersen MR, Hansen BG, Mortensen UH & Larsen TO (2013a). *Aspergillus nidulans* synthesize

insect juvenile hormones upon expression of a heterologous regulatory protein and in response to grazing by *Drosophila melanogaster* larvae. PLoS One 8: e73369

Nielsen MT, Nielsen JB, Anyaogu DC, Holm DK, Nielsen KF, Larsen TO & Mortensen UH (2013b). Heterologous Reconstitution of the Intact Geodin Gene Cluster in *Aspergillus nidulans* through a Simple and Versatile PCR Based Approach. PloS one 8: 10.1371/annotation-/c05c3fd1-dd00-4840-891d-693c614aaaf9

Nierman W, May G, Kim H, Anderson M, Chen D & Denning D (2005). What the *Aspergillus* genomes have told us. Medical Mycology 43: S3-S5

Nowrousian M, Masloff S, Pöggeler S & Kück U (1999). Cell differentiation during sexual development of the fungus *Sordaria macrospora* requires ATP citrate lyase activity. Molecular and Cellular Biology 19: 450-460

Nowrousian M, Stajich JE, Chu M, Engh I, Espagne E, Halliday K, Kamerewerd J, Kempken F, Knab B & Kuo H-C (2010). De *novo* assembly of a 40 Mb eukaryotic genome from short sequence reads: *Sordaria macrospora*, a model organism for fungal morphogenesis. PLoS genetics 6: e1000891

O'Connell RJ, Thon MR, Hacquard S, Amyotte SG, Kleemann J, Torres MF, Damm U, Buiate EA, Epstein L & Alkan N (2012). Lifestyle transitions in plant pathogenic *Colletotrichum* fungi deciphered by genome and transcriptome analyses. Nature Genetics 44: 1060-1065

Ohashi H, Ishikawa M, Ito J, Ueno A, Gleich GJ, Kita H, Kawai H & Fukamachi H (1997). Sulochrin inhibits eosinophil degranulation. The Journal of Antibiotics 50: 972-974

Palmer JM & Keller NP (2010). Secondary metabolism in fungi: does chromosomal location matter? Current Opinion in Microbiology 13: 431-436

Pandit S, Lohmar J, Ahmed S, Etxebeste O, Espeso E & Calvo A (2018). UrdA Controls Secondary Metabolite Production and the Balance between Asexual and Sexual Development in *Aspergillus nidulans*. Genes 9: 570

Panigrahi GK, Mudiam MK, Vashishtha VM, Raisuddin S & Das M (2015a). Activity-guided chemo toxic profiling of *Cassia occidentalis* (CO) seeds: detection of toxic compounds in body fluids of CO-exposed patients and experimental rats. Chemical Research in Toxicology 28: 1120-1132

Panigrahi GK, Suthar MK, Verma N, Asthana S, Tripathi A, Gupta SK, Saxena JK, Raisuddin S & Das M (2015b). Investigation of the interaction of anthraquinones of *Cassia occidentalis* seeds with bovine serum albumin by molecular docking and spectroscopic analysis: Correlation to their in vitro cytotoxic potential. Food Research International 77: 368-377

Panigrahi GK, Verma N, Singh N, Asthana S, Gupta SK, Tripathi A & Das M (2018). Interaction of anthraquinones of *Cassia occidentalis* seeds with DNA and Glutathione. Toxicology Reports 5: 164-172

Paoletti M, Seymour FA, Alcocer MJ, Kaur N, Calvo AM, Archer DB & Dyer PS (2007). Mating type and the genetic basis of self-fertility in the model fungus *Aspergillus nidulans*. Current Biology 17: 1384-1389

Park B-C, Park Y-H, Yi S, Choi YK, Kang E-H & Park H-M (2014). Transcriptional regulation of *fksA*, a β-1, 3-glucan synthase gene, by the APSES protein StuA during *Aspergillus nidulans* development. Journal of Microbiology 52: 940-947

Park H-S, Lee M-K, Han K-H, Kim M-J & Yu J-H (2019). Developmental Decisions in *Aspergillus nidulans*. In Biology of the Fungal Cell, pp 63-80. Springer

Park H-S, Ni M, Jeong KC, Kim YH & Yu J-H (2012). The role, interaction and regulation of the velvet regulator VelB in *Aspergillus nidulans*. PLoS one 7: e45935

Park M-Y, Kwon H-J & Sung M-K (2009). Evaluation of aloin and aloe-emodin as anti-inflammatory agents in aloe by using murine macrophages. Bioscience, Biotechnology, and Biochemistry 73: 828-832

Patakova P (2013). Monascus secondary metabolites: production and biological activity. Journal of Industrial Microbiology & Biotechnology 40: 169-181

Perrin RM, Fedorova ND, Bok JW, Cramer Jr RA, Wortman JR, Kim HS, Nierman WC & Keller NP (2007). Transcriptional regulation of chemical diversity in *Aspergillus fumigatus* by LaeA. PLoS pathogens 3: e50

Peti W & Page R (2013). Molecular basis of MAP kinase regulation. Protein Science 22: 1698-1710

Pietta P-G (2000). Flavonoids as antioxidants. Journal of Natural Products 63: 1035-1042

Pinto M, Sousa M & Nascimento M (2005). Xanthone derivatives: new insights in biological activities. Current Medicinal Chemistry 12: 2517-2538

Pippi B, Lana A, Moraes R, Güez C, Machado M, De Oliveira L, Lino von Poser G & Fuentefria A (2015). *In vitro* evaluation of the acquisition of resistance, antifungal activity and synergism of B razilian red propolis with antifungal drugs on *Candida* spp. Journal of Applied Microbiology 118: 839-850

Pockrandt D, Ludwig L, Fan A, König GM & Li SM (2012). New Insights into the Biosynthesis of Prenylated Xanthones: Xptb from *Aspergillus nidulans* Catalyses an O-Prenylation of Xanthones. ChemBioChem 13: 2764-2771

Pöggeler S, Nowrousian M & Kück U (2006). Fruiting-body development in ascomycetes. In Growth, Differentiation and Sexuality, pp 325-355. Springer

Pontecorvo G, Roper J, Chemmons L, MacDonald K & Bufton A (1953). The genetics of *Aspergillus nidulans*. In Advances in Genetics, pp 141-238. Elsevier

Punt PJ & van den Hondel CA (1992). Transformation of filamentous fungi based on hygromycin b and phleomycin resistance markers. In Methods in Enzymology, pp 447-457. Elsevier

Purschwitz J, Müller S, Kastner C, Schöser M, Haas H, Espeso EA, Atoui A, Calvo AM & Fischer R (2008). Functional and physical interaction of blue-and red-light sensors in *Aspergillus nidulans*. Current Biology 18: 255-259

Quan Y, Gong L, He J, Zhou Y, Liu M, Cao Z, Li Y & Peng C (2019). Aloe emodin induces hepatotoxicity by activating NF-κB inflammatory pathway and P53 apoptosis pathway in zebrafish. Toxicology Letters 306: 66-79

Räisänen R (2019). Fungal colorants in applications–focus on *Cortinarius* species. Coloration Technology 135: 22-31

Räisänen R, Nousiainen P & Hynninen PH (2001). Emodin and dermocybin natural anthraquinones as high-temperature disperse dyes for polyester and polyamide. Textile Research Journal 71: 922-927

Rattan RS (2010). Mechanism of action of insecticidal secondary metabolites of plant origin. Crop Protection 29: 913-920

Rauscher S, Pacher S, Hedtke M, Kniemeyer O & Fischer R (2016). A phosphorylation code of the *Aspergillus nidulans* global regulator VelvetA (VeA) determines specific functions. Molecular Microbiology 99: 909-924

Regulin A & Kempken F (2018). Fungal genotype determines survival of *Drosophila melanogaster* when competing with *Aspergillus nidulans*. PLoS one 13: e0190543

Rodríguez-Urra ABn, Jiménez C, Nieto MI, Rodríguez J, Hayashi H & Ugalde U (2012). Signaling the induction of sporulation involves the interaction of two secondary metabolites in *Aspergillus nidulans*. ACS Chemical Biology 7: 599-606

Rohlfs M, Albert M, Keller NP & Kempken F (2007). Secondary chemicals protect mould from fungivory. Biology Letters 3: 523-525

Rojo F, Weise F & Alonso JC (1993). Purification of the β product encoded by the *Streptococcus pyogenes* plasmid pSM19035: a putative DNA recombinase required to resolve plasmid oligomers. FEBS Letters 328: 169-173

Romero-Calvo I, Ocón B, Martínez-Moya P, Suárez MD, Zarzuelo A, Martínez-Augustin O & de Medina FS (2010). Reversible Ponceau staining as a loading control alternative to actin in Western blots. Analytical Biochemistry 401: 318-320

Saiki RK, Gelfand DH, Stoffel S, Scharf SJ, Higuchi R, Horn GT, Mullis KB & Erlich HA (1988). Primer-directed enzymatic amplification of DNA with a thermostable DNA polymerase. Science 239: 487-491

Sanchez JF, Chiang Y-M, Szewczyk E, Davidson AD, Ahuja M, Oakley CE, Bok JW, Keller N, Oakley BR & Wang CC (2010). Molecular genetic analysis of the orsellinic acid/F9775 gene cluster of *Aspergillus nidulan*s. Molecular Biosystems 6: 587-593

Sanchez JF, Entwistle R, Hung J-H, Yaegashi J, Jain S, Chiang Y-M, Wang CC & Oakley BR (2011). Genome-based deletion analysis reveals the prenyl xanthone biosynthesis pathway in *Aspergillus nidulans*. Journal of the American Chemical Society 133: 4010-4017

Sarkar A, Funk AN, Scherlach K, Horn F, Schroeckh V, Chankhamjon P, Westermann M, Roth M, Brakhage AA & Hertweck C (2012). Differential expression of silent polyketide biosynthesis gene clusters in chemostat cultures of *Aspergillus nidulans*. Journal of Biotechnology 160: 64-71

Scazzocchio C (2009). Aspergillus: a multifaceted genus. Encyclopedia of Microbiology

Scherer M, Wei H, Liese R & Fischer R (2002). *Aspergillus nidulans* catalase-peroxidase gene (*cpeA*) is transcriptionally induced during sexual development through the transcription factor StuA. Eukaryotic Cell 1: 725-735

Schimmel TG, Coffman AD & Parsons SJ (1998). Effect of butyrolactone I on the producing fungus, *Aspergillus terreus*. Appl Environ Microbiol 64: 3707-3712

Schindler D & Nowrousian M (2014). The polyketide synthase gene *pks4* is essential for sexual development and regulates fruiting body morphology in *Sordaria macrospora*. Fungal Genetics and Biology 68: 48-59

Schinke J, Gulko MK, Christmann M, Valerius O, Stumpf SK, Stirz M & Braus GH (2016). The DenA/DEN1 interacting phosphatase DipA controls septa positioning and

phosphorylation-dependent stability of cytoplasmatic DenA/DEN1 during fungal development. PLoS genetics 12: e1005949

Schmittgen TD & Livak KJ (2008). Analyzing real-time PCR data by the comparative C T method. Nature Protocols 3: 1101

Schoustra SE, Slakhorst M, Debets AJ & Hoekstra RF (2005). Comparing artificial and natural selection in rate of adaptation to genetic stress in *Aspergillus nidulans*. Journal of Evolutionary Biology 18: 771-778

Seo J-A, Guan Y & Yu J-H (2005). FluG-dependent asexual development in *Aspergillus nidulans* occurs via derepression. Genetics 172: 1535-1544

Sewall T, Mims C & Timberlake W (1990). Conidium differentiation in *Aspergillus nidulans* wild-type and wet-white (*wetA*) mutant strains. Developmental Biology 138: 499-508

Shank EA & Kolter R (2009). New developments in microbial interspecies signaling. Current Opinion in Microbiology 12: 205-214

Shieh D-E, Chen Y-Y, Yen M-H, Chiang L-C & Lin C-C (2004). Emodin-induced apoptosis through p53-dependent pathway in human hepatoma cells. Life Sciences 74: 2279-2290

Shwab EK, Bok JW, Tribus M, Galehr J, Graessle S & Keller NP (2007). Histone deacetylase activity regulates chemical diversity in *Aspergillus*. Eukaryotic Cell 6: 1656-1664

Sibounnavong P, Soytong K, Divina C & Sofrio P (2009). In–vitro biological activities of *Emericella nidulans*, a new fungal antagonist against *Fusarium oxysporum* f. sp. *lycopersici*. Journal of Agricultural Technology 5: 75-84

Simpson TJ (2012). Genetic and biosynthetic studies of the fungal prenylated xanthone shamixanthone and related metabolites in *Aspergillus* spp. revisited. ChemBioChem 13: 1680-1688

Singh S, Braus-Stromeyer SA, Timpner C, Tran VT, Lohaus G, Reusche M, Knüfer J, Teichmann T, von Tiedemann A & Braus GH (2010). Silencing of Vlaro2 for chorismate synthase revealed that the phytopathogen *Verticillium longisporum* induces the cross-pathway control in the xylem. Applied Microbiology and Biotechnology 85: 1961-1976

Skromne I, Sánchez O & Aguirre J (1995). Starvation stress modulates the expression of the *Aspergillus nidulans brlA* regulatory gene. Microbiology 141: 21-28

Sohn K & Yoon K (2002). Ultrastructural study on the cleistothecium development in *Aspergillus nidulans*. Mycobiology 30: 117-127

Southern EM (1975). Detection of specific sequences among DNA fragments separated by gel electrophoresis. J Mol Biol 98: 503-517

Srinivas G, Babykutty S, Sathiadevan PP & Srinivas P (2007). Molecular mechanism of emodin action: transition from laxative ingredient to an antitumor agent. Medicinal Research Reviews 27: 591-608

Studt L, Wiemann P, Kleigrewe K, Humpf H-U & Tudzynski B (2012). Biosynthesis of Fusarubins Accounts for Pigmentation of *Fusarium fujikuroi* Perithecia. Applied and Environmental Microbiology 78: 4468

Suck RW & Krupinska K (1996). Repeated probing of Western blots obtained from Coomassie brilliant blue-stained or unstained polyacrylamide gels. BioTechniques 21: 418-422

Sugihara N, Tsuruta Y & Furuno K (1998). Effect of potassium sorbate on cellular GSH level and lipid peroxidation in cultured rat hepatocytes. Biological & Pharmaceutical Bulletin 21: 524-526

Swart K, van Heemst D, Slakhorst M, Debets F & Heyting C (2001). Isolation and characterization of sexual sporulation mutants of *Aspergillus nidulans*. Fungal Genetics and Biology 33: 25-35

Szewczyk E, Chiang Y-M, Oakley CE, Davidson AD, Wang CC & Oakley BR (2008). Identification and characterization of the asperthecin gene cluster of *Aspergillus nidulans*. Appl Environ Microbiol 74: 7607-7612

Szewczyk E, Nayak T, Oakley CE, Edgerton H, Xiong Y, Taheri-Talesh N, Osmani SA & Oakley BR (2006). Fusion PCR and gene targeting in *Aspergillus nidulans*. Nature Protocols 1: 3111-3120

Szwalbe AJ, Williams K, Song Z, de Mattos-Shipley K, Vincent JL, Bailey AM, Willis CL, Cox RJ & Simpson TJ (2019). Characterisation of the biosynthetic pathway to agnestins A and B reveals the reductive route to chrysophanol in fungi. Chemical Science 10: 233-238

Taghavi F, Moosavi-Movahedi A, Bohlooli M, Alijanvand HH, Salami M, Maghami P, Saboury A, Farhadi M, Yousefi R & Habibi-Rezaei M (2013). *Potassium sorbate* as an AGE activator for human serum albumin in the presence and absence of glucose. International Journal of Biological Macromolecules 62: 146-154

Thieme KG, Gerke J, Sasse C, Valerius O, Thieme S, Karimi R, Heinrich AK, Finkernagel F, Smith K, Bode HB, Freitag M, Ram AFJ & Braus GH (2018). Velvet domain protein VosA represses the zinc cluster transcription factor SclB regulatory network for *Aspergillus nidulans* asexual development, oxidative stress response and secondary metabolism. PLoS genetics 14: e1007511

Towbin H, Staehelin T & Gordon J (1979). Electrophoretic transfer of proteins from polyacrylamide gels to nitrocellulose sheets: procedure and some applications. Proceedings of the National Academy of Sciences 76: 4350-4354

Trienens M, Keller NP & Rohlfs M (2010). Fruit, flies and filamentous fungi–experimental analysis of animal–microbe competition using *Drosophila melanogaster* and *Aspergillus* mould as a model system. Oikos 119: 1765-1775

Ugalde U & Corrochano LM (2007). Spore formation in food-relevant fungi. Mycology Series 25: 53-55

Untergasser A, Cutcutache I, Koressaar T, Ye J, Faircloth BC, Remm M & Rozen SG (2012). Primer3—new capabilities and interfaces. Nucleic Acids Research 40: e115

Valiante V, Heinekamp T, Jain R, Härtl A & Brakhage AA (2008). The mitogen-activated protein kinase MpkA of *Aspergillus fumigatus* regulates cell wall signaling and oxidative stress response. Fungal Genetics and Biology 45: 618-627

Vargas-Pérez I, Sánchez O, Kawasaki L, Georgellis D & Aguirre J (2007). Response regulators SrrA and SskA are central components of a phosphorelay system involved in stress signal transduction and asexual sporulation in *Aspergillus nidulans*. Eukaryotic Cell 6: 1570-1583

Vienken K, Scherer M & Fischer R (2005). The Zn (II) 2Cys6 putative *Aspergillus nidulans* transcription factor repressor of sexual development inhibits sexual development under low-carbon conditions and in submersed culture. Genetics 169: 619-630

Vining LC (1990). Functions of secondary metabolites. Annual Review of Microbiology 44: 395-427

Wang C, Wu X, Chen M, Duan W, Sun L, Yan M & Zhang L (2007). Emodin induces apoptosis through caspase 3-dependent pathway in HK-2 cells. Toxicology 231: 120-128

Wang J, Huang H, Liu P, Tang F, Qin J, Huang W, Chen F, Guo F, Liu W & Yang B (2006). Inhibition of phosphorylation of p38 MAPK involved in the protection of nephropathy by emodin in diabetic rats. European Journal of Pharmacology 553: 297-303

Wang J, Wei D & Chou K (2008). Drug candidates from traditional chinese medicines. Current Topics in Medicinal Chemistry 8: 1656-1665

Wang S, Chen T, Chen R, Hu Y, Chen M & Wang Y (2012). Emodin loaded solid lipid nanoparticles: preparation, characterization and antitumor activity studies. International Journal of Pharmaceutics 430: 238-246

Wei H, Scherer M, Singh A, Liese R & Fischer R (2001). *Aspergillus nidulans* α-1, 3 glucanase (mutanase), *mutA*, is expressed during sexual development and mobilizes mutan. Fungal Genetics and Biology 34: 217-227

Wei W-T, Lin S-Z, Liu D-L & Wang Z-H (2013). The distinct mechanisms of the antitumor activity of emodin in different types of cancer. Oncology Reports 30: 2555-2562

Weinberg ED (1969). Biosynthesis of secondary metabolites: roles of trace metals. In Advances in Microbial Physiology, pp 1-44. Elsevier

Wells JM, Cole RJ & Kirksey JW (1975). Emodin, a toxic metabolite of *Aspergillus wentii* isolated from weevil-damaged chestnuts. Applied Microbiology 30: 26-28

Wen L, Lin Y-C, She Z-G, Du D-S, Chan W-L & Zheng Z-H (2008). Paeciloxanthone, a new cytotoxic xanthone from the marine mangrove fungus *Paecilomyces* sp.(Tree1-7). Journal of Asian Natural Products Research 10: 133-137

Williams DH, Stone MJ, Hauck PR & Rahman SK (1989). Why are secondary metabolites (natural products) biosynthesized? Journal of Natural Products 52: 1189-1208

Wink M (2003). Evolution of secondary metabolites from an ecological and molecular phylogenetic perspective. Phytochemistry 64: 3-19

Wink M & Schimmer O (2018). Molecular modes of action of defensive secondary metabolites. Annual Plant Reviews online: 10.1007/s40614-018-00181-z

Winkelmann G (1986). Iron complex products (siderophores). Biotechnology 4: 215-243

Wolf J & Mirocha C (1973). Regulation of sexual reproduction in *Gibberella zeae* (*Fusarium roseum*'Graminearum') by F-2 (zearalenone). Canadian Journal of Microbiology 19: 725-734

Woodcock D, Crowther P, Doherty J, Jefferson S, DeCruz E, Noyer-Weidner M, Smith S, Michael M & Graham M (1989). Quantitative evaluation of *Escherichia coli* host strains for tolerance to cytosine methylation in plasmid and phage recombinants. Nucleic Acids Research 17: 3469-3478

Woodman ME (2008). Direct PCR of intact bacteria (colony PCR). Current Protocols in Microbiology 9: A. 3D. 1-A. 3D. 6

Wyatt GR & Davey KG (1996). Cellular and molecular actions of juvenile hormone. II. Roles of juvenile hormone in adult insects. In Advances in Insect Physiology, pp 1-155. Elsevier

Xiao P, He L & Wang L (1984). Ethnopharmacologic study of Chinese rhubarb. Journal of Ethnopharmacology 10: 275-293

Xue J, Chen F, Wang J, Wu S, Zheng M, Zhu H, Liu Y, He J & Chen Z (2015). Emodin protects against concanavalin A-induced hepatitis in mice through inhibiting activation of the p38 MAPK-NF-κB signaling pathway. Cellular Physiology and Biochemistry 35: 1557-1570

Yang Y-C, Lim M-Y & Lee H-S (2003). Emodin isolated from *Cassia obtusifolia* (Leguminosae) seed shows larvicidal activity against three mosquito species. Journal of Agricultural and Food Chemistry 51: 7629-7631

Zasloff M (1987). Magainins, a class of antimicrobial peptides from Xenopus skin: isolation, characterization of two active forms, and partial cDNA sequence of a precursor. Proceedings of the National Academy of Sciences 84: 5449-5453

Zeise K & Von Tiedemann A (2002). Host specialization among vegetative compatibility groups of *Verticillium dahliae* in relation to *Verticillium longisporum*. Journal of Phytopathology 150: 112-119

Zonneveld BJ (1988). Effect of carbon dioxide on fruiting in *Aspergillus nidulans*. Transactions of the British Mycological Society 91: 625-629

List of abbreviations

%	Percent
°C	Degree Celsius
µg	Microgram
µl	Microliter
AspGD	Aspergillus genome database
bp	Base pairs
kb	Kilo bases
cm	Centimeter
mm	Millimeter
COP9	Constitutive photomorphogenesis 9
CSN	COP9 signalosome
MAP	Mitogen-activated (kinase)
PKS	Polyketide synthase
C-terminus	Carboxy terminus
GFP	Green fluorescent protein
d	Day(s)
DTT	Dithiothreitol
EDTA	Ethylenediaminetetraacetic acid
etc	et cetera
e.g.	exempli gratia and means “for example”
g	Gram
h	Hour(s)
H2A	Histone
S15	AN5997
LC-MS	Liquid chromatography-coupled mass spectrometry
CAD	Charged aerosol detector
TLC	Thin layer chromatogram
kDa	Kilo Dalton
LB	Lysogeny broth
M	Molar (mol/l)
mg	Milligram
min	Minute(s)
l	Liter
ml	Milliliter
MM	Minimal medium
mM	Millimolar
mm	Millimeter
PABA	4-Aminobenzoic acid
KSB	Potassium Sorbate
MSB	Menadione Sodium Bisulfite
MeOH	Methanol

EtOH	Ethanol
NAD(H)	Nicotinamide adenine dinucleotide
NADP(H)	Nicotinamide adenine dinucleotide phosphate
ROS	Reactive oxygen species
nat$_{R}$	Nourseothricin resistance marker
N-source	Nitrogen source
N-terminal	Amino-terminal
o/n	Over night
DNA	Deoxyribonucleic acid
cDNA	Complementary DNA
mRNA	Messenger RNA
PCR	Polymerase chain reaction
phleo$_{RM}$	Phleomycin recyclable resistance marker
PKS	Polyketide synthase
ptrA	Pyrithiamin recyclable resistance marker
qRT-PCR	Quantitative real-time PCR
P	P value
$_{p}$	Promoter
rpm	Rounds per minute
SMs	Secondary metabolites
SM_3d	Secondary metabolites from three days of sexual growth
SM_5d	Secondary metabolites from five days of sexual growth
rt	Room temperature
wt	Wild type
OE	Overexpression
Δ	Deletion
$_{com}$	complementation

Table of figures

FIGURE 1. LIFE CYCLES OF *A. NIDULANS*. 5
FIGURE 2. DETACHED HÜLLE CELLS OF *A. NIDULANS*. 8
FIGURE 3. SEXUAL STRUCTURE OF *A. NIDULANS*. 9
FIGURE 4. THE SEXUAL DEVELOPMENT REGULATORY NETWORK IN *A. NIDULANS*. 11
FIGURE 5. THE CHROMOSOME LOCATIONS OF *MDP/XPT* CLUSTERS IN *A. NIDULANS*. 20
FIGURE 6. PROPOSED BIOSYNTHETIC PATHWAY OF PRENYL XANTHONES. 22
FIGURE 7. THE REGULATION MODELS OF SECONDARY METABOLISM AND FUNGAL DEVELOPMENT IN *A. NIDULANS*. 25
FIGURE 8. SCHEMATIC DIAGRAM OF A RESISTANCE RECYCLABLE MARKER IN A FRAGMENT CONSTRUCT. 36
FIGURE 9. RESTRICTION MAP AND SOUTHERN HYBRIDIZATION AFTER THE MARKER WAS RECYCLED. 43
FIGURE 10. THE GENE *MDPG* WAS UPREGULATED IN OE*MDPG* MUTANT STRAIN (AGB1235) IN COMPARISON TO WILD TYPE (AGB552). 53
FIGURE 11. DELETION OF GENES OF *MDP/XPT* CLUSTERS RESULTED IN THE ACCUMULATION OF VARIOUS COMPOUNDS INCLUDING EMODIN AND CHRYSOPHANOL IN *A. NIDULANS*. 54
FIGURE 12. DELETION OF GENES OF *MDP/XPT* CLUSTERS RESULTED IN THE ACCUMULATION OF VARIOUS INTERMEDIATES OF EPI-/SHAMIXANTHONE IN *A. NIDULANS*. 56
FIGURE 13. DELETION OF GENES OF *MDP/XPT* CLUSTERS RESULTED IN THE ACCUMULATION OF VARIOUS EMODIN, BENZOPHENONE AND XANTHONE DERIVATIVES IN *A. NIDULANS*. 58
FIGURE 14. A DYNAMIC CHANGE OF ACCUMULATED COMPOUNDS IN *A. NIDULANS MDP/XPT* DELETION STRAINS WAS OBSERVED AFTER THREE OR FIVE DAYS OF SEXUAL GROWTH. 60
FIGURE 15. SECONDARY METABOLITES PRODUCED BY *MDP/XPT* CLUSTERS WERE ACCUMULATED IN HÜLLE CELLS. 62
FIGURE 16. THE COMPLEMENTATION OF *MDPG* WAS RESTORED TO WILD TYPE. 63
FIGURE 17. THE SM PRODUCTION OF THE COMPLEMENTATION OF *MDPC* WAS PARTIALLY RESTORED TO WILD TYPE. 64
FIGURE 18. DELETION OF GENES OF THE *MDP/XPT* CLUSTERS LED TO A REPRESSION OF SEXUAL DEVELOPMENT OF *A. NIDULANS*. 66
FIGURE 19. DELETION OF GENES OF *MDP/XPT* CLUSTERS PRODUCED SMALLER HÜLLE CELLS WITH REDUCED ACTIVITY. 67
FIGURE 20. SMS OF Δ*MDPC* REPRESSED THE SEXUAL FRUITING BODY DEVELOPMENT OF *A. NIDULANS* WILD TYPE. 70
FIGURE 21. DELETION STRAINS OF *MDP/XPT* CLUSTERS EXHIBITED NO EFFECT ON THE ASEXUAL DEVELOPMENT OF *A. NIDULANS*. 71
FIGURE 22. DELETION OF GENES *MDPC* AND *MDPL* HAD NO EFFECT ON THE GENE EXPRESSION OF *SAKA*. 73
FIGURE 23. DELETION OF THE GENE *MDPC* CHANGED THE EXPRESSION OF *VELB* AND *STUA* IN THE LATE STAGE OF SEXUAL DEVELOPMENT. 74
FIGURE 24. DELETION OF GENES *MDPC* AND *MDPL* EXHIBITED NO IMPACT ON THE PROTEIN LEVEL OF SAKA OR PHOSPHORYLATED SAKA. 75
FIGURE 25. DELETION OF GENES *MDPC*, *MDPL*, *MDPD*, *XPTA* AND *XPTB* OF *MDP/XPT* CLUSTERS CAUSED *A. NIDULANS* OXIDATIVE AND ACIDIC STRESS SENSITIVITY. 77
FIGURE 26. PRECURSORS OF EPI-/SHAMIXANTHONE REPRESSED THE RESTING AND REPRODUCTIVE STRUCTURE DEVELOPMENT OF DIFFERENT FUNGI. 81

FIGURE 27. EMODIN, A PRECURSOR OF EPI-/SHAMIXANTHONE, IS ONE OF THE KEY FACTORS FOR REPRESSION OF DEVELOPMENT OF DIFFERENT FUNGI AND THE EGG DEPOSITING BEHAVIOR OF FLIES. 82
FIGURE 28. TYPICAL FUNGAL XANTHONE METABOLITES DERIVED FROM EMODIN SKELETON. 84
FIGURE 29. SIMPLIFIED BIOSYNTHETIC PATHWAY OF EPI/SHAMIXANTHONE IN THIS STUDY. 86
FIGURE 30. COMPARISON OF SECONDARY METABOLITES OF Δ*MDPC* STRAIN FROM THREE AND FIVE DAYS OF SEXUAL GROWTH. 95
FIGURE 31. COMPARISON OF SECONDARY METABOLITES OF *A. NIDULANS* WILD TYPE FROM THREE AND FIVE DAYS OF SEXUAL GROWTH. 97
FIGURE 32. EMODINS EXHIBITED A BROAD BIOACTIVITY ON FUNGAL AND INSECT REPRODUCTION AND SURVIVAL STRUCTURES. 100
FIGURE 33. EMODINS DISTURBED THE INTRACELLULAR ROS BALANCE RESULTING IN THE REPRESSED SEXUAL DEVELOPMENT OF *A. NIDULANS*. 102

List of tables

TABLE 1. GENE DESIGNATION OF *MDP/XPT* CLUSTERS OF *ASPERGILLUS NIDULANS* (ARNAUD *ET AL*., 2012). 18
TABLE 2. FUNGAL STRAINS USED IN THIS STUDY 30
TABLE 3. PRIMERS FOR QRT-PCR USED IN THIS STUDY 33
TABLE 4. PLASMIDS USED AND CONSTRUCTED IN THIS STUDY 40
TABLE 5. PRIMERS USED IN THIS STUDY FOR DNA SEQUENCE AMPLIFICATION AND PLASMID CONSTRUCTION 41
TABLE 6. METABOLITE MARKERS IDENTIFIED BY HPLC-MS 59

Acknowledgements

First and foremost, I would like to thank Prof. Dr. Gerhard Braus for his constant support and many inspiring discussions during my PhD study in his department. I appreciate his excellent supervision and expertise he invested into my work. I am also very thankful to him for financial support during the last period of my PhD studies.

I want to thank Dr. Jennifer Gerke for being my supervisor. She introduced me into this project and constantly help and guide my work. Our many meetings and discussions, she gave me a lot of helpful ideas. I also want to thank for her encouragement as well as patient during my whole PhD study.

I want to thank Prof. Dr. Stefanie Pöggeler and Prof. Dr. Petr Karlovsky for being members of my thesis committee and their helpful discussions and suggestions during our meetings. I also want to thank Prof. Dr. Rolf Daniel, Jun.-Prof. Dr. Kai Heimel and PD Dr. Michael Hoppert for being my thesis examination board.

I am gratefull to conduct my PhD studies as a member of the doctoral program “Microbiology and Biochemistry” of the Göttingen Graduate School for Neuroscience, Biophysics and Molecular Biosciences (GGNB). It was a great opportunity for scientific learning and exchanging with other researchers. I am also thankful to GGNB team for timely notice and reminder and patient reply.

My appreciation goes to Dr. Rebekka Harting, Dr. Daniela Nordzieke and Gertrud Stahlhut. They kindly provide the tested fungal plates and help me analyze the results. I also want to thank Prof. Dr. Frank Kempken from Christian-Albrechts-Uni, Kiel for the biotest on fly egg laying part.

I want to thank all former and current members of my lab 0.107, Christoph, Hugo, Alex, Maxin, Linnet and many lab interns. I really enjoy the time we had in the lab. I also thank all members of the Department of Molecular Microbiology and Genetics for the nice working atmosphere. In particular I thank Verena Grosse for technical teaching in the beginning of my PhD study and Benedict Dirnberger, Fruzsina Bakti, Cindy Meister, Miriam Kolog Gulko, Anja Abelmann and Jessica Starke for proof reading my thesis and for all the fun we had in the lab. I also want to thank my lunch team, Dan, Xuebin and Wanping.

Last but certainly not least, all my love goes to my parents, my elder sister and my boyfriend. Without your love and your constant support, this would never have been possible. Of course, I also want to thank myself for my persistence, optimistic attitude and good health.